Theses and Dissertations　　　　　　　　　　1. Thesis and Dissertation Collection, all items

1956

Helium gas turbines for nuclear power.

Phillips, Kenneth Elwin

Monterey, California: U.S. Naval Postgraduate School

HELIUM GAS TURBINES FOR NUCLEAR POWER

Kenneth Elwin Phillips

HELIUM GAS TURBINES

FOR

NUCLEAR POWER

* * *

Kenneth E. Phillips

HELIUM GAS TURBINES

FOR NUCLEAR POWER

by

Kenneth Elwin Phillips

Lieutenant, United States Navy

Submitted in partial fulfillment
of the requirements
for the degree of
MASTER OF SCIENCE
IN
MECHANICAL ENGINEERING

United States Naval Postgraduate School
Monterey, California

1 9 5 6

Thesis
P.121

This work is accepted as fulfilling

the thesis requirements for the degree of

MASTER OF SCIENCE

IN

MECHANICAL ENGINEERING

from the

United States Naval Postgraduate School

In recent years great progress has been made in the gas turbine field. The improvements made in high temperature materials, compressor and turbine design, and compact heat exchangers have made the gas turbine power plant a serious competitor of steam plants and diesel engines for many applications. There are, however, many problems still existing that tend to make conventional gas turbines unattractive.

The use of residual fuels in the open cycle results in ash deposits and corrosion in the turbines which seriously limits the operating life of the units. Furthermore, open cycle plants are limited in power rating since the components become too large for outputs greater than about 20,000 HP. The closed cycle gas turbine plant eliminates these problems since only clean air circulates through the cycle and high pressures permit components of a practical size for outputs much larger than 20,000 HP. For a ship propulsion unit where the power requirements vary over a wide range, the closed cycle has the additional advantage of good part load efficiency. A major factor in the slow progress of the closed cycle plant has been the inability to manufacture a reliable air heater cheaply enough to permit the gas turbine plant to compete with conventional steam plants.

The future of the gas turbines may depend on how well they can be adapted for use with nuclear power. At the present time the only ship propulsion plant employing a nuclear reactor is essentially a steam plant. The size of this plant is large since a two loop system is required in order that energy may be conveyed from the reactor to the

secondary working fluid. A simpler and smaller plant would be one in which there is only one fluid serving both as the working fluid and reactor coolant. Such a plant is a closed cycle gas turbine plant using helium at high pressure. Helium has good coolant characteristics including a negligible cross section for neutron absorption. If pure, it is not subject to induced activity. By proper design of the cooling channels and filtering system, fission products can be prevented from being carried through that portion of the cycle which is external to the reactor. This would require only the reactor to be shielded. It has been presumed up to this point that helium is a satisfactory gas turbine fluid. Although helium turbines have never been built, the following general statements can be made by comparing the properties of helium with air:

(1) Better heat transfer characteristics of helium results in smaller heat exchangers.

(2) Lower molecular weight of helium requires more stages in the turbo-machines for the same peripheral speed.

(3) Higher velocity of sound in helium permits higher peripheral speeds before Mach effect occurs.

It would appear from these statements that the advantage of smaller heat exchangers for a helium cycle may be more than offset by requiring more expensive turbines and compressors as well as a costlier and less available gas. Design criteria for helium compressors are based on stress limitations, whereas for air compressors the Mach effect becomes the limiting factor. Thus, the higher peripheral speed permitted for the helium compressors will partially counteract the effect of lower

iii

molecular weight on the number of stages required. Furthermore, improved efficiency and fewer stages of compression may result by employing a higher effectiveness regenerator than would be practical with air.

It is the writer's objective to investigate a 50,000 HP closed-cycle helium gas turbine power plant for ship propulsion and determine the approximate sizes of the major components. Unfortunately, the scope of this report does not cover many of the interesting problems which would have to be investigated and solved before this plant could become a reality. Some of these are discussed briefly in Chapter IX.

It has been necessary to include a list of symbols at the beginning of each chapter since the same symbols may have different meanings in different chapters.

The writer wishes to express his deep appreciation for the encouragement and assistance given him by Professor M. H. Vavra and Professor H. M. Wright in the preparation of this report. The writer is also grateful for the fine clerical support given him by his typist, Mrs. Marilyn Heard.

TABLE OF CONTENTS

LIST OF ILLUSTRATIONS

viii

LIST OF TABLES

CHAPTER I

THERMODYNAMIC PROPERTIES OF HELIUM

Symbols used in this chapter:

Symbol	Description	Units
B_o	virial coefficient	ft^3/lb
c_p	specific heat at constant pressure	BTU/lb - °F
c_v	specific heat at constant volume	BTU/lb - °F
f	reheat factor for ∞ stages	-----
h	enthalpy	BTU/lb
k	thermal conductivity	BTU/ft^2 - hr - °F/ft
P	pressure	psia
R	gas constant	$\dfrac{ft - lb_f}{lb_m - °F}$
T	absolute temperature	°R
t	temperature	°F
v	specific volume	ft^3/lb
γ	ratio of $\dfrac{c_p}{c_v}$	----
Δ	increment	----
η	efficiency	----
μ	absolute viscosity	lb/hr - ft
ψ	corresponds to $\dfrac{\gamma -1}{\gamma}$	----

Subscript	Definition
o	reference quantity
c	compressor or compression process

1

Subscript	Definition
i	initial
f	final
s	isentropic process
t	turbine or expansion

General

In studying a cycle that uses fluids such as steam or air, or one that behaves like an ideal gas, there are tables, charts and equations which can be used to obtain accurate thermodynamic information. This is not the case for helium. Several equations of state have been proposed based on theory and empirical data obtained at low temperatures. Which of these equations, if any, is applicable at higher temperatures will be known only after more extensive empirical data are available. Until then, extrapolation from the lower temperatures will have to suffice. The extrapolation methods used in this investigation are based on the research done by Akin [1]. His tables for enthalpy, entropy, and specific volume extend to 600°F whereas the highest temperature in the cycle being investigated is 1350°F. His extrapolation formulas for absolute viscosity and thermal conductivity extend to temperatures beyond 1350°F.

Absolute Viscosity, μ

Akin found Keesom's [2] equation for μ accurate within 1% for temperatures between -450 and 2000°F. This equation, plotted in Figure 1-1, is:

$$\mu = 8.315 \, T^{0.647} \times 10^{-4} \quad lb/hr\text{-}ft \quad (1\text{-}1)$$

2

Thermal Conductivity, k

The following equation is based on kinetic theory and test results at temperatures below 212°F. It is plotted in Figure 1-1.

$$k = \mu c_v \epsilon \qquad BTU/ft^2 - hr - °F/ft$$

$$or \quad k = 1.8166 \mu \qquad for \quad t > 80°F \qquad (1-2)$$

Specific Volume, v

Akin's results on specific volume are based on the Beattie-Bridgeman equation of state. Comparisons with the co-volume equation of state show good agreement in the range of pressures and temperatures encountered in this report. Because of its simpler form, the latter equation has been used throughout.

$$P = \frac{RT}{v - B_o} \qquad psia \qquad (1-3)$$

where

$$B_o = 0.306 \left(\frac{1}{T}\right)^{\frac{1}{4}} - 1.845 \left(\frac{1}{T}\right)^{\frac{3}{4}} - 0.822 \left(\frac{1}{T}\right)^{\frac{5}{4}} \qquad (1-3a)$$

and

$$R = 2.6829 \qquad \frac{ft^3 - lb_f}{lb_m - °F - in^2}$$

Equation (1-3a) is plotted in Figure 1-2. The specific volume for temperatures from 0°F to 1400°F when calculated from equation (1-3) is 0.047 to 0.040 ft^3/lb greater than that obtained by assuming ideal gas behavior at the same temperature.

Enthalpy, h

For enthalpies below 600°F, Akin's tables have been used. The extrapolation formula for a constant pressure process can be expressed

3

as:

$$h_t = h_o + c_{p_o}(t - t_o) + f\left(\tfrac{1}{T}, P\right) \tag{1-4}$$

where $h_o = h$ at $-440°F$

and $c_{p_o} = 1.241$ BTU/lb-°F

At temperatures above 400°F it is apparent from the tables that for a constant pressure process:

$$h_{t_2} = h_{t_1} + c_p(t_2 - t_1) \quad \text{BTU/lb} \tag{1-5}$$

where $t_1 > 400$ °F

and $c_p = 1.24$ BTU/lb-°F

Since extrapolation is necessary above 600°F, (1-5) becomes:

$$h_t = h_{600°F} + 1.24(t - 600) \quad \text{BTU/lb} \tag{1-5a}$$

Figure 1-3 contains plots of h vs. P for temperatures from 100°F to 600°F.

Isentropic Work of Expansion and Compression

For an ideal gas the work of compression for a reversible-adiabatic process is:

$$\Delta h_s = T_i\, c_p \left[\left(\frac{P_f}{P_i}\right)^{\frac{\gamma-1}{\gamma}} - 1\right] \quad \text{BTU/lb} \tag{1-6}$$

4

Similarly, the work of expansion is:

$$\Delta h_s = T_i \, c_p \left[1 - \left(\frac{P_f}{P_i} \right)^{\frac{\gamma-1}{\gamma}} \right] \quad BTU/lb \qquad (1\text{-}7)$$

An analysis of **Akin's** tables reveals that these equations are not applicable for helium if both c_p and γ are assumed to be constant. Since c_p is constant (1.24 BTU/lb °F) equations (1-6) and (1-7) were solved for $\frac{\gamma-1}{\gamma}$ using various combinations of T_i, P_i, and P_f/P_i. The results indicated that $\frac{\gamma-1}{\gamma}$ is a function of P_i only. Since this function differs for the compression and expansion processes, $\frac{\gamma-1}{\gamma}$ has been replaced by ψ_c and ψ_t respectively.

$$\Delta h_s = T_i \, c_p \left[\left(\frac{P_f}{P_i} \right)^{\psi_c} - 1 \right] \quad BTU/lb \qquad (1\text{-}6a)$$

$$\Delta h_s = T_i \, c_p \left[1 - \left(\frac{P_f}{P_i} \right)^{\psi_t} \right] BTU/lb \qquad (1\text{-}7a)$$

Figure 1-4 contains plots of ψ_c and ψ_t vs. P_i.

Reheat Factor, $1+f_\infty$

The values of ψ_c and ψ_t are also applicable to expressions for evaluating reheat factors. Assuming ideal gas behavior and replacing $\frac{\gamma-1}{\gamma}$ by ψ_c or ψ_t, the reheat factor, $1+f_\infty$, becomes:

$$1+f_\infty = \eta_c \frac{\left[\left(\frac{P_f}{P_i} \right)^{\psi_c / \eta_c} - 1 \right]}{\left[\left(\frac{P_f}{P_i} \right)^{\psi_c} - 1 \right]} \qquad \text{for compression}$$

$$\qquad (1\text{-}8)$$

5

$$1+f_\infty = \frac{1}{\eta_t} \frac{\left[1 - \left(\frac{P_f}{P_i}\right)^{\gamma_t \eta_t}\right]}{\left[1 - \left(\frac{P_f}{P_i}\right)^{\gamma_t}\right]} \qquad \text{for expansion}$$

(1-9)

A more detailed analysis of reheat factors is given in Chapter IV on "Compressors".

By means of the aforementioned formulas and/or the plots, all the thermodynamic properties that are required in the following cycle analysis can be obtained.
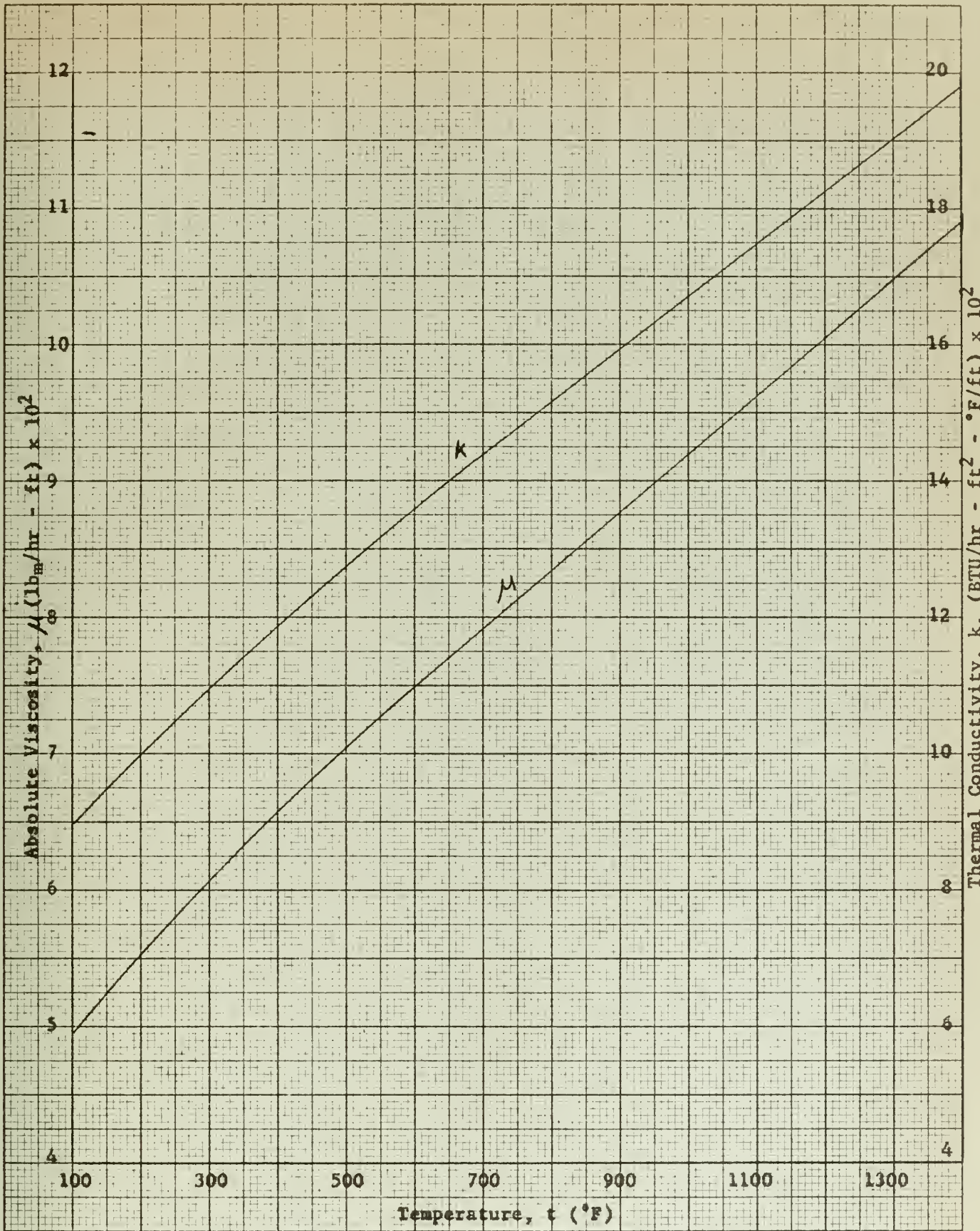
Figure 1-1   Variation of Thermal Conductivity and
Absolute Viscosity with Temperature
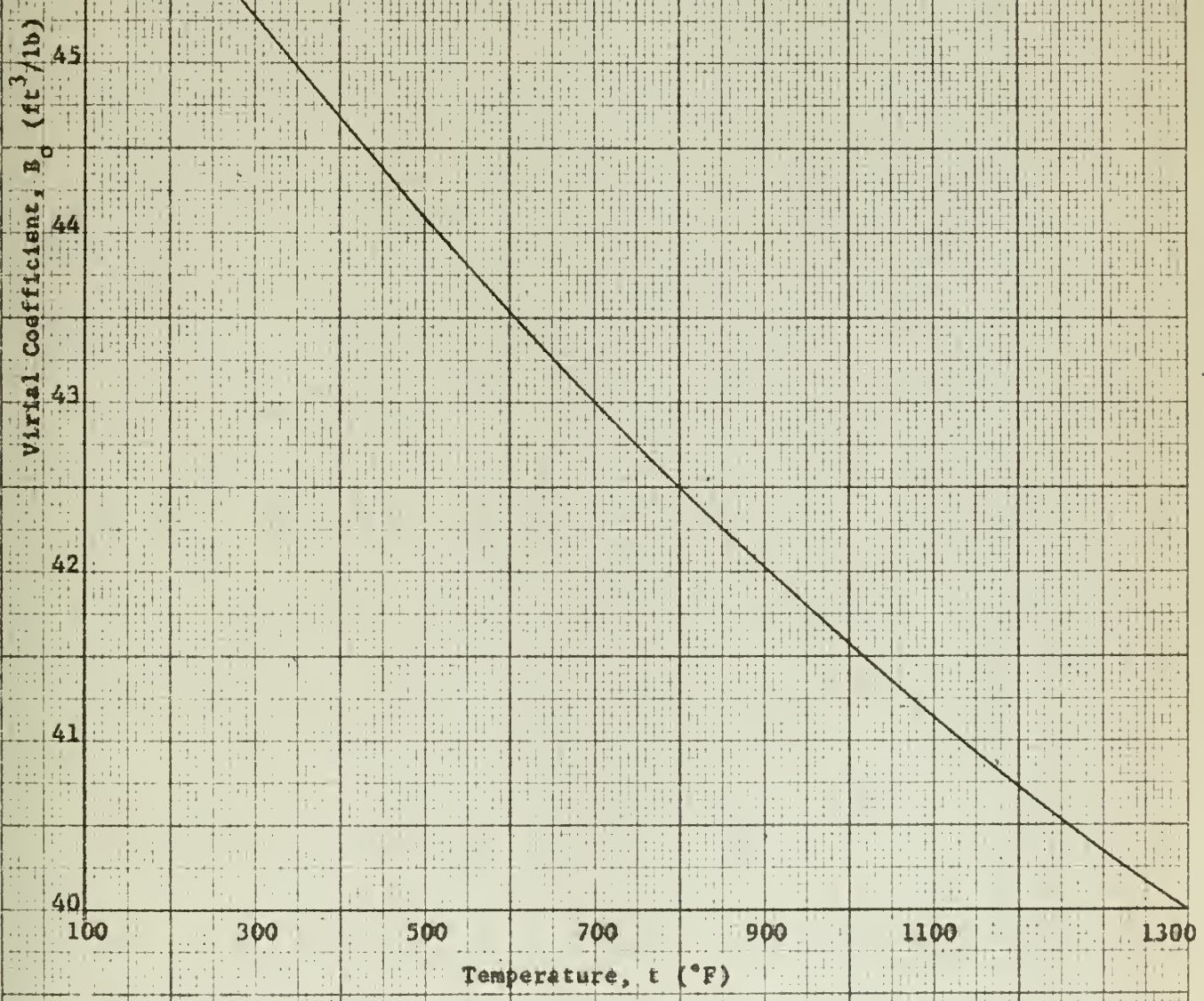
Figure 1-2   Variation of B_o with Temperature

8

Figure 1-3   Variation of Enthalpy with Pressure for Specified Temperatures

9

Figure 1-3   Variation of Enthalpy with Pressure for
(continued)   Specified Temperatures

10
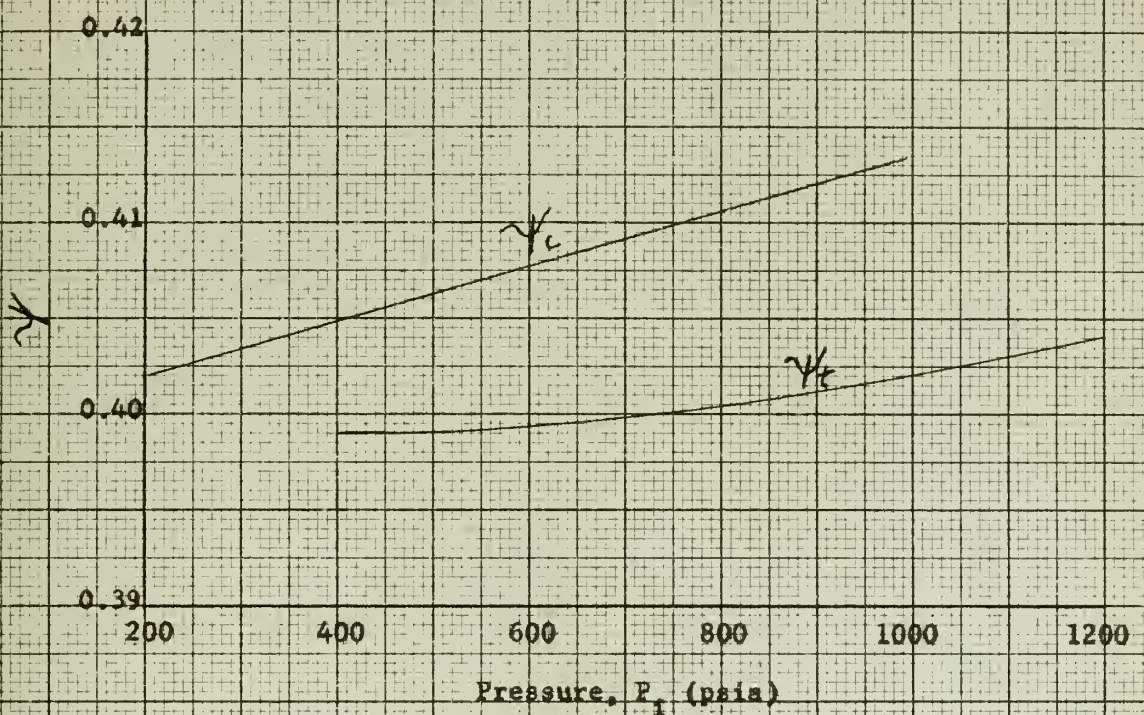
Figure 1-4   Variation of ψ_c and ψ_t
with Initial Pressure

11

CHAPTER II

PRELIMINARY CYCLE ANALYSIS

Symbols used in this chapter:

Symbol	Description	Units
B_o	virial coefficient	ft^3/lb
c_p	specific heat at constant pressure	BTU/lb - °F
c_v	specific heat at constant volume	BTU/lb - °F
ΔH_s	total isentropic enthalpy change for the compressor or turbine	BTU/lb
h	enthalpy	BTU/lb
k	thermal conductivity	BTU/ft^2 - hr - °F/ft
$\dot{m}$	mass rate of flow	lb/sec
P	pressure	psia
R	gas constant	$\dfrac{ft - lb_f}{lb_m - °F}$
T	absolute temperature	°R
t	temperature	°F
v	specific volume	ft^3/lb
γ	ratio of $\dfrac{c_p}{c_v}$	----
Δ	increment	----
η	efficiency	----
μ	absolute viscosity	lb/hr - ft
ψ	corresponds to $\dfrac{\gamma - 1}{\gamma}$	----

12

Subscript	Definition
o	reference quantity
c	compressor or compression process
i	initial
f	final
R	regenerator
s	isentropic process
t	turbine or expansion
Th	thermal

General

Since it is the objective of this report to analyze a 50,000 HP closed-cycle gas turbine plant, it is of prime importance to select a set of conditions which will result in a plant of high thermal efficiency and reasonable size which is still practical and economical to build, operate and maintain. To make such a selection one must know the following:

(a) Components of the cycle

(b) Reasonable estimate of the machine efficiencies

(c) Anticipated losses associated with the various components and interconnecting piping.

(d) Regenerator effectiveness

(e) Limiting temperatures, both upper and lower

(f) Highest pressure permissible in the cycle.

Components of the Cycle

This is not a study of various types and arrangements of cycles, hence a cycle of minimum complexity was chosen. The basic cycle is

13

similar to the conventional plant built and operated by Escher-Wyss [3] and consists of a single heat source, regenerator, precooler, compressors with intercooling, and two turbines. For the heat source, the conventional air heater is replaced by a homeogeneous reactor, the core consisting of a graphite and highly enriched uranium mixture. Since auxiliary equipment, including control apparatus, has little effect on the thermodynamics of the cycle it is not included here. A diagrammatic sketch of the basic cycle is shown in Figure 2-1.

Machine Efficiencies

Assigning efficiencies to the two compressors and two turbines can at best be only a first approximation. Turbo-machines are built today with overall efficiencies over 80% when used in conventional cycles. However, for a given cycle such as the one being investigated, practical design considerations may preclude these high efficiencies and a conservative estimate is in order. No distinction is made in the preliminary analysis between internal and overall machine efficiencies and no separate mechanical efficiency is specified. The efficiencies for Compressor No. 2 and Turbine No. 2 are lower than for the No. 1 units in the event that radial flow turbo-machines are practical.

MACHINE	EFFICIENCY (Assumed)
Turbine No. 1	0.85
Turbine No. 2	0.80
Compressor No. 1	0.84
Compressor No. 2	0.80

14
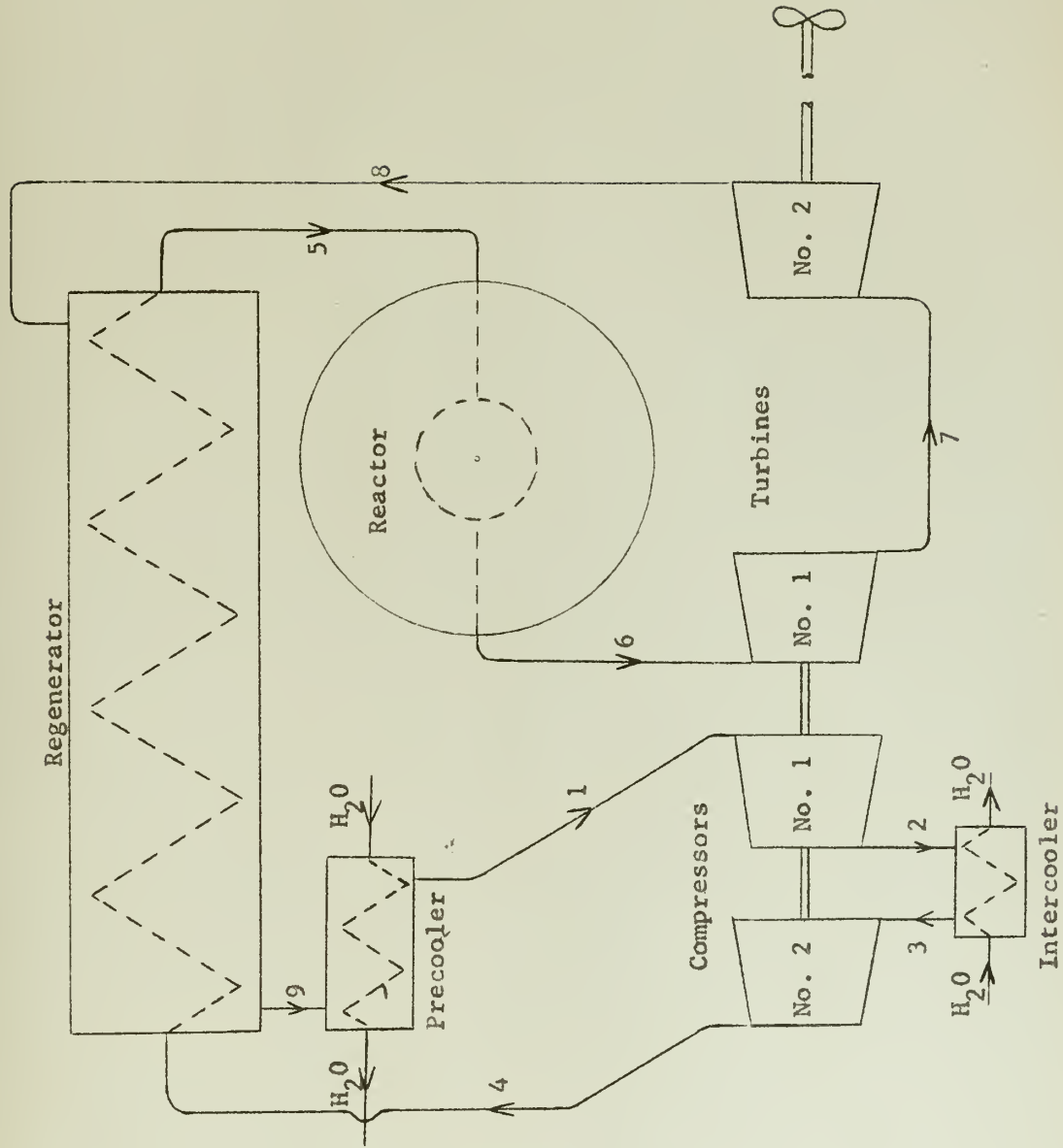
Figure 2-1   Schematic Diagram of a Closed Cycle Gas Turbine Plant

The losses associated with each component are expressed here as a ratio of the static pressure loss across the component to the inlet static pressure. Again, these are only estimates based on rough calculations and experience and include not only the drop across the component but also associated inlet and exit piping effects.

COMPONENT	$\frac{\Delta P}{P_i}$ (Assumed)
Reactor	0.010
Regenerator	
High Pressure Side	0.015
Low Pressure Side	0.010
Precooler	0.0075
Intercooler	0.005

Regenerator Effectiveness

The regenerator effectiveness is defined as:

$$\eta_R \equiv \frac{h_5 - h_4}{h_8 - h_4} \tag{2-1}$$

A high effectiveness is usually desirable from the standpoint of high thermal efficiency. It is not practically feasible to have η_R greater than 0.9 because of the large amount of surface required. In the preliminary analysis η_R is taken as 0.7, 0.8 and 0.9 to indicate its effect on efficiency.

Limiting Temperatures of Working Fluid

The lower temperature is dependent primarily on the cooling medium, in this case sea water. For a given plant a decrease in the lower

16

temperature will improve plant efficiency. However, since a ship may

operate in tropic waters as well as arctic waters, a conservative

lower limit of 100°F is chosen. The upper temperature limit depends

on materials and is gradually increasing as materials and cooling

techniques are improved. Temperatures of 1450 and 1500°F are common

in present-day gas turbine cycles, but because of the high pressure

encountered in this closed cycle an upper temperature of 1350°F is

assumed.

Maximum Pressure

The maximum pressure in the cycle has a slight effect on effi-

ciency due to the variation of γ_c and γ_t with pressure. More

important, however, is the effect of pressure on the size of the plant.

Higher pressures mean smaller specific volumes, hence smaller flow

areas. Based on steam plant design a maximum cycle pressure of 1000

psia seems reasonable for a plant of this size.

Cycle Analysis

Now, with the foregoing assumptions, together with the thermody-

namic information from Chapter I, the cycle of Figure 2-1 has been

analyzed by standard methods to obtain thermodynamic properties at

each point for pressure ratios between 1.25 and 5.0. In addition,

the following performance indices are plotted in Figures 2-2, 2-3 and

2-4 respectively:

    (a) Thermal efficiency based on work output at turbine shaft

    (b) Helium rate

    (c) Work ratio

17
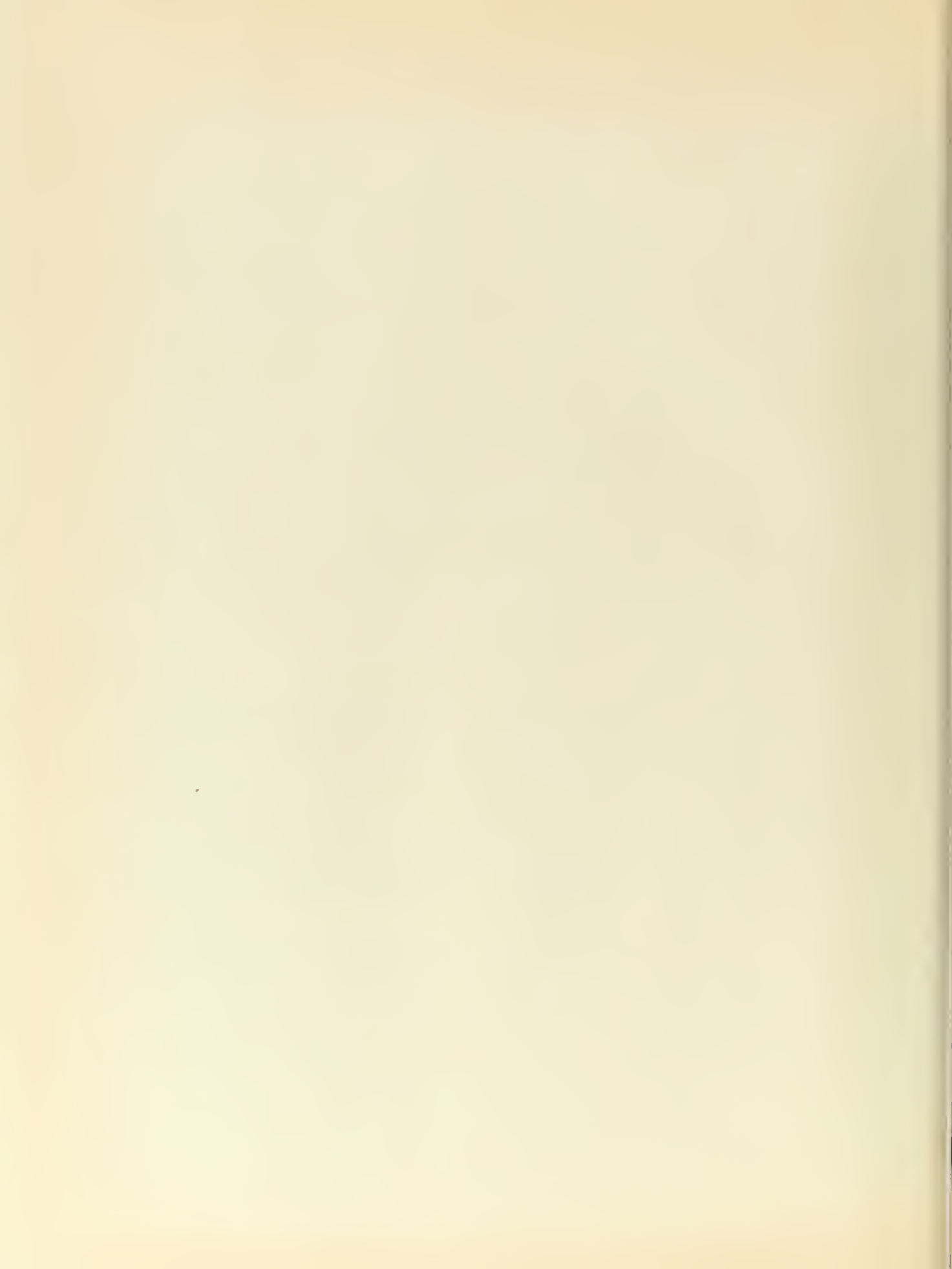
A list of equations used in the analysis follows:

$$v = \frac{2.6829\,T}{P} + B_o \qquad ft^3/lb \qquad\qquad (1\text{-}3)$$

$$\Delta H = \frac{\Delta H_s}{\eta_c} \qquad\qquad (2\text{-}2)$$

$$\Delta H = \Delta H_s \times \eta_t \qquad\qquad (2\text{-}3)$$

$$h_t = h_{600°F} + 1.24\,(t - 600)\ BTU/lb \qquad\qquad (1\text{-}5a)$$

$$\Delta H_s = 1.24\,T_i \left[\left(\frac{P_f}{P_i}\right)^{Y_c} - 1 \right]\ BTU/lb \qquad\qquad (1\text{-}6a)$$

$$\Delta H = 1.24\,T_i \left[1 - \left(\frac{P_f}{P_i}\right)^{Y_t} \right] BTU/lb \qquad\qquad (1\text{-}7a)$$

$$\eta_{th} = \frac{h_7 - h_8}{h_6 - h_5} \qquad\qquad (2\text{-}4)$$

$$\text{Helium Rate} = \frac{2545}{h_7 - h_8} \qquad lb/hp\text{-}hr \qquad\qquad (2\text{-}5)$$

18

$$\text{Work Ratio} = \frac{h_7 - h_8}{h_6 - h_8} \qquad (2\text{-}6)$$

$$\eta_R = \frac{h_5 - h_4}{h_3 - h_4} \qquad (2\text{-}1)$$

Conclusion

In studying Figure 2-2 we observe the following points of maximum efficiency:

η_R	P_4/P_1	η_{th}
0.7	3.00	0.268
0.8	2.65	0.292
0.9	2.25	0.329

If this cycle is to compete with other power plants it must have a higher thermal efficiency and/or be smaller in size. A high effectiveness regenerator provides the higher efficiency at the expense of increased size of plant. At the lower effectiveness, not only is the thermal efficiency less, but the larger pressure ratio will result in several more stages for the turbo-machines. Placing emphasis on the higher efficiency and fewer stages, the remainder of this report considers only the cycle having $P_4/P_1 = 2.25$ and $\eta_R = 0.9$. Table 2-2 lists the thermodynamic properties at each point in this cycle.

19

TABLE 2-1

PLANT PERFORMANCE AS A FUNCTION OF PRESSURE RATIO

Pressure Ratio P_4/P_1	Plant Thermal Efficiency, η th			Helium Rate (lb/hp-hr)	Work Ratio
	η R = 0.9	η R = 0.8	η R = 0.7		
1.25	0.184	0.122	0.091	51.7	0.378
1.50	0.279	0.210	0.169	24.4	0.413
1.75	0.312	0.253	0.212	17.7	0.410
2.00	0.325	0.274	0.237	14.8	0.400
2.25	0.329	0.285	0.252	13.2	0.388
2.50	0.327	0.290	0.261	12.2	0.375
2.75	0.323	0.291	0.265	11.6	0.362
3.00	0.318	0.291	0.268	11.1	0.351
4.00	0.290	0.275	0.261	10.4	0.308
5.00	0.261	0.252	0.244	10.6	0.270

TABLE 2-2

THERMODYNAMIC PROPERTIES FOR CYCLE HAVING $P_4/P_1 = 2.25$ AND $\eta_R = 0.9$

Location (Fig.2-1)	P (psia)	h(BTU/lb)	t(°F)	v(ft^3/lb)
1	444.4	701.5	100	3.428
2	666.7	848.8	216.9	2.768
3	663.4	703.7	100	2.309
4	1000	861.9	224.9	1.883
5	985	1667.8	874.8	3.677
6	975.2	2256.9	1350	5.019
7	631.2	1951.0	1106.3	6.692
8	452.2	1757.3	951.3	8.413
9	447.7	951.4	301.5	4.607

$\dot{m}$ = 182.4 lb/sec (For Net output = 50,000 HP)

η_{th} = 0.329

Helium
 Rate = 13.2 lb/hp-hr

Work
 Ratio = 0.388

Figure 2-2   Effect of Pressure Ratio and Regenerator Effectiveness on Plant Thermal Efficiency

22
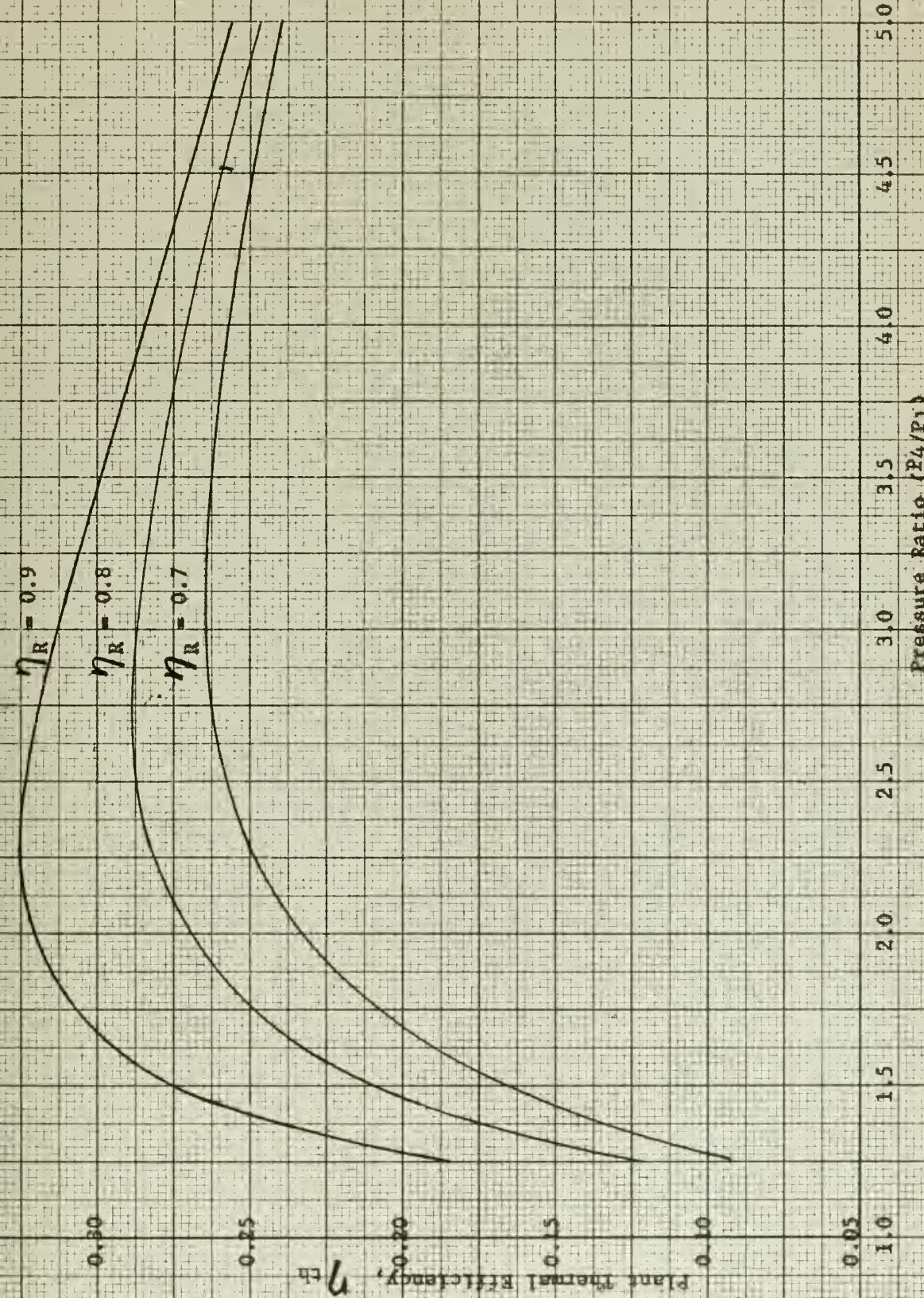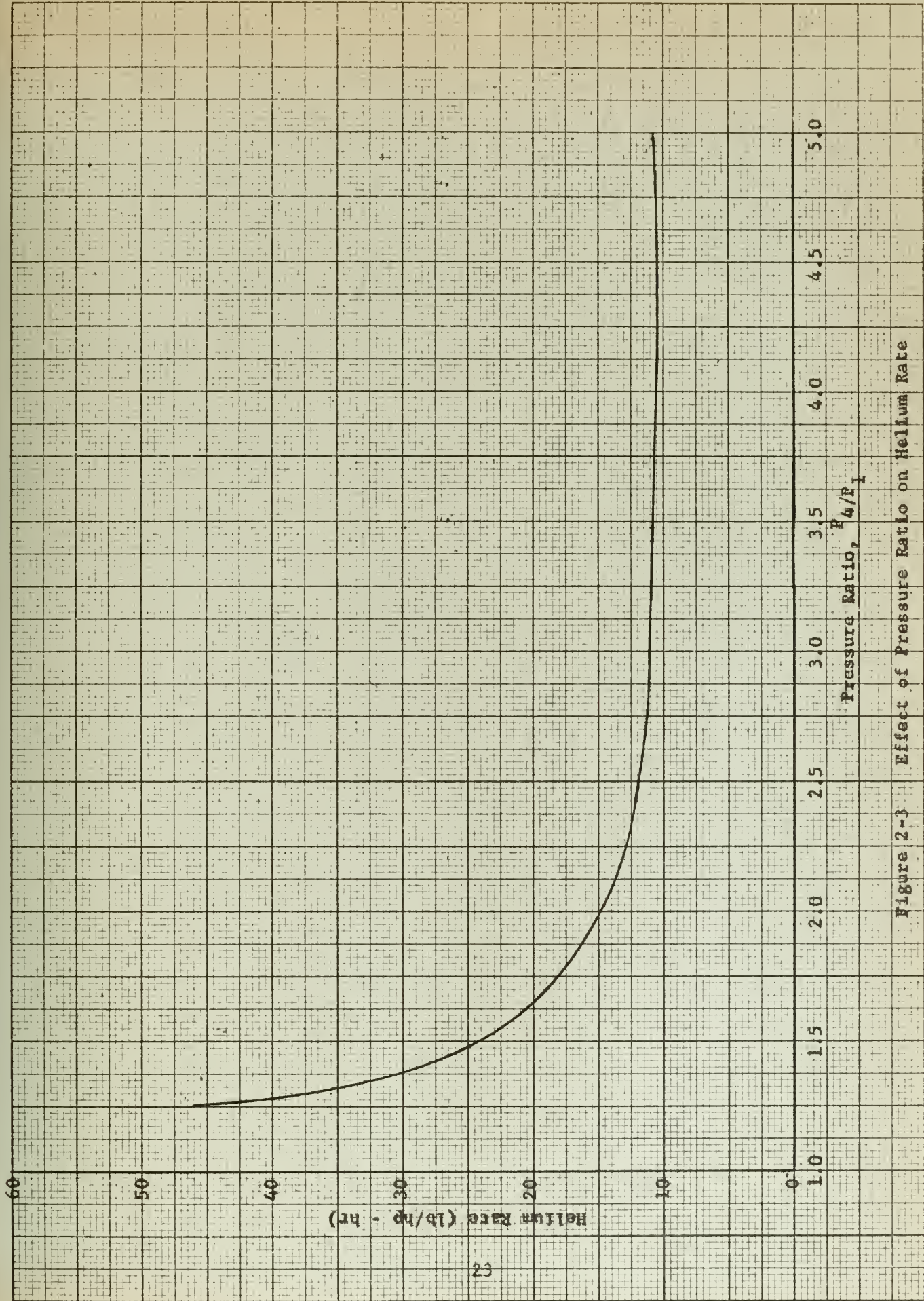
Figure 2-3   Effect of Pressure Ratio on Helium Rate

Pressure Ratio, P_4/P_1

Helium Rate (lb/hp - hr)

23

Figure 2-4   Effect of Pressure Ratio on Work Ratio

24
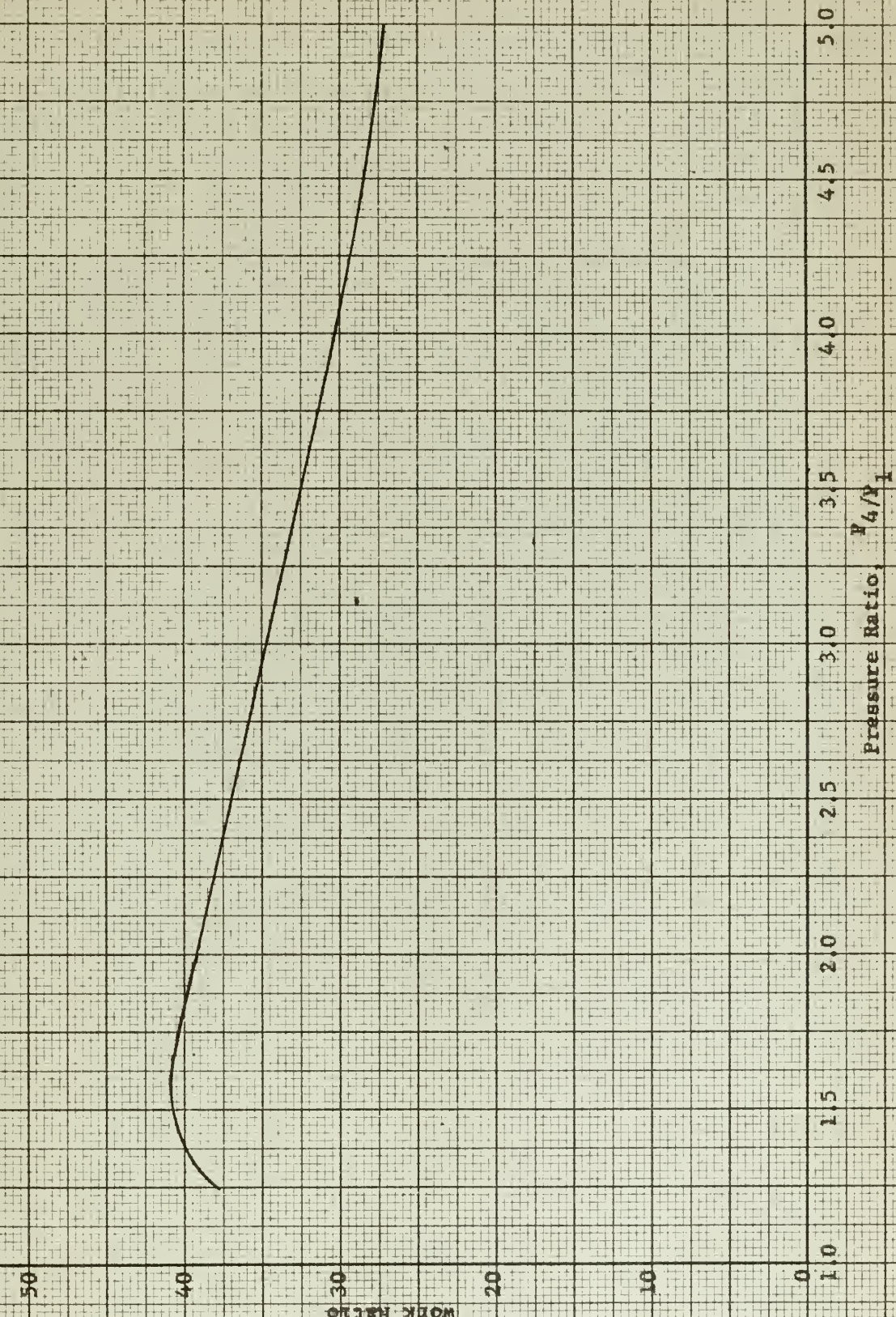
CHAPTER III

HEAT EXCHANGERS

Symbols used in this chapter:

Symbol	Description	Units
A	heat transfer area per tube	ft^2
a	free flow area per tube	ft^2
a_t	frontal area per tube	ft^2
a	fin longitudinal length	in.
c	fin thickness	in.
c_p	specific heat at constant pressure	BTU/lb - °F
D	heat exchanger shell inside diameter	ft
D_h	hydraulic diameter	ft
d	tube diameter	in.
h	convection heat transfer coefficient	BTU/ft^2 - hr - °F
k	thermal conductivity	BTU/ft^2 - hr - °F/ft
L	heat exchanger tube length	ft
λ	fin radial length	in.
m	(defined by equation 3-10a, page 33)	----
$\dot{m}$	mass rate of flow	lb/sec
N	total number of tubes	----
Nu	Nusselt number	----
P	pressure	psia
Pr	Prandtl number	----
Re	Reynolds number	----
s	tube center to center spacing	in.

Symbol	Description	Units
t	temperature	°F
U	overall heat transfer coefficient	BTU/ft^2 - hr - °F
V	velocity	ft/sec
v	specific volume	ft^3/lb
W	ratio $\dfrac{(\dot{m}\,c_p)_c}{(\dot{m}\,c_p)_h}$	----
δ	wall thickness or boundary length thickness	in.
Δ	increment	----
ζ	friction factor	----
η_f	fin efficiency	----
η_o	fin temperature effectiveness	----
μ	absolute viscosity	lb/hr - ft
ρ	density	lb/ft^3
ϕ	dimensionless overall heat transfer coefficient	----
ψ	dimensionless convection heat transfer coefficient	----
Ω	ratio of heat transfer areas, $\dfrac{A_c}{A_h}$	----
Φ	ratio of fluid flow areas, $\dfrac{a_c}{a_h}$	----

Subscript	Definition
c	cold fluid
e	exit
f	fin
h	hot fluid

26

Subscript	Definition
i	inlet, inside, or initial
o	outside
t	tube
w	wall

General

Having selected a pressure ratio of 2.25 from the preliminary analysis, the components will now be more closely investigated to determine if they can be of practical design. Since one of the more important requirements is the size of the plant, a design study of the regenerator, intercooler and precooler is necessary. Before going into this study, some review of heat transfer theory as used herein may be advantageous.

Heat Transfer Theory

In the usual type of heat exchanger heat transfer occurs between two fluids of different temperatures separated by a wall of finite thickness. The quantity of heat, dQ, transmitted through an element of area, dA, can be expressed as:

$$\frac{dQ}{dA} = U\left(t_h - t_c\right) \qquad (3\text{-}1)$$

where U is the overall heat transfer coefficient associated with area dA.

If the wall surface is a plane, i.e., no extended surface:

$$\frac{1}{UA} = \frac{1}{A_h h_h} + \frac{\delta}{A_w k} + \frac{1}{A_c h_c} \qquad (3\text{-}2)$$

27

If $U = U_h$: $A = A_h$

$$\frac{1}{U_h} = \frac{1}{h_h} + \frac{\delta}{\frac{A_w}{A_h}k} + \frac{1}{\frac{A_c}{A_h}h_c} \qquad (3\text{-}2a)$$

Kays[4] has modified (3-2a) to include extended surfaces on both sides of the wall:

$$\frac{1}{U_h} = \frac{1}{\eta_{o_h}h_h} + \frac{\delta}{\frac{A_w}{A_h}k} + \frac{1}{\frac{A_c}{A_h}\eta_{o_c}h_c} \qquad (3\text{-}3)$$

where $\eta_{o_h} A_h$ = effective surface area on hot side

and $\eta_{o_c} A_c$ = effective surface area on cold side.

For thin walled surfaces the term $\dfrac{\delta}{\frac{A_w}{A_h}k}$ is negligible:

$$\frac{1}{U_h} = \frac{1}{\eta_{o_h}h_h} + \frac{1}{\frac{A_c}{A_h}\eta_{o_c}h_c} \qquad (3\text{-}3a)$$

Combining the techniques of Kays and Traupel[5] it is convenient to change (3-3a) to a dimensionless form:

$$\frac{1}{\phi_h} = \frac{1}{\eta_{o_h}\psi_h} + \frac{\Phi}{\eta_{o_c}\psi_c\, W\,\Omega} \qquad (3\text{-}4)$$

where $\phi \equiv \dfrac{U}{\rho c_p V} \qquad (3\text{-}4a)$

28

$$\gamma \equiv \frac{h}{\rho c_p V} \qquad \text{(also known as Stanton Number)} \qquad \text{(3-4b)}$$

$$W \equiv \frac{(\dot{m} c_p)_c}{(\dot{m} c_p)_h} \qquad \text{(3-4c)}$$

$$\Phi \equiv \frac{a_c}{a_h} \qquad \text{(3-4d)}$$

$$\Omega \equiv \frac{A_c}{A_h} \qquad \text{(3-4e)}$$

Considering the hot fluid only, the heat loss, dQ, for a temperature change dt can be expressed as:

$$dQ_h = -(\dot{m} c_p)_h \, dt_h = -(\rho \, a \, V c_p)_h \, dt_h \qquad \text{(3-5)}$$

Combining (3-5) with (3-1):

$$\phi_h \frac{dA_h}{a_h} = -\frac{dt_h}{t_h - t_c} \qquad \text{(3-6)}$$

If we assume that the configuration and dimensions of the heat exchanger elements do not change along the direction of the flow, then $dA_h = \frac{A_h}{L} dx$, where x is a lengthwise coordinate, L is length of the surface and A_h is the total hot side area. Integrating equation (3-6):

$$\int_0^L \frac{\phi_h A_h}{a_h L} \, dx = -\int_{t_i}^{t_e} \frac{1}{t_h - t_c} \, dt_h \qquad \text{(3-7)}$$

29

or

$$\frac{A_h}{Q_h} \int_0^l \phi_h \, d\left(\frac{x}{L}\right) = - \int_{t_i}^{t_e} \frac{1}{t_h - t_c} \, dt_h \qquad (3\text{-}7a)$$

ϕ_h will change as the fluid flow proceeds along the surface and its function of x must be known before the integral can be evaluated. Likewise, t_h - t_c changes and its function of t_h must be known. Usually these functions are not known and it is common practice to simplify (3-7) as follows:

$$\frac{A_h}{Q_h} \overline{\phi}_h = \frac{(t_i - t_e)_h}{\overline{\Delta t}} \qquad (3\text{-}7b)$$

where $\quad \overline{\phi}_h \equiv \int_0^l \phi_h \, d\left(\frac{x}{L}\right)$

and $\quad \overline{\Delta t} \equiv - \dfrac{t_i - t_e}{\displaystyle\int_{t_i}^{t_e} \frac{1}{t_h - t_c} \, dt_h}$

Bowman, Mueller and Nagle[6] have determined relations for $\overline{\Delta t}$ for many types of heat exchangers. For the longitudinal counter-flow exchanger $\overline{\Delta t}$ is the familiar log mean temperature difference:

$$\overline{\Delta t} = \frac{(t_{h_i} - t_{c_e}) - (t_{h_e} - t_{c_i})}{\ln \dfrac{(t_{h_i} - t_{c_e})}{(t_{h_e} - t_{c_i})}} \qquad (3\text{-}8)$$

Close approximation is obtained if $\overline{\phi}$ is evaluated by equation (3-4) using average values of ψ_c and ψ_h.

Up to this point the type of extended surface has not been speci-
fied. Once this is specified there remains the problem of evaluating
η_o.

η_o A has been defined as the effective heat transfer area. For a
finned surface this effective area can be expressed as the sum of the
wall area A_W (not including fin base), and an effective fin area.
From the definition of fin efficiency, η_f, this effective fin area is
$\eta_f A_f$ where A_f is the total surface area of the fin.

$$\eta_o A = A_w + \eta_f A_f$$

$$A_w = A - A_f$$

$$\therefore \; \eta_o = 1 - \frac{A_f}{A}\left(1 - \eta_f\right) \tag{3-9}$$

For several types of fins the solutions for η_f are known.
(Gardner[7])

As an example, for a bar fin of constant thickness shown in
Figure 3-1:
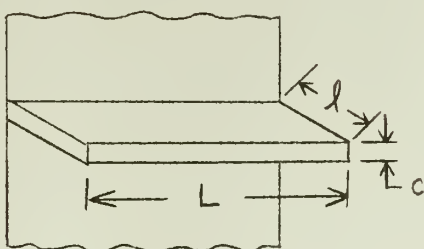
Figure 3-1

$$\eta_f = \frac{\tanh(m\ell)}{m\ell} \tag{3-10}$$

$$\text{where} \quad m = \sqrt{\frac{2h(L+c)}{k_f L c}}$$

31

$$\text{If } \quad L >> c : \quad m = \sqrt{\frac{2h}{k_f c}} \tag{3-10a}$$

It is noted that Gardner's solutions for η_f are based on several assumptions. Of these, the following may result in appreciable error:

  (1) The heat transfer coefficient, h, is uniform over the
      entire fin surface.

  (2) The temperature of the base of the fin is uniform.

  (3) Temperature gradients normal to the fin surface are
      neglected.

  (4) Heat transfer through the outermost end is negligible.

The only type of heat exchanger involved in this investigation is tubular with external fins. By introducing the hydraulic diameter, D_h:

$$D_h \equiv \frac{4\, a_h}{A_h / L} \tag{3-11}$$

equation (3-7b) becomes:

$$\frac{L}{D_h} = \frac{1}{4\, \overline{\Phi}_h} \left[\frac{(t_i - t_e)_h}{\Delta t} \right] \tag{3-12}$$

The above equation will be one of the principal equations employed in this investigation for design of the heat exchangers.

Pressure Drops

Fluid pressure drop in the heat exchanger must be considered in addition to heat transfer aspects. It has been found both experimen-tally and analytically that the two are interdependent. Improvement in

32

heat transfer characteristics results in increased pressure drop, so a
compromise has to be made in most designs. The relation used by
Traupel[5], McAdams[8] and others for longitudinal flow inside of tubes
is:

$$\Delta P = \zeta \, \frac{L}{d_i} \, \frac{V^2}{2 g V} \qquad (3\text{-}13)$$

where ζ is the coefficient of resistance. It is identical to $4f$
in McAdams.

For turbulent flow through smooth tubes[8]:

$$\zeta = 0.184 \, Re^{-0.2} \qquad (3\text{-}14)$$

$$5000 < Re < 500{,}000$$

Similarly, for determining pressure drop outside of the tubes (on
finned side), equation (3-13) and (3-14) are applicable if the diameter
is replaced by an equivalent diameter:

$$D_{eq} = \frac{4 \times free \ flow \ area}{wetted \ perimeter} \approx \frac{4 a_h}{A_\eta / L} \qquad (3\text{-}11a)$$

The difference between D_h and D_{eq} is that D_{eq} includes the wetted
perimeter of the exchanger shell. The error in assuming $D_h = . D_{eq}$ is
small for most heat exchangers.

In addition to the pressure drops due to pipe friction there are
static pressure changes due to acceleration or deceleration of the flow
at the heat exchanger ends and changes in specific volume. Since these

33

effects depend on pipe sizes, types of headers, etc., they are left for further discussion in Chapter VII.

Correlation of Heat Transfer and Pipe Friction

Equation (3-4b) can be expressed in terms of other dimensionless quantities as follows:

$$\gamma = \frac{Nu}{Re \cdot Pr} \tag{3-15}$$

where $Nu \equiv \dfrac{hd}{K}$ (Nusselt No.) (3-15a)

$$Pr \equiv \frac{c_p \mu}{K} \qquad \text{(Prandtl No.)} \quad \text{(3-15b)}$$

$$Re \equiv \frac{dV}{\mu v} \qquad \text{(Reynolds No.)} \quad \text{(3-15c)}$$

For turbulent flow inside of tubes according to McAdams[8]:

$$Nu = 0.023 \, Re^{0.8} \cdot Pr^{0.4} \tag{3-16}$$

Equation (3-16) can be used for turbulent flow outside of tubes providing that the hydraulic diameter is used in lieu of d.

From equations (3-14), (3-15) and (3-16):

$$\gamma = \frac{\zeta}{8 \, Pr^{0.6}} \tag{3-17}$$

To summarize, the principal working equations for tubular heat

exchangers having longitudinal fins are:

$$\frac{L}{D_h} = \frac{1}{4} \frac{(t_i - t_e)_h}{\Delta t} \left[\frac{1}{\eta_{o_h} Y_h} + \frac{\Phi}{Y_c W \Omega} \right] \qquad (3\text{-}12)$$

$$\Delta P = \zeta \frac{L}{d_i} \frac{V^2}{2gV} \qquad (3\text{-}13)$$

Type of Heat Exchanger

The feasibility of this cycle depends to a large extent on the size of the three heat exchangers; namely, regenerator, precooler and intercooler. By far the largest of these will be the regenerator. For an ordinary shell and circular tube regenerator analysis reveals that to satisfy the pressure drop and size limitations extremely small tubes (less than 0.2 in. diameter) placed very close together (less than 0.3 in. center to center) are required.

Construction difficulties, if the above dimensions were specified, would be of sufficient severity to render the design impractical. However, the addition of longitudinal fins to the exterior walls of the tubes in this type of heat exchanger will cause a salutory effect. Analysis reveals that tube size and spacing may be increased, and the total number of tubes decreased. Although this may not be as good a design as could be obtained by employment of more compact surfaces such as were investigated by Kays, London and Johnson[4] the reduced complexity in design and analysis warrants its use here.

A similar design is investigated for the precooler and intercooler,

35

the difference being in dimensions. In all cases, the hotter fluid is outside the tubes (on the finned side). Figures 3-3 and 3-4 show the finned tubes and tube arrangement respectively. Although the analysis assumes that the fins extend the entire length, L, of the tube, boundary layer buildup between the fins will require the use of several shorter fins staggered along the tube. This has been discussed by Gloyer[9] with the conclusion that the minimum fin spacing should be not less than one boundary layer thickness,   .
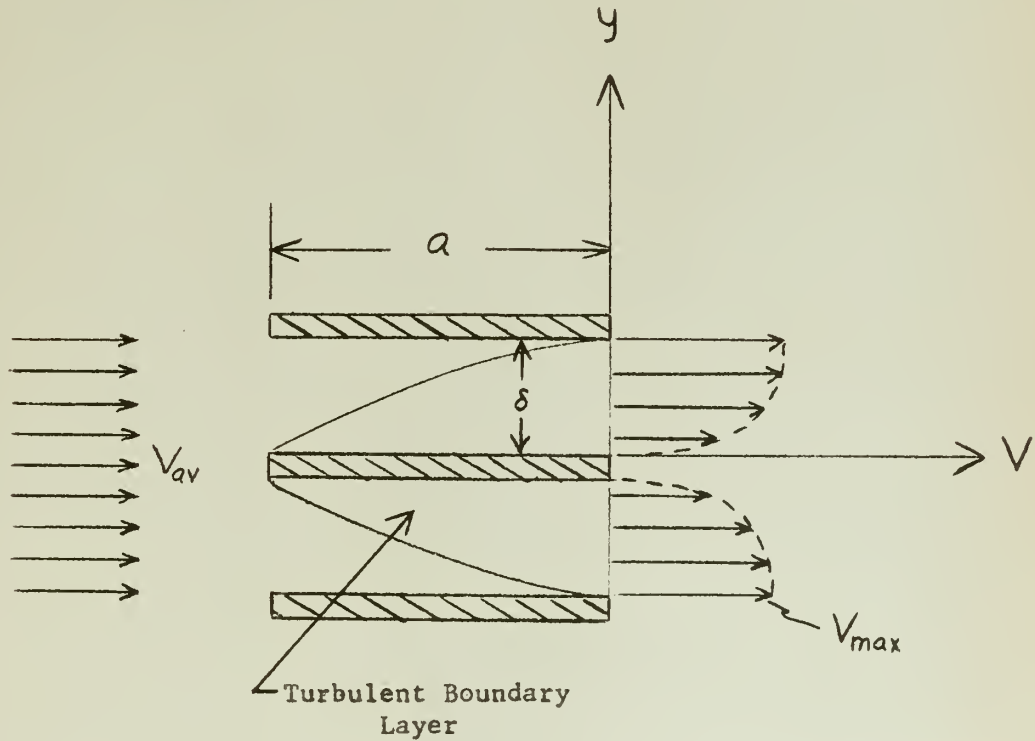
Figure 3-2

Von Karman's[10] equation for turbulent boundary layer thickness, δ, is:

$$\delta = 0.1183 \, a^{4/5} \left(\frac{\nu \mu}{V_{max}} \right)^{1/5} \; in. \qquad (3-18)$$

36
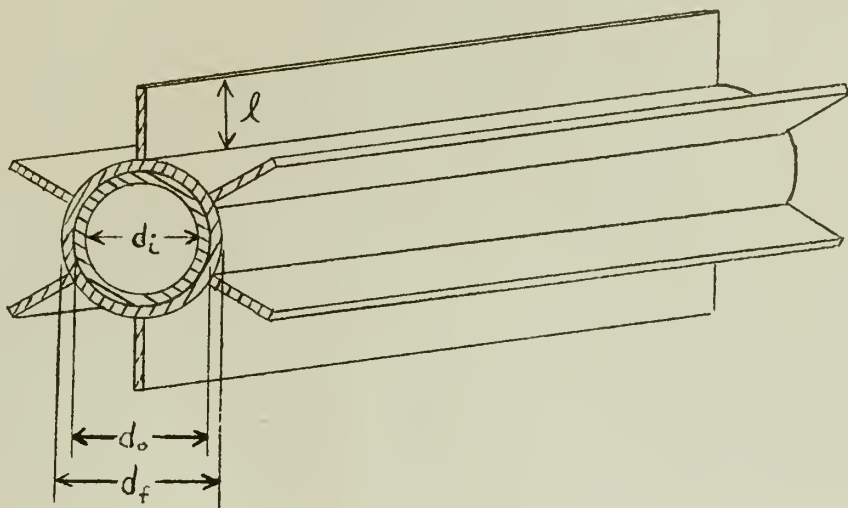
Figure 3-3   Heat Exchanger Tube
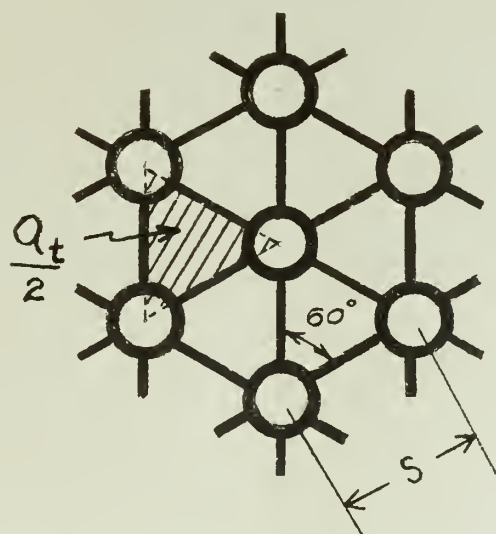
Figure 3-4   Tube Arrangement

37

For moderate Re:

$$\frac{V_{av}}{V} = \left(\frac{y}{\delta}\right)^{1/7} \tag{3-19}$$

$$V_{max} = \frac{8}{7} V_{av} \tag{3-19a}$$

In all three heat exchangers the tubes will have six longitudinal brass fins ($k_f \approx 60 \dfrac{BTU}{ft^2 - hr - °F/ft}$). For good heat transfer the fins must have good metal-to-metal contact with the tube. The assembly shown in Figure 3-3 consists of two concentric tubes, the outer one having the six external fins. These outer tubes will be quite short (six to ten inches) and could be made in one machine shop operation. These would then have to be brazed to the inner tube in a manner to insure intimate contact.

In this analysis it has been found convenient to employ areas associated with one tube. For the equi-angular arrangement that has been selected, the frontal area per tube, Q_t, is equal to twice the area of one of the triangles formed by the centers of three adjacent tubes. The formulas for this and other areas are:

$$\frac{A_h}{L} = \left[\pi d_f + 6(2\ell - c)\right]\frac{1}{12} \quad \frac{ft^2}{ft} \tag{3-20}$$

$$\frac{A_c}{L} = \frac{\pi d_i}{12} \quad \frac{ft^2}{ft} \tag{3-21}$$

$$\frac{A_f}{L} = \frac{12\ell}{12} = \ell \quad \frac{ft^2}{ft} \tag{3-22}$$

38

$$Q_c = \frac{\pi d_i^2}{4 \times 144} \quad ft^2 \tag{3-23}$$

$$Q_t = \frac{s^2 \sin 60°}{144} \ ft^2 \tag{3-24}$$

$$Q_h = Q_t - \left[\frac{\pi d_f^2}{4} + 6Lc\right]\frac{1}{144} \ ft^2 \tag{3-25}$$

Other equations which are used in the analysis are:

$$\frac{V_c}{V_h} = \frac{Q_h V_c \dot{m}_c}{Q_c V_h \dot{m}_h} \tag{3-26}$$

$$D^2 = \frac{4 Q_t N}{\pi} \quad ft^2 \tag{3-27}$$

$$N = \frac{m_h V_h}{Q_h V_h} = \frac{m_c V_c}{Q_c V_c} \tag{3-28}$$

39
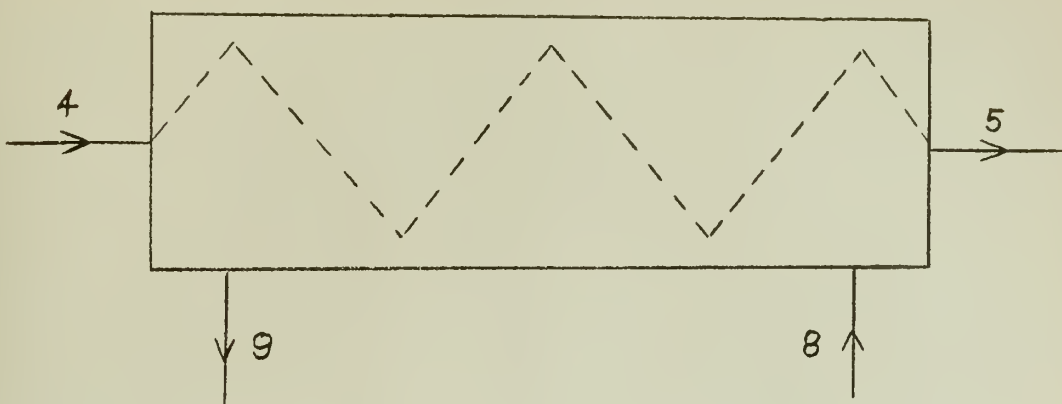
Regenerator

Figure 3-5   Schematic Representation of the Regenerator

TABLE 3-1

PROPERTIES OF HELIUM ENTERING AND LEAVING REGENERATOR

Location (Fig. 3-5)	t (°F)	P (psia)	h (BTU/lb)	v (ft³/lb)
4	224.9	1000	361.9	1.883
5	874.8	985	1667.8	3.677
8	951.3	452.2	1757.3	8.413
9	301.5	447.7	951.4	4.606

$\dot{m}$ = 182.4 lb/sec

$\overline{\Delta t}$ = 76.6 °F

40

Since this analysis is based on average values of such quantities as v, c_p, k, μ, Re, Pr, ψ, and ϕ, they are evaluated at the arithmetic mean temperatures. To distinguish the hotter fluid outside the tubes from the cooler fluid inside the tubes the terms "hot side" and "cold side" will be used henceforth.

TABLE 3-2

AVERAGE PROPERTIES OF FLUIDS IN THE REGENERATOR

Quantity	Hot Side	Cold Side	Units
t	626.4	549.8	°F
v	6.510	2.780	ft^3/lb
k	0.138	0.132	BTU/ft^2 - hr - °F/ft
μ	0.0759	0.0725	lb/hr - ft
Pr	0.681	0.680	----
c_p	1.24	1.24	BTU/lb - °F

Precooler

The basic difference between the regenerator and the precooler is that the fluid inside the tubes for the latter is sea water rather than helium. The heat transmitted to the water is lost, but the lower temperature for compression results in less compressor work required, and because of the higher temperature differential in the regenerator, in a higher overall cycle efficiency. The precooler, as in the case of the regenerator, consists of externally finned circular tubes with single pass counterflow. The tubes and tube arrangement are also the same as in the regenerator with a slight modification of dimensions.

41
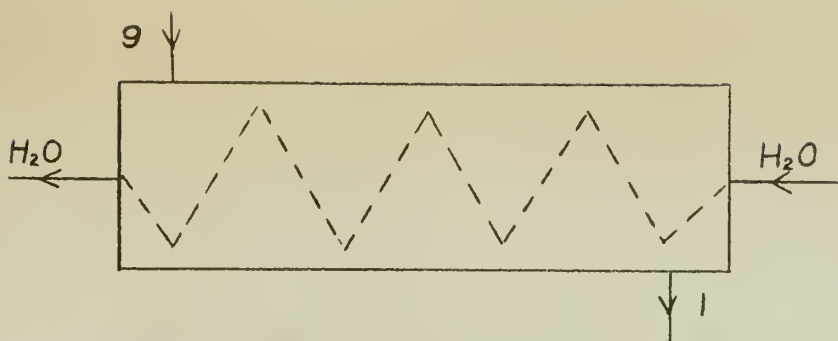
Figure 3-6   Schematic Representation of the Precooler

TABLE 3-3

PROPERTIES OF FLUIDS ENTERING AND LEAVING PRECOOLER

Location	t (°F)	P (psia)	h (BTU/lb)	v (ft^3/lb)
1	100	444.4	701.5	3.428
9	301.5	447.7	951.4	4.607
H$_2$O in	60	----	----	.01604
H$_2$O out	90	----	----	.01610

$$\dot{m}_h = 182.4 \text{ lb/sec}$$

$$\overline{\Delta t} = 103 \text{ °F}$$

TABLE 3-4

AVERAGE PROPERTIES OF FLUIDS IN THE PRECOOLER

Quantity	Helium	H$_2$O	Units
t	200.8	75	°F
v	4.018	0.01607	ft^3/lb
μ	0.0558	2.22	lb/hr - ft
c_p	1.24	1.0	BTU/lb - °F
k	0.10	0.346	BTU/ft^2 - hr - °F/ft
Pr	0.692	6.42	----

42
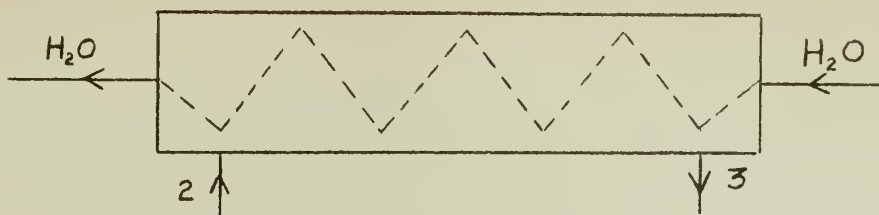
Figure 3-7   Schematic Representation of the Intercooler

TABLE 3-5

PROPERTIES OF FLUIDS ENTERING AND LEAVING INTERCOOLER

Location	t (°F)	P (psia)	h (BTU/lb)	v (ft^3/lb)
2	216.9	666.7	848.8	2.768
3	100	663.4	703.7	2.309
H_2O in	60	----	----	0.01604
H_2O out	90	----	----	0.01610

$$\dot{m}_h = 182.4 \text{ lb/sec}$$

$$\overline{\Delta t} = 75.4 \text{ °F}$$

TABLE 3-6

AVERAGE PROPERTIES OF FLUIDS IN THE INTERCOOLER

Quantity	Helium	H_2O	Units
t	158.5	75	°F
v	2.538	0.01607	ft^3/lb
μ	0.0532	2.22	lb/hr - ft
c_p	1.24	1.0	BTU/lb - °F
k	0.096	0.346	BTU/ft^2 - hr - °F/ft
Pr	0.687	6.42	----

Selection of Tube Dimensions

The dimensions that appear in Table 3-7 are the result of many trial and error calculations. There are, no doubt, other combinations which will produce equally good results. It is intended that the ones used here represent a reasonable design for this cycle.

Calculations

Values in Tables 3-8 and 3-9 were obtained from substitution of known and assumed quantities into equations outlined earlier in this chapter. It can be seen that there occur several relations and variables. However, there is only one independent variable and it is convenient to choose V_h as this variable. Figures 3-8, 3-9, and 3-10 show the variation of ΔP, L, D and total volume with V_h for the three units.

The final selection of V_h depends on how large a pressure drop and/or size can be tolerated. The choices of V_h and the corresponding heat exchanger dimensions listed in Table 3-11 are based on the values assumed for $\Delta P/P_i$ in Chapter II. A knowledge of end effects was necessary to make the selection since in some cases the ΔP due to the end effects is larger than ΔP due to pipe friction. This is covered in more detail in Chapter VII.

TABLE 3-7

TUBE DIMENSIONS

	Regenerator	Intercooler	Precooler	Units
d_i	0.30	0.40	0.40	in.
d_o	0.35	0.50	0.50	"
d_f	0.40	0.60	0.60	"
ℓ	0.20	0.20	0.20	"
c	0.025	0.05	0.05	"
s	0.80	1.00	1.00	"

TABLE 3-8

HEAT EXCHANGER AREAS AND ASSOCIATED QUANTITIES

	Regenerator	Intercooler	Precooler	Units
$A_{h/L}$	0.2922	0.3321	0.3321	ft^2/ft
$A_{c/L}$	0.07854	0.1047	0.1047	"
$A_{f/L}$	0.20	0.20	0.20	"
a_h	0.00277	0.00363	0.00363	ft^2
a_c	0.000491	0.000873	0.000873	"
a_t	0.003849	0.006014	0.006014	"
D_h	0.0379	0.0437	0.0437	ft
Φ	0.1774	0.2405	0.2405	----
Ω	0.2688	0.3152	0.3152	----
W	1.0	3.897	6.717	----

45

TABLE 3-9

LIST OF CONSTANTS FOR THE REGENERATOR, PRECOOLER AND INTERCOOLER

Quantity *	Regenerator	Precooler	Intercooler	Reference Equation
V_c/V_h	2.407	0.1388	0.127	(3-26)
Re_h/V_h	276.1	700	1165	(3-15c)
Re_c/V_c	446.5	3360	3360	(3-15c)
$h_h/\psi_h V_h$	685.7	1110	1759	(3-4b)
$h_c/\psi_c V_c$	1605.7	224,000	224,000	(3-4b)
ψ_h/ζ_h	0.1575	0.1558	0.1566	(3-17)
ψ_c/ζ_c	0.1575	0.04098	0.04098	(3-17)
$m\ell/N_{h_h}$	0.0667	0.0471	0.0471	(3-10a)
$\Delta P_h/L\zeta_h V_h^2$	4.365×10^{-4}	6.14×10^{-4}	9.73×10^{-4}	(3-13)
$\Delta P_c/L\zeta_c V_c^2$	15.53×10^{-4}	2010×10^{-4}	2010×10^{-4}	(3-13)
$L \cdot \phi_h$	0.0805	0.02137	0.01694	(3-12)
D^2/N	0.00490	0.00765	0.00765	(3-27)
NV_h	4.288×10^5	2.02×10^5	1.2753×10^5	(3-28)

* all units are as indicated in the list of symbols at the beginning of the Chapter.
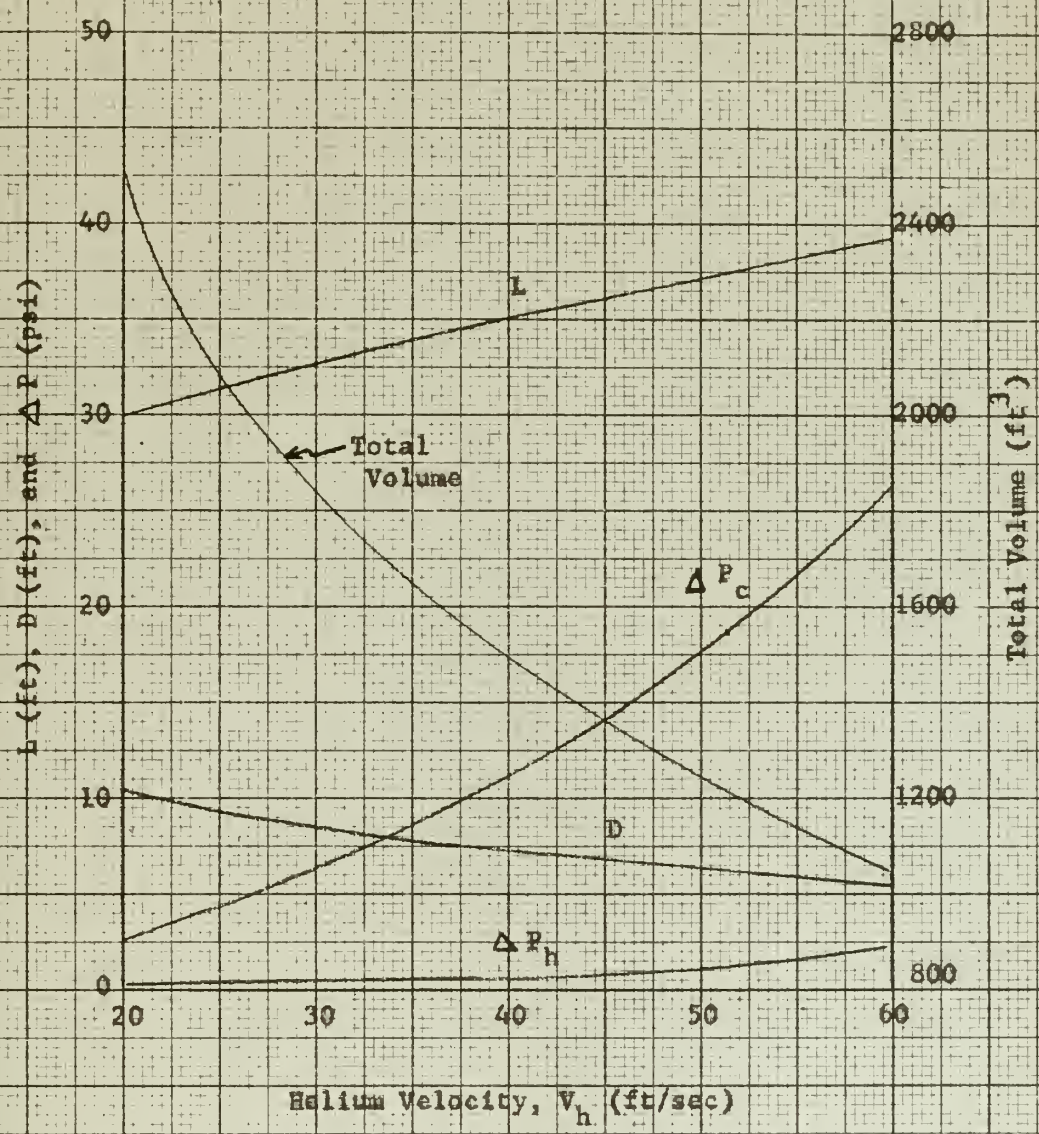
Figure 3-8   Variation of Regenerator Characteristics
with Average Helium Velocity
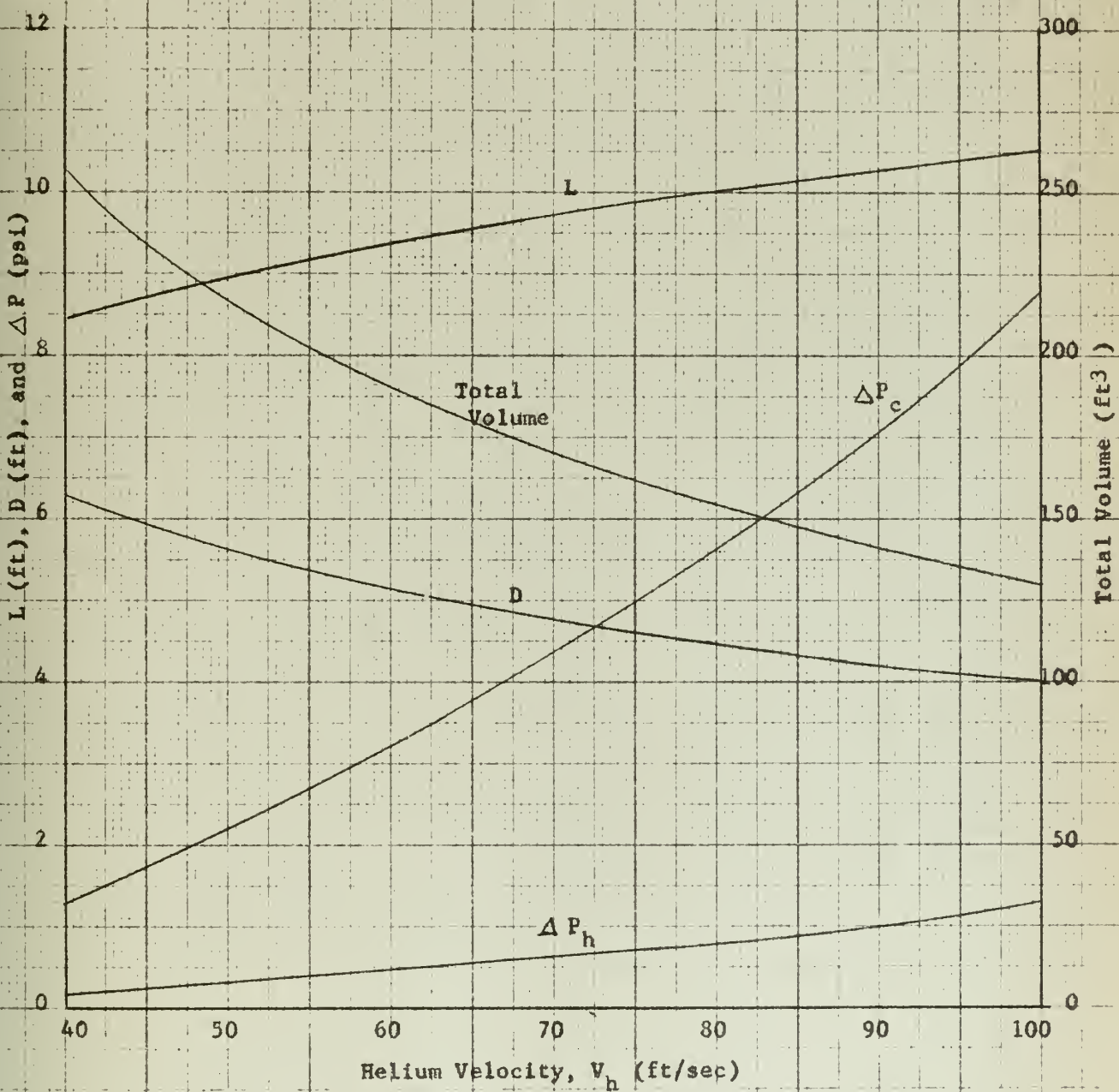
Figure 3-9   Variation of Precooler Characteristics with Average
Helium Velocity
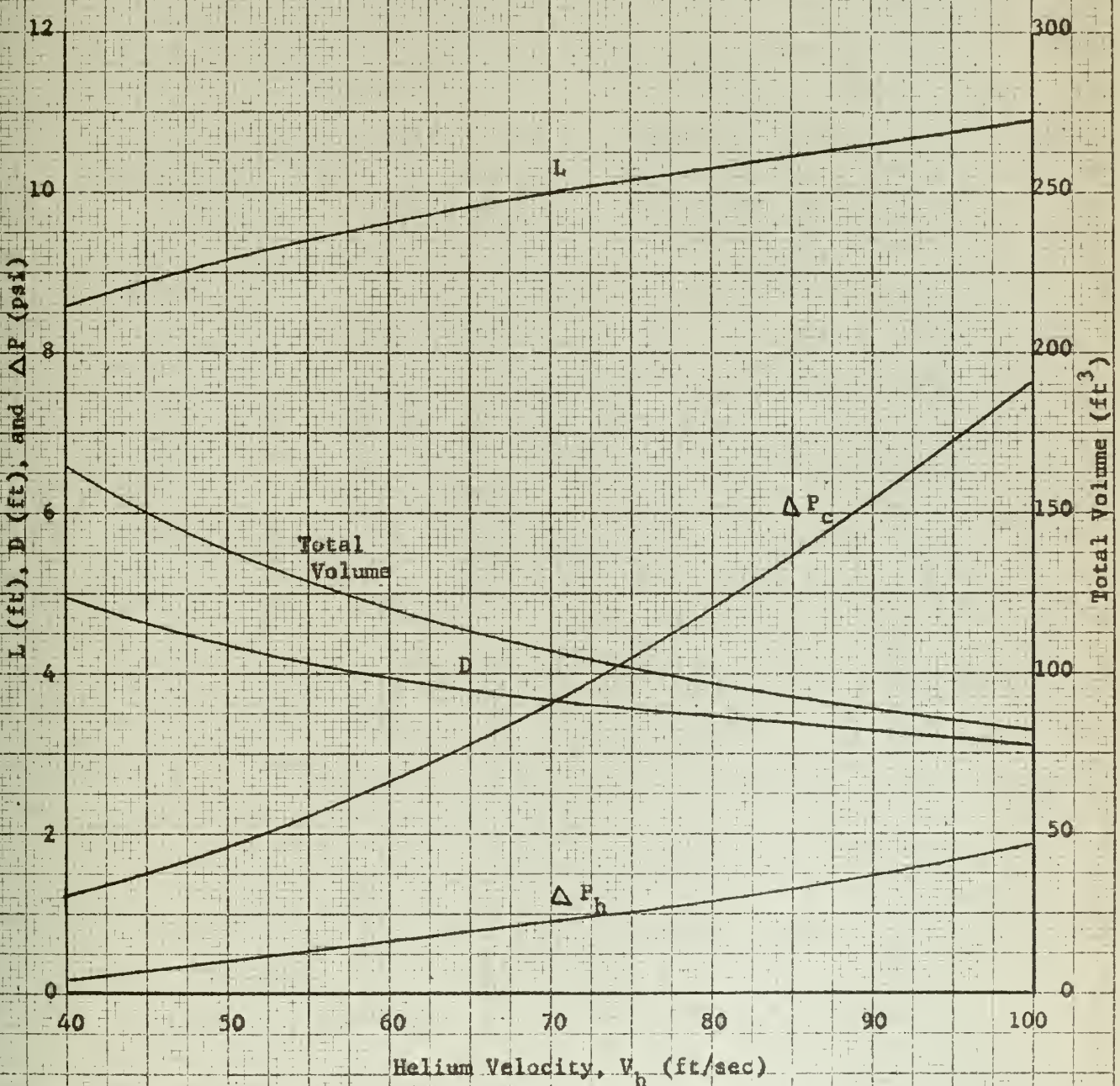
Figure 3-10 — Variation of Intercooler Characteristics with Average Helium Velocity

TABLE 3-10

DATA FOR SELECTED HEAT EXCHANGERS

	Regenerator	Precooler	Intercooler	Units
V_h	41.5	75	75	ft/sec
V_c	100	10.4	9.5	"
L	35.7	9.9	10.2	ft
D	7.19	4.52	3.61	"
N	10,330	2690	1700	Tubes
Volume	1450	161	104	ft^3
ΔP_h	0.76	0.715	1.05	psi
ΔP_c	12.03	4.87	4.17	"
a	10.6	21.4	24.5	in.

CHAPTER IV

COMPRESSORS

Symbols used in this chapter:

Symbol	Description	Units
A	annulus area	in.^{2}
C	force coefficient	---
c	chord	in.
c_p	specific heat at constant pressure	BTU/lb - °F
D	ratio $\dfrac{\text{Last stage isentropic enthalpy change}}{\text{First stage \quad " \qquad " \qquad "}}$	---
d	diameter	in.
F	blade force	lb_f
f	reheat factor	---
g	conversion factor, 32.17	$\dfrac{lb_m}{lb_f}\dfrac{ft}{sec^2}$
H	total enthalpy	BTU/lb
h	static enthalpy	BTU/lb
or	blade height	in.
J	conversion factor, 778	$\dfrac{ft - lb}{BTU}$
L	ratio $\dfrac{\text{last stage actual enthalpy change}}{\text{first } \quad " \qquad " \qquad " \qquad "}$	---
$\dot{m}$	mass flow	lb/sec
N	rotational speed	rpm
n	no. of stages	---
P	pressure	psia
r	radius	in.

Symbol	Description	Units
s	entropy	BTU/lb - °F
or	blade spacing	in.
T	absolute temperature	°R
U	peripheral velocity	ft/sec
V	absolute velocity	ft/sec
v	specific volume	ft^3/lb
W	relative velocity	ft/sec
α	absolute flow angle	degrees
β	relative flow angle	degrees
Δ	increment	---
ϵ	drag force/lift force	---
η	efficiency	---
ρ	density	lbs/ft^3
τ	defined by equation (4-8)	---
ϕ	defined by equation (4-7)	---
χ	degree of reaction	---
ω	rotational speed	rad/sec

Subscript	Description
C	compressor
c	center, mean
D	drag
DP	drag profile
e	exit
i	inlet, initial

Subscript	Description
L	lift
m	axial
n	last stage
R	rotor, relative
S	stator
s	stage, isentropic
th	theoretical
u	tangential
x	arbitrary stage

General

Before proceeding with a design study of the two compressors, the type of compressors must be selected. From Table 2-2 the energy imparted to the gas in the two compressors is 147.3 and 158.2 BTU/lb respectively. Analysis reveals that each compressor, if centrifugal, would consist of two or more stages in order to prevent excessive peripheral speeds. Rather than employ several centrifugal stages where efficiencies are usually low due to losses occurring between stages, two axial flow compressors have been selected.

The flow channel associated with an axial flow compressor is illustrated in Figure 4-1 and the corresponding h-s diagram in Figure 4-2.
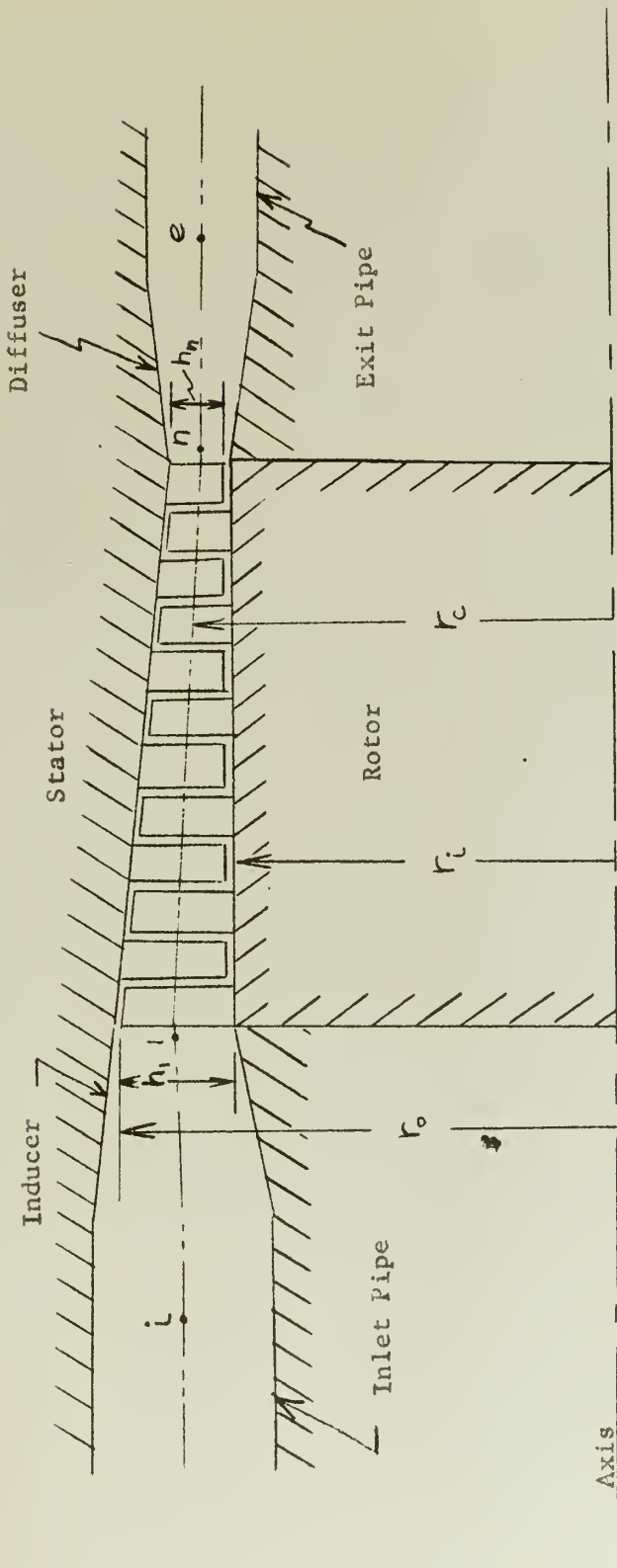
Figure 4-1   Schematic Representation of an Axial Flow Compressor

54
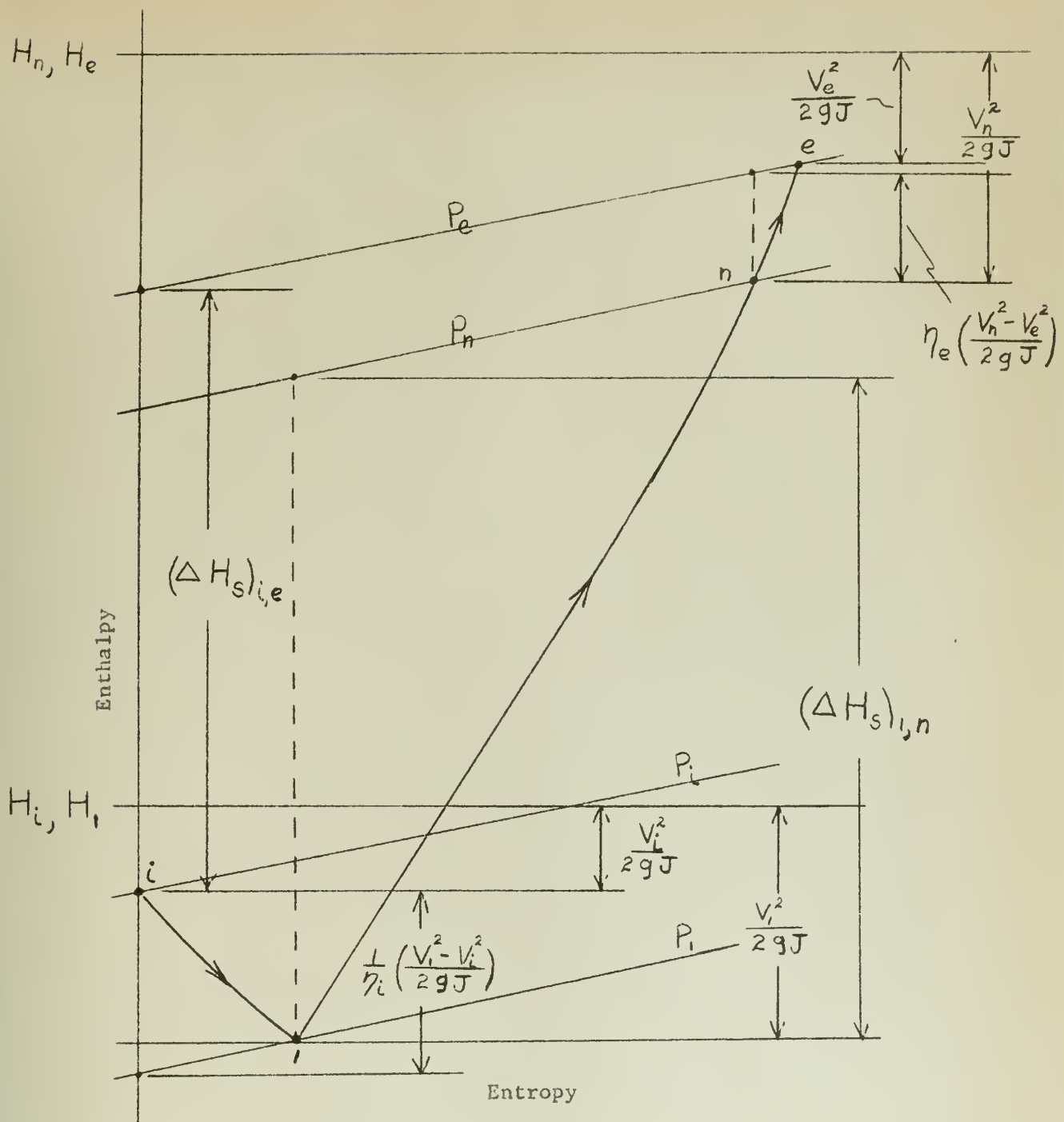
Figure 4-2   Typical Enthalpy-Entropy Diagram for an Axial
Flow Compressor

55

From Figure 4-2, where it is assumed that the flow in the inducer and diffuser sections is steady and adiabatic, the following equations are obtained if geopotential energy differences are ignored:

$$H = \frac{V^2}{2gJ} + h \qquad = \text{constant} \qquad (4-1)$$

$$\eta_i \equiv \frac{(\Delta h)_{i,1}}{(\Delta h_s)_{i,1}} \qquad (4-2)$$

$$\eta_e \equiv \frac{(\Delta h_s)_{n,e}}{(\Delta h)_{n,e}} \qquad (4-3)$$

$$\left(\Delta H_s\right)_{1,n} = \left(\Delta H_s\right)_{i,e} + \frac{1}{\eta_i}\left(\frac{V_1^2 - V_i^2}{2gJ}\right) - \eta_e\left(\frac{V_n^2 - V_e^2}{2gJ}\right) \qquad (4-4)$$

$$\left(\Delta H\right)_{1,n} = \left(\Delta H\right)_{i,e} + \frac{V_1^2 - V_i^2}{2gJ} - \frac{V_n^2 - V_e^2}{2gJ} \qquad (4-4a)$$

Compressor Stage Performance

Before the compressor design can be carried out the type of stage must be selected. In this design only one type of stage was considered; namely, a non-symmetric stage where the absolute velocity entering the rotor is axial. Figures 4-3 and 4-4 show this type of stage and a corresponding h-s diagram.
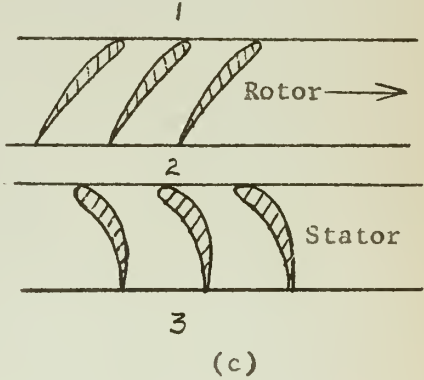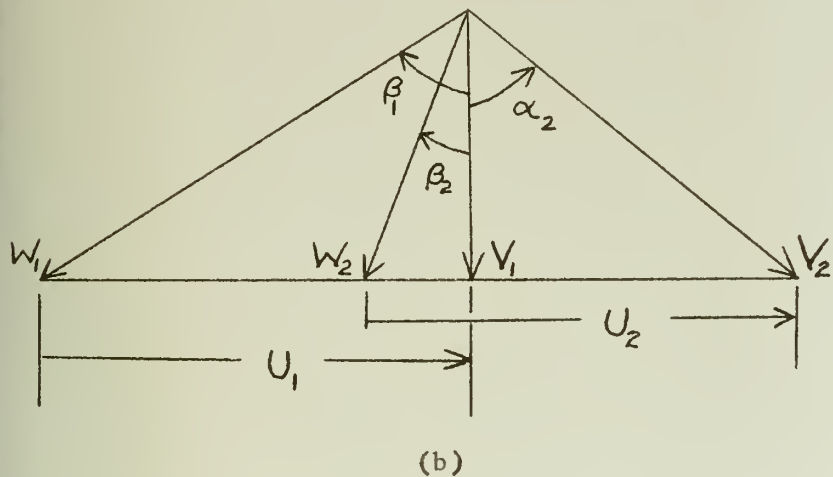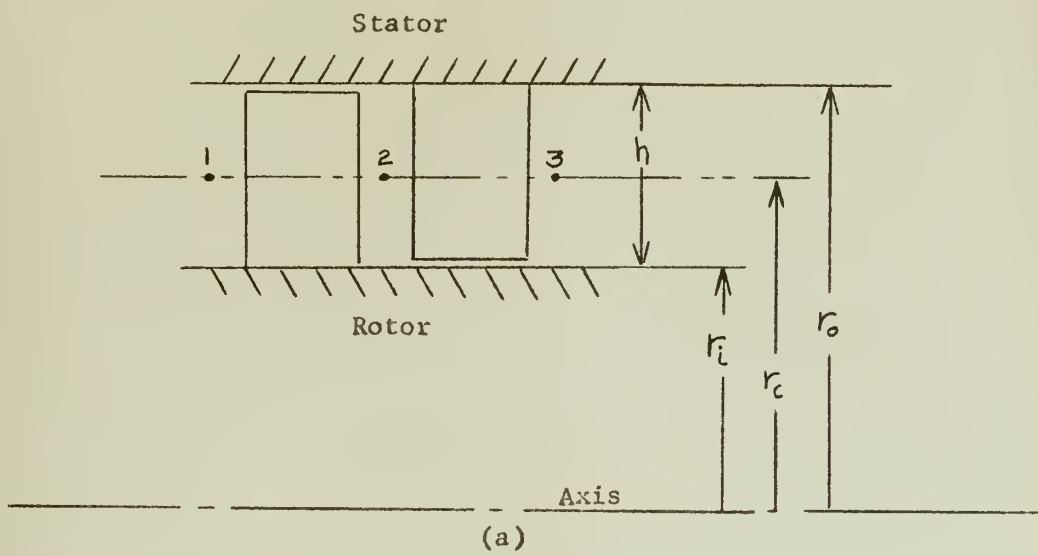
Figure 4-3   Schematic Representation of an Axial Flow Compressor
                Stage and Corresponding Velocity Diagram

57
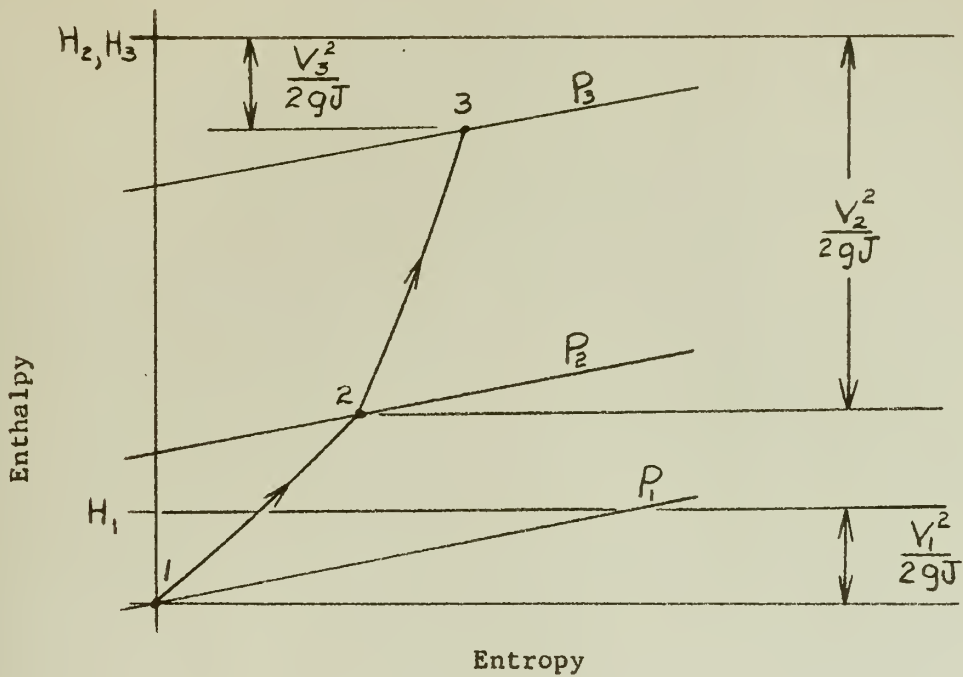
Figure 4-4   Typical h-s diagram for an axial flow compressor stage

For the purpose of developing convenient working equations for calculating stage performance the velocity diagram of Figure 4-3 is changed to a dimensionless form by dividing all vectors by U to obtain Figure 4-5. It is assumed here that $U_1 = U_2$.
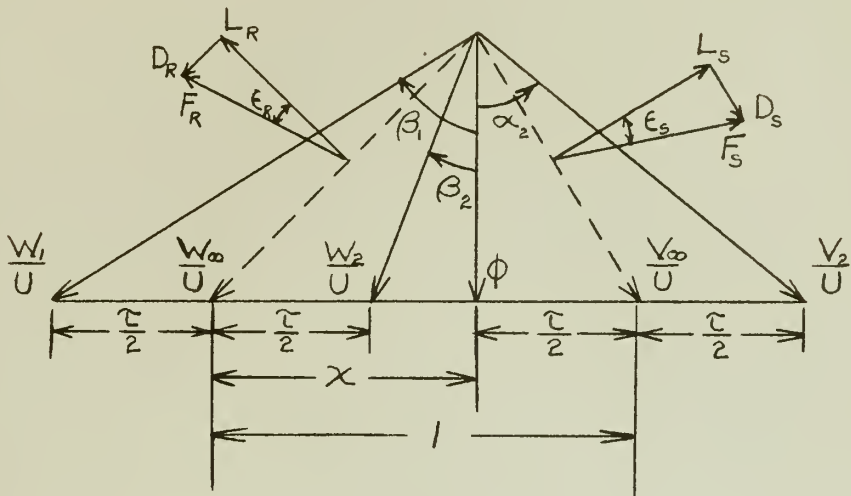
Figure 4-5   Dimensionless velocity diagram for axial flow
compressor stage.

In Figure 4-5 several new terms have been introduced.   They are:

$$\epsilon_R \equiv \frac{\text{Drag Force}}{\text{Lift Force}} \quad \text{for rotor blade} \qquad (4-5)$$

$$\epsilon_S \equiv \frac{\text{Drag Force}}{\text{Lift Force}} \quad \text{for stator blade} \qquad (4-5a)$$

$$x \equiv \frac{W_{u_1} + W_{u_2}}{2U} = 1 - \frac{\tau}{2} \qquad (4-6)$$

$$\phi \equiv \frac{V_m}{U} = \frac{V_i}{U} \qquad (4\text{-}7)$$

$$\tau \equiv \frac{V_{u_2} - V_{u_1}}{U} = \frac{W_{u_2} - W_{u_1}}{U} \qquad (4\text{-}8)$$

or

$$\tau = \frac{V_{u_2}}{U} \qquad \text{for} \quad \alpha_i = 0 \qquad (4\text{-}8a)$$

Expressions for stage efficiency are based on airfoil theory assuming incompressible flow and will not be derived here. Referring to Figure 4-5; if the product $\epsilon_R \epsilon_S$ is ignored with respect to ϵ_R or ϵ_S,

$$P_3 - P_1 = \frac{U^2 \phi \tau}{vg} \left[\frac{1 - x - \epsilon_S \phi}{\phi + \epsilon_S (1-x)} + \frac{x - \epsilon_R \phi}{\phi + \epsilon_R x} \right] \qquad (4\text{-}9)$$

$$(P_3 - P_1)_{th} = \frac{U^2 \tau}{vg} \qquad \left(\epsilon_R = \epsilon_S = 0 \right) \qquad (4\text{-}9a)$$

$$\eta_s \equiv \frac{P_3 - P_1}{(P_3 - P_1)_{th}} = \phi \left[\frac{1 - x - \epsilon_S \phi}{\phi + \epsilon_S (1-x)} + \frac{x - \epsilon_R \phi}{\phi + \epsilon_R x} \right] \qquad (4\text{-}10)$$

$$\text{where} \quad \epsilon = \frac{C_D}{C_L} \qquad (4\text{-}5)$$

$$C_D = C_{DP} + 0.020 \frac{s}{h} + 0.018 \, C_L^2 \qquad (4\text{-}11)$$

$$C_{L_R} = \frac{2\tau \left(\frac{s}{c}\right)_R}{W_\infty / U} \qquad (4\text{-}12)$$

$$C_{L_S} = \frac{2\tau \left(\frac{s}{c}\right)_S}{V_\infty / U} \qquad (4\text{-}12a)$$

Equation (4-11) was obtained from Howell[11] and is based on cascade tests and experimental single-stage and multiple-stage compressor data. These tests also show that the profile drag coefficient, C_{DP}, is primarily a function of the ratio s/c. This relation is plotted in Figure 4-6. (Howell)

Figures 4-7 and 4-8 contain plots of additional test results[11], showing a relation between fluid deflection, exit flow angle and ratio s/c.

In addition to the stage efficiency, calculation of energy input per stage is necessary for determining the number of stages required. This can be expressed as:

$$(\Delta H)_{3,1} = \frac{U}{gJ} \left(V_{u_2} - V_{u_1}\right) = \frac{U^2 \tau}{gJ} \qquad (4\text{-}13)$$

61
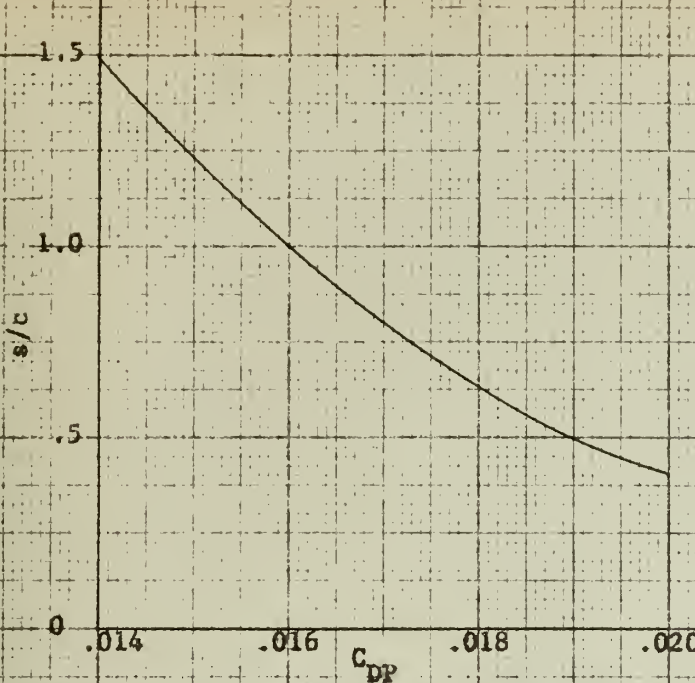
Figure 4-6   Nominal Values of Drag
            Profile Loss Coefficient
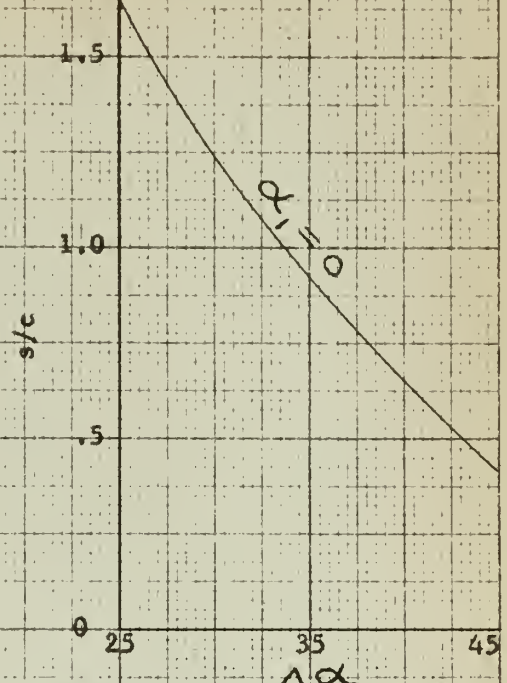
Figure 4-7   Nominal Values
             of Fluid
             Deflection
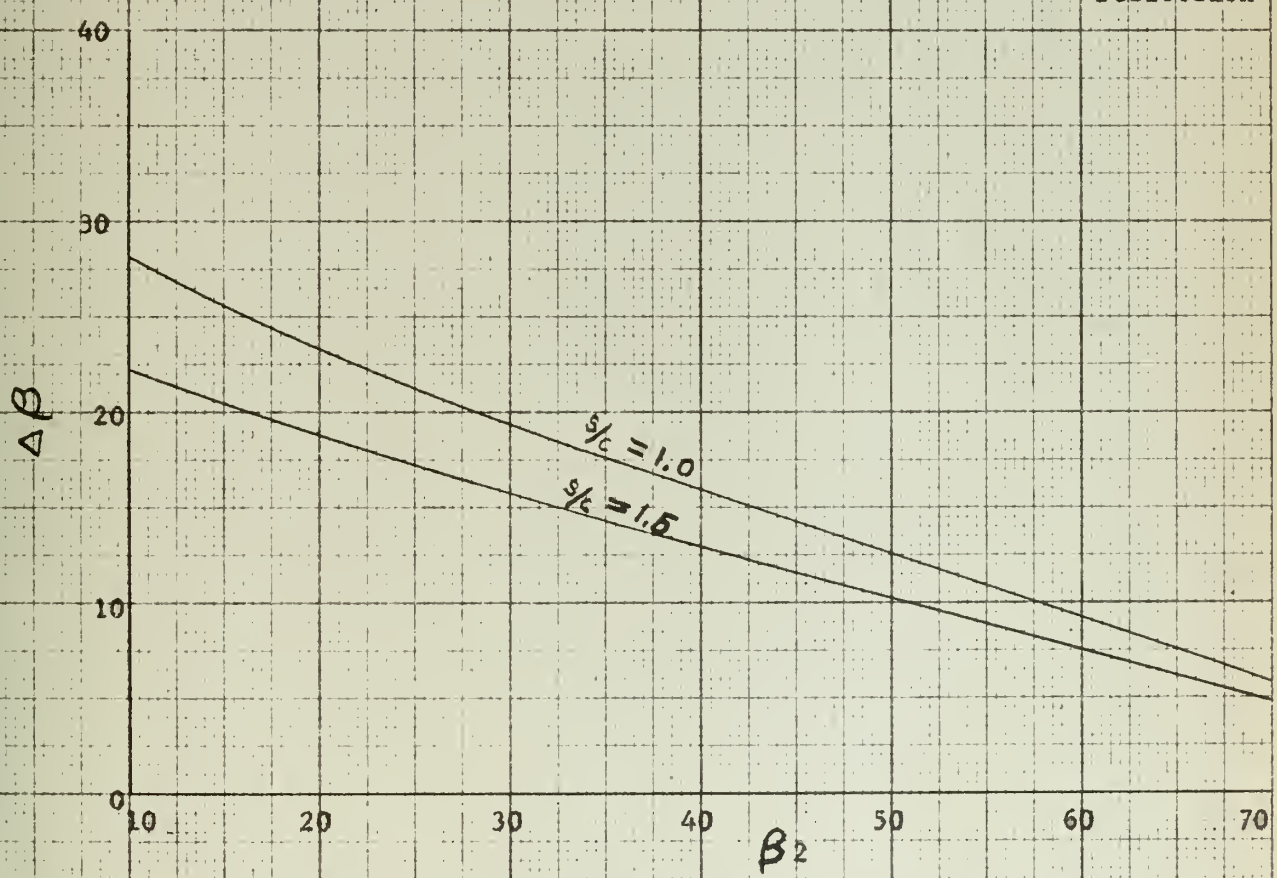
Figure 4-8   Nominal Values of Fluid Deflection

$$\left(\Delta H_s\right)_{3,1} = \left(\Delta H\right)_{3,1} \times \eta_s = \frac{U^2 \tau \, \eta_s}{g J} \qquad (4\text{-}14)$$

For $V_1 = V_3$:

$$\left(\Delta h_s\right)_{3,1} = \frac{U^2 \tau \, \eta_s}{g J} \qquad (4\text{-}14a)$$

The degree of reaction is defined as the ratio of actual enthalpy rise in the rotor to actual enthalpy rise in the stage.

Degree of reaction $\equiv \dfrac{h_2 - h_1}{h_3 - h_1} = \dfrac{h_2 - h_1}{H_3 - H_1} = \dfrac{\left(\Delta h\right)_{2,1}}{\left(\Delta H\right)_{3,1}} \qquad (4\text{-}15)$

If the relative flow in the rotor blade is steady and adiabatic:

$$H_R = h + \frac{W^2}{2 g J} - \frac{U^2}{2 g J} = \text{constant} \qquad (4\text{-}16)$$

For $U_1 = U_2$ and $W_{m_1} = W_{m_2}$:

$$h_2 - h_1 = \frac{W_1^2 - W_2^2}{2 g J} = \frac{W_{u_1}^2 - W_{u_2}^2}{2 g J} \qquad (4\text{-}17)$$

63

From (4-8), (4-13), (4-15) and (4-17):

$$\text{Degree of reaction} = \frac{W_{u_1} + W_{u_2}}{2U} = X \qquad (4-6)$$

Determining Number of Stages

In a multistage compressor, the stage performance varies from stage to stage in some continuous manner. By evaluating the perform- ance of the first and last stages where the stream properties are known and assuming some reasonable relation between these and the other stages' it is possible to express U, τ and η_s for any stage in terms of the two known stages.

The relations assumed in the analysis are:

$$\frac{U_x}{U_1} = \left(\frac{U_n}{U_1}\right)^{\frac{x-1}{n-1}} \qquad (4-18)$$

$$\frac{\tau_x}{\tau_1} = \left(\frac{\tau_n}{\tau_1}\right)^{\frac{x-1}{n-1}} \qquad (4-19)$$

$$\frac{\eta_x}{\eta_1} = \left(\frac{\eta_n}{\eta_1}\right)^{\frac{x-1}{n-1}} \qquad (4-20)$$

From (4-14a) it follows that:

$$\left(\Delta h_s\right)_x = \frac{U_x^2}{gJ}\, \tau_x\, \eta_x = \left(\Delta h_s\right)_1 \left[\frac{\left(\Delta h_s\right)_n}{\left(\Delta h_s\right)_1}\right]^{\frac{x-1}{n-1}} \qquad (4-21)$$

64

$$\sum_{x=1}^{n} (\Delta h_s)_x = (1+f)(\Delta H_s)_{1,n} = (\Delta h_s)_1 \left[1 + D + \sum_{x=2}^{n-1} D^{\frac{x-1}{n-1}} \right] \qquad (4\text{-}22)$$

$$\text{where} \quad D \equiv \frac{(\Delta h_s)_n}{(\Delta h_s)_1} = \left(\frac{U_n}{U_1} \right)^2 \frac{\tau_n \, \eta_n}{\tau_1 \, \eta_1} \qquad (4\text{-}22a)$$

or

$$\frac{(1+f)(\Delta H_s)_{1,n}}{(\Delta h_s)_1} \equiv n' = 1 + D + D^{\frac{1}{n-1}} \left(\frac{D^{\frac{n-2}{n-1}} - 1}{D^{\frac{1}{n-1}} - 1} \right) \qquad (4\text{-}22b)$$

where n' = number of stages required if for
all stages $(\Delta h_s)_x = (\Delta h_s)_1$

Similarly:

$$(\Delta h)_x = \frac{U_x^2}{g \, J} \, \tau_x = (\Delta h)_1 \left[\frac{(\Delta h)_n}{(\Delta h)_1} \right]^{\frac{x-1}{n-1}} \qquad (4\text{-}23)$$

$$\sum_{x=1}^{n} (\Delta h)_x = (\Delta H)_{1,n} \qquad (4\text{-}24)$$

$$\frac{(\Delta H)_{1,n}}{(\Delta h)_1} \equiv n'' = 1 + L + L^{\frac{1}{n-1}} \left(\frac{L^{\frac{n-2}{n-1}} - 1}{L^{\frac{1}{n-1}} - 1} \right) \qquad (4\text{-}25)$$

$$\text{where} \quad L \equiv \frac{(\Delta h)_n}{(\Delta h)_1} = \left(\frac{U_n}{U_1} \right)^2 \frac{\tau_n}{\tau_1} \qquad (4\text{-}25a)$$

and n'' = Number of stages required if for
all stages $(\Delta h)_x = (\Delta h)_1$

Since there must be an integral number of stages the solution of equation (4-22b) for $(\Delta h_s)_1$ generally will not be the same as the value obtained from the first stage calculations. Thus a correction to the peripheral speed is usually necessary. Unless this correction is large, the effect on stage efficiency will be small. The total energy input can then be calculated with equation (4-25).

The overall compressor efficiency is defined as:

$$\eta_c \equiv \frac{(\Delta H_s)_{i,e}}{(\Delta H)_{i,e}} \qquad (4\text{-}26)$$

where

$$(\Delta H_s)_{i,e} = c_p T_i \left[\left(\frac{P_e}{P_i}\right)^{\frac{k_c}{}} - 1 \right] \qquad (1\text{-}6a)$$

and

$$(\Delta H)_{i,e} = (\Delta H)_{i,n} + \frac{V_n^2 - V_e^2}{2gJ} - \frac{V_1^2 - V_i^2}{2gJ} \qquad (4\text{-}4a)$$

The reheat factor, f, appears in equation (4-22b). Equations (1-8) and (1-9) give the reheat factors for an infinite number of stages for both expansion and compression processes. Referring to Figure 4-9 the reheat factor for n stages of compression is obtained from:

$$1 + f \equiv \frac{\displaystyle\sum_{x=1}^{n} (\Delta h_s)_x}{h_{f'} - h_i} \qquad (4\text{-}27)$$

66
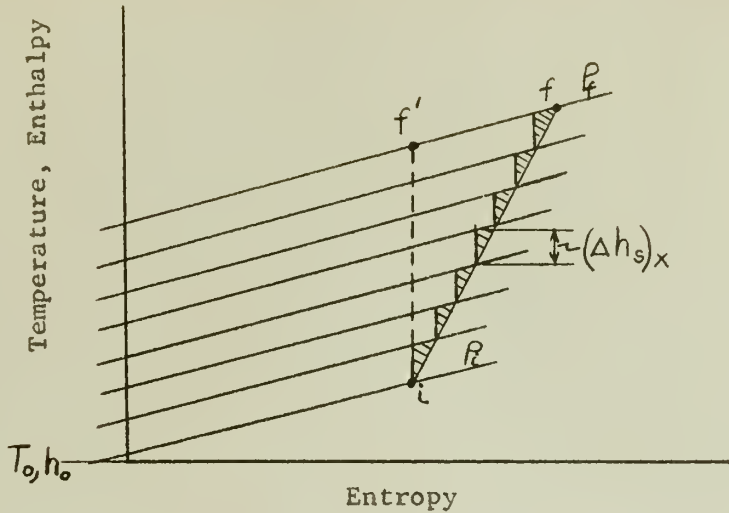
Figure 4-9

For an infinite number of stages (4-27) becomes:

$$1 + f_\infty = \frac{\sum\limits_{x=1}^{\infty} dh_s}{h_{f'} - h_i} \tag{4-27a}$$

Since dh = Tds + vdp for either a reversible or irreversible process and dh = Tds when P = constant:

$$\left(\Delta h\right)_{P=Const.} = \int_{S_1}^{S_2} Tds \quad = \quad \text{area under a constant pressure line on T-S diagram}$$

67

$$\left(\Delta h_s\right)_x = \text{area between the stage inlet and}$$

exit constant pressure lines on the

T-S diagram extending to a reference

absolute temperature.

The difference between $\displaystyle\sum_{x=1}^{\infty} dh_s$ and $\displaystyle\sum_{x=1}^{n} (\Delta h_s)_x$ is the small triangular areas shown in Figure 4-9. Assuming the constant pressure lines to be parallel and $(\Delta h_s)_x$ constant for all stages, the area of i-f'-f consists of n^2 small triangles.

Equations (4-27) and (4-27a) can be combined as follows:

$$\frac{f}{f_\infty} = \frac{h_{f'}-h_i - \displaystyle\sum_{x=1}^{n} (\Delta h_s)_x}{h_{f'}-h_i - \displaystyle\sum_{x=1}^{\infty} dh_s}$$

or $$\frac{f}{f_\infty} = \frac{\text{area i-f-f' \ less n small triangles}}{\text{area i-f-f'}}$$

$$= \frac{n^2-n}{n^2} = \frac{n-1}{n}$$

$$f = f_\infty \frac{n-1}{n} \tag{4-28}$$

Compressor No. 1

Having previously decided on the type of blading it is now necessary to determine an optimum combination of the many variables involved. First of all, a high stage efficiency is desired. To calculate this, practical values for $(s/c)_R$, $(h/c)_S$ and $(h/c)_R$ must be selected from

experience. The quantities, C_{DP}, $(s/c)_S$, and $\Delta\beta$, can be obtained from test data of Figures 4-6, 4-7 and 4-8. Then for given values of β_2 the remaining quantities in the dimensionless velocity diagram, Figure 4-5, and the stage efficiency can be calculated.

The effect of a bad choice of $(h/c)_S$ and $(h/c)_R$ is not great, since these quantities change the stage efficiency slightly. The values assumed for a preliminary investigation were 3.0 and 2.0 respectively. The choice of $(s/c)_R$ is more critical. From a consideration of dimensions, especially blade heights, $(s/c)_R$ of less than 1.0 proves to be impractical. Therefore, stage efficiencies were calculated for $(s/c)_R$ of 1.0 and 1.5. Figure 4-10 shows the plot of η_s vs. β_2 for these two ratios. It can be seen that the maximum efficiency in both cases will occur at some smaller angle than has been plotted. At the smaller angles the blade heights become smaller than practical design permits. In addition, consideration must be given to Compressor No. 2 and Turbine No. 1 since their rpm will be the same as Compressor No. 1. For the same blading in Compressor No. 2 the smaller specific volume will result in even smaller blade heights. Too high a rpm will result in a large through flow velocity in Turbine No. 1 and consequently a low turbine efficiency.

In conventional designs using air as the working fluid, the maximum peripheral speed is usually determined from Mach effects because of the relatively low velocity of sound in air. The velocity of sound in helium is approximately three times as great so that allowable stress becomes the controlling factor. The materials that are presently being used for compressor rotors and blades will permit a U_{max} of about 1200 ft/sec.
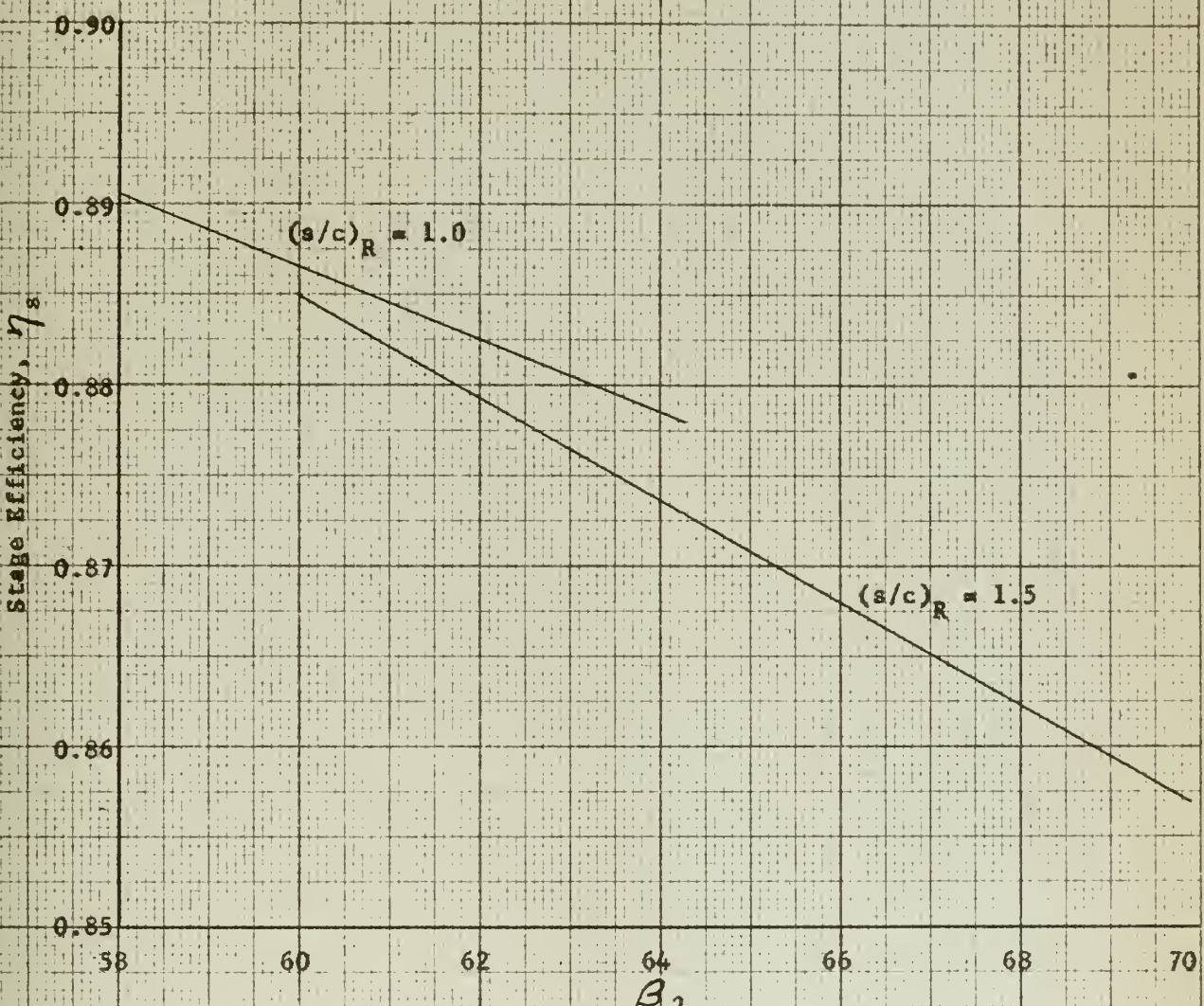
Figure 4-10   Effect of β_2 and $(s/c)_R$ on Compressor Stage Efficiency

The y-axis is labeled "Stage Efficiency, η_s" with values 0.85, 0.86, 0.87, 0.88, 0.89, 0.90.

The x-axis is labeled β_2 with values 58, 60, 62, 64, 66, 68, 70.

Curves labeled $(s/c)_R = 1.0$ and $(s/c)_R = 1.5$.

Figure 4-11 shows plots of N vs. β_2 for last stage blade heights of 1.0 and 1.4 inches. For calculation of the last stage blade heights it is assumed that the same blading is employed as in the first stage. From the plot it can be deduced that for given values of h_n and η_s the compressor having the smallest value of $(s/c)_R$ has the lowest rpm. The compressors in this cycle require high rpm if small blade heights and large diameters are to be avoided. High turbine rpm results in a blade height to mean diameter ratio which is too large, so some compromise has to be made. Preliminary calculations indicate that 7000 rpm is satisfactory for Turbine No. 1 and the two compressors. Another factor to be considered is the number of stages required for different values of $(s/c)_R$.

TABLE 4-1

EFFECT OF $(s/c)_R$ ON COMPRESSOR BLADING

$(s/c)_R$	1.0	1.5	Units
N	7000	7000	rpm
β_2	62.2	64.4	degrees
h_n	1.4	1.4	inches
η_s	.882	.873	----
n	7 or 8	10	stages

71
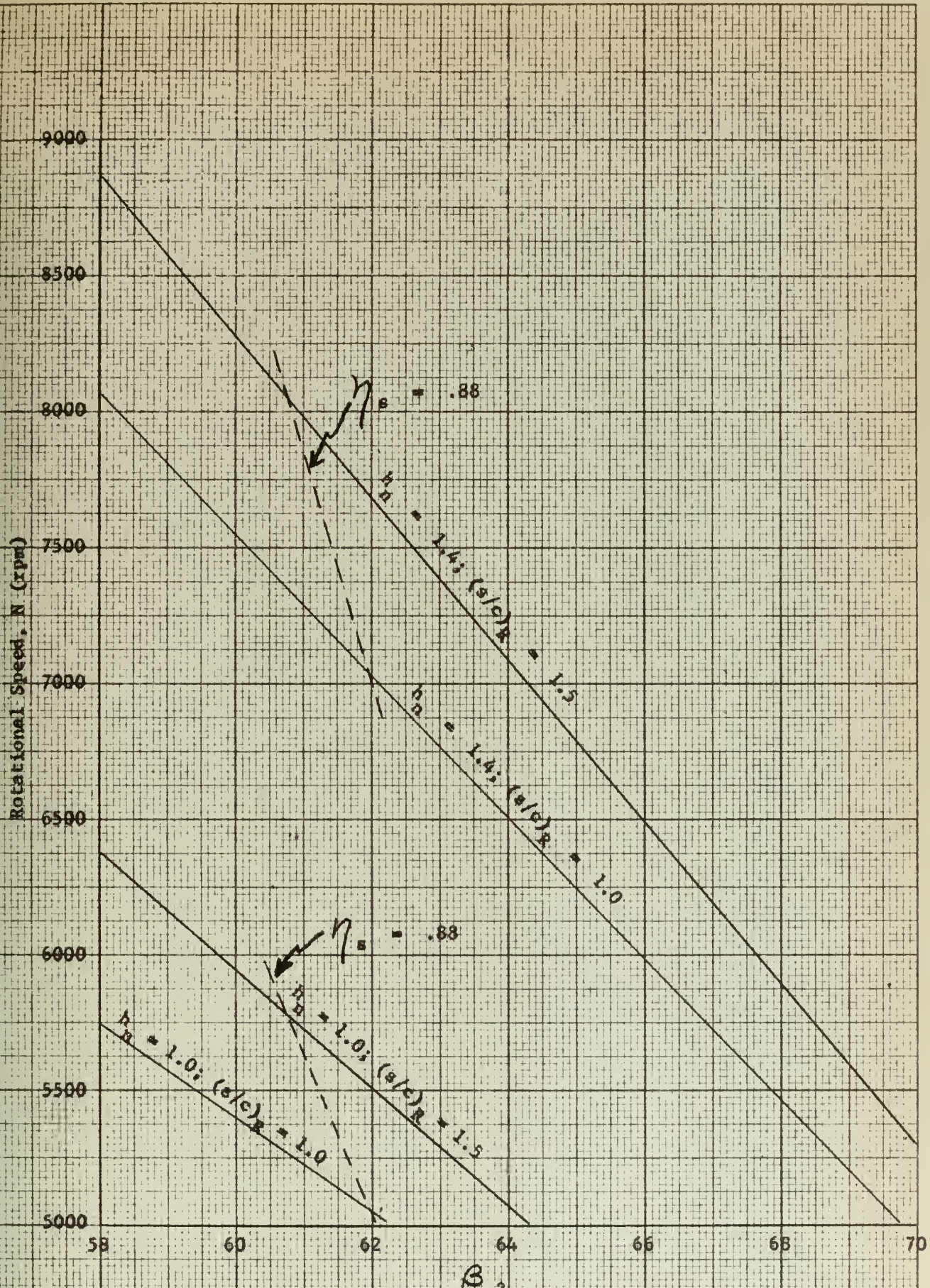
Figure 4-11   Effect of β_2, h_n and $(s/c)_R$ on Compressor Rotational
Speed

72

From the comparison in Table 4-1 the blading having a space to chord ratio of 1.0 appears to be the most favorable and is used in subsequent analysis.

The results of preliminary calculations indicate that an $(h/c)_R$ or 3 results in a very small chord so it was changed to 2.0.

In order to make all rotor disks of the same dimensions, the blade root diameter will be constant. The first and last stage data that result are listed in Table 4-2.

TABLE 4-2

DATA FOR FIRST AND LAST STAGES OF COMPRESSOR NO. 1

	First Stage	Last Stage	Units
α_1	0	0	degrees
$(s/c)_R$	1.0	1.0	----
$(h/c)_R$	2.0	1.63*	----
$(h/c)_S$	2.0	1.63*	----
β_2	62.0	62.0	degrees
β_1	70.6	70.6	"
ϕ	0.3522	0.3522	----
τ	0.3376	0.3376	----
x	0.8312	0.8312	----
α_2	43.8	43.8	degrees
$(s/c)_S$	0.48	0.48	----
η_S	0.8812	0.8755	----
ϵ_R	0.0482	0.0513	----
ϵ_S	0.0438	0.0440	----

* h/c for last stage = h/c for first stage x $\dfrac{h_n}{h_1}$

Since there must be an integral number of stages the calculation

of work imput per stage, dimensions, and velocities requires a series

of approximations. Table 4-3 contains first approximations of U, V_1,

A , h and d_c, for a fixed compressor speed of 7000 rpm. Before

proceeding with the analysis, some additional information is necessary;

namely, the inlet and exit pipe velocities and the inducer and diffuser

efficiencies. The velocities were selected after taking into consider-

ation the size of pipe required and the efficiencies are typical values

for conventional designs. These are indicated in Table 4-4 along with

calculated results.

The following equations, supplementary to those listed previously,

are also applicable:

$$A = \frac{\dot{m}\, v}{V_1} \times 144 = \pi h d_c \quad in^2 \tag{4-29}$$

$$N = \frac{720\, U}{\pi d_c} \quad rpm \tag{4-30}$$

TABLE 4-3

FIRST APPROXIMATION DATA FOR FIRST AND LAST STAGES OF COMPRESSOR NO. 1

	First Stage	Last Stage	Units
N	7000	7000	rpm
U*	1200	1190	ft/sec
V_1*	423	420	ft/sec
A *	213	172	in^2
h*	1.72	1.40	in
d_c*	39.32	39.00	in

* First approximation

TABLE 4-4

ADDITIONAL DATA FOR COMPRESSOR NO. 1

V_i	400	ft/sec
V_e	400	"
η_i	0.75	----
η_e	0.85	----
$(\Delta H_s)_{i,e}$	124.1	BTU/lb
$(\Delta H_s)_{i,n}^{*}$	124.3	"
$(\Delta h_s)_{i}^{*}$	17.14	"
n'^{*}	7.34	----
$1+f$	1.0117	----
n	7	stages
D	0.9773	----
L	0.9837	----
n'	6.920	----
n''	6.941	----
$(\Delta h_s)_{i}$	18.17	BTU/lb
$(\Delta h)_{i}$	20.60	"
$(\Delta H)_{i,n}$	143.05	"
$\eta_{i,n}$	0.868	----
η_c	0.867	----

* First approximation

We observe in Table 4-4 that the actual $(\Delta h_s)_1$ required for seven stages differs from the first approximation. Therefore, some changes must be made in U and some of the dimensions if N is to remain at 7000 rpm. These changes can be made by use of the following equations:

$$U_1 = U_1^* \left[\frac{(\Delta h_s)_1}{(\Delta h_s)_1^*}\right]^{\frac{1}{2}} \qquad (4\text{-}31)$$

$$d_{c_1} = d_c^* \frac{U_1}{U_1^*} \qquad (4\text{-}32)$$

$$Y_1 = V_1^* \frac{U_1}{U_1^*} \qquad (4\text{-}33)$$

$$A_1 = A_1^* \frac{U_1^*}{U_1} \qquad (4\text{-}34)$$

Corrected results for the first and last stages are indicated in Table 4-5.

TABLE 4-5

FINAL DATA FOR FIRST AND LAST STAGES OF COMPRESSOR NO. 1

	First Stage	Last Stage	Units
U	1235	1225	ft/sec
N	7000	7000	rpm
V_1	436	432	ft/sec
V_2	604	599	"
W_1	1310	1300	"
W_2	928	920	"
A	207	167	in^2
h	1.63	1.33	in
d_i	38.87	38.87	"
d_c	40.50	40.20	"
d_o	42.13	41.53	"
c	0.82	0.82	"
s_R	0.82	0.82	"
s_S	0.39	0.39	"

Compressor No. 2

The same blading is used in Compressor No. 2 as was used in Com-
pressor No. 1 and the rpm is fixed at 7000. Figure 4-12 shows the
variation of h_n and n as a function of U. A mean peripheral speed of
1050 ft/sec was selected in order to obtain a satisfactory last stage
blade height. The root diameter is constant as in Compressor No. 1.

Table 4-2 is applicable with the following exceptions for the
last stage:
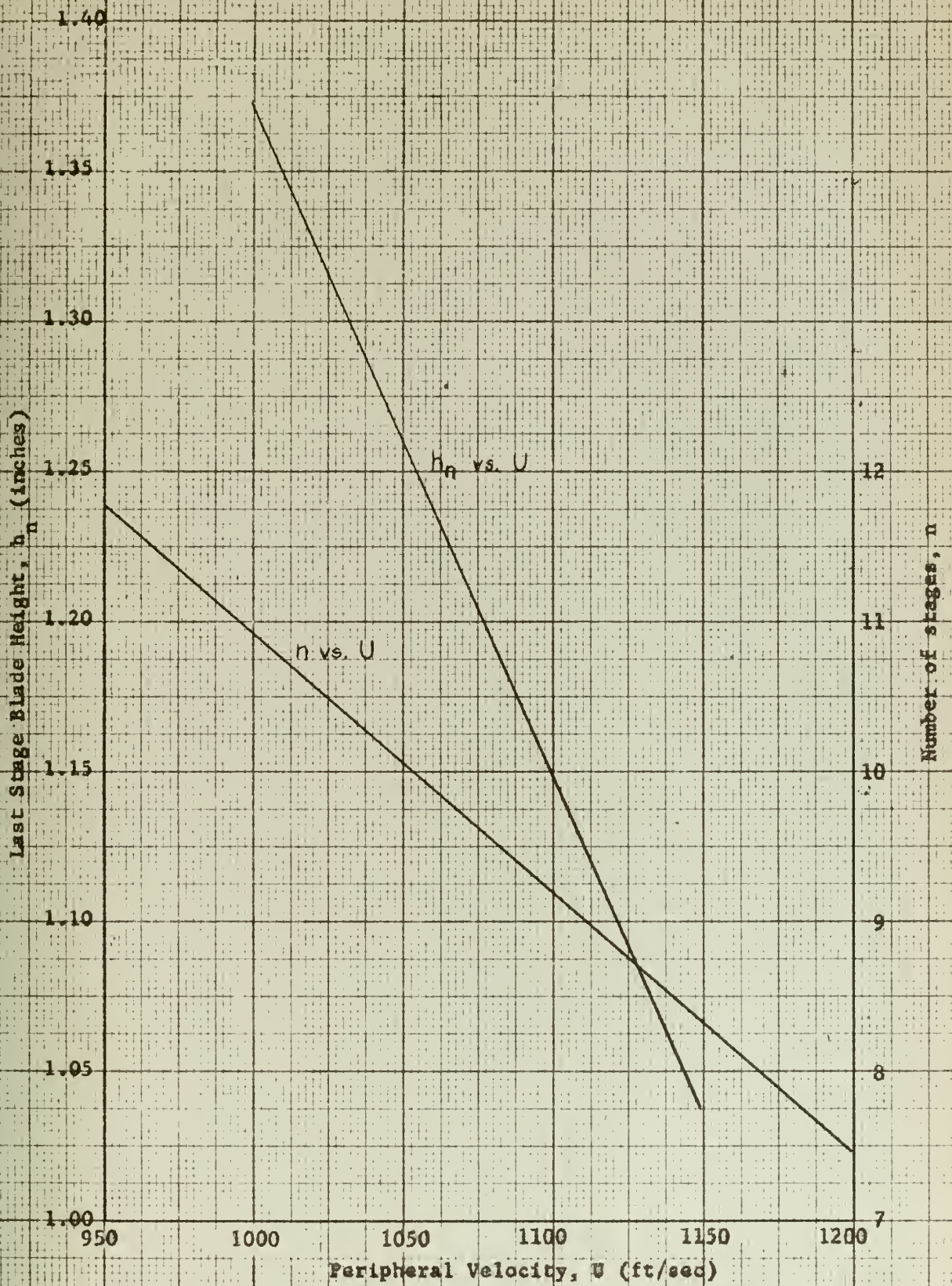
Figure 4-12   Effect of Peripheral Velocity on Number of Stages and Last Stage Blade Heights of Compressor No. 2

$$\left(h/c \right)_R = \left(h/c \right)_S = 1.66$$

$$\eta_s = 0.8762$$

Calculated results are listed in Tables 4-6, 4-7 and 4-8.

TABLE 4-6

FIRST APPROXIMATION DATA FOR FIRST AND LAST STAGES OF COMPRESSOR NO. 2

	First Stage	Last Stage	Units
$U*$	1050	1037	ft/sec
N	7000	7000	rpm
V_1*	370	365	ft/sec
$A*$	164	134	in^2
$h*$	1.52	1.26	in.
d_c*	34.38	33.90	"

* First Approximations

TABLE 4-7

ADDITIONAL DATA FOR COMPRESSOR NO. 2

V_i	300	ft/sec
V_e	450	"
η_i	0.75	----
η_e	0.75	----
$(\Delta H_s)_{i,e}$	126.6	BTU/lb
$(\Delta H_s)_{i,n}^*$	128.83	"
$(\Delta h_s)_i^*$	13.12	"
n'*	9.97	----
1+f	1.0157	----
n	10	stages
D	0.9793	----
L	0.9849	----
n'	9.9005	----
n"	9.9189	----
$(\Delta h_s)_i$	13.20	BTU/lb
$(\Delta h)_i$	14.98	"
$(\Delta H)_{i,n}$	148.58	"
$\eta_{1,n}$	.867	----
η_c	.840	----

TABLE 4-8

FINAL DATA FOR FIRST AND LAST STAGES OF COMPRESSOR NO. 2

	First Stage	Last Stage	Units
U	1050	1037	ft/sec
N	7000	7000	rpm
V_1	370	365	ft/sec
V_2	513	507	"
W_1	1115	1100	"
W_2	788	778	"
A	164	134	in^2
h	1.52	1.26	in.
d_i	32.86	32.64	"
d_c	34.38	33.90	"
d_o	36.90	35.16	"
c	0.76	0.76	"
s_R	0.76	0.76	"
s_S	0.37	0.37	"

CHAPTER V

TURBINES

Symbols used in this chapter:

Symbol	Description	Units
d	diameter	in.
f	reheat factor	---
g	conversion factor, 32.17	$\frac{lb_m}{lb_f} \frac{ft}{sec^2}$
H	total enthalpy	BTU/lb
h	blade height	in.
or		
	enthalpy	BTU/lb
J	conversion factor, 778	$\frac{ft - lb}{BTU}$
K	coefficient defined in equation (5-10b)	---
$\dot{m}$	mass flow	lbs/sec
N	rotational speed	rpm
n	number of stages	---
P	absolute pressure	psia
r	radius	in.
T	absolute temperature	°R
U	peripheral speed	ft/sec
V	absolute flow velocity	ft/sec
v	specific volume	ft^3/lb
W	relative flow velocity	ft/sec
α	absolute flow angle	degrees
β	relative flow angle	degrees

Symbol	Description	Units
Δ	increment	----
η	efficiency	----
λ	defined by equation (5-16)	----
ν	defined by equation (5-15)	----
ϕ	coefficient defined by equation (5-7)	----
$\Chi$	defined by equation (5-20)	----
χ	degree of reaction	----
ψ	coefficient defined by equations (5-12) and (5-13)	----
ω	rotational speed	rad/sec

Subscript	Description
B	blade
c	center, mean
e	exit
i	inlet, initial
m	axial
n	last stage
o	outer
R	relative
s	isentropic
T	turbine
u	tangential

General

This chapter consists of a design study of the two turbines in the cycle. As in Chapter IV for the compressors, a one-dimensional flow

83

analysis is performed to determine turbine diameters, blade heights, number of stages and blade shapes at a mean streamline. The flow is assumed to be steady and adiabatic in both moving and stationary channels so that the total enthalpy, H, in the stationary channels and the total relative enthalpy, H_R, in the moving channels are constant along the streamlines. Analysis reveals that if a centripetal turbine is employed an excessive peripheral speed will be required to produce the necessary work output. Therefore, the entire analysis that follows is based upon an axial flow turbine.
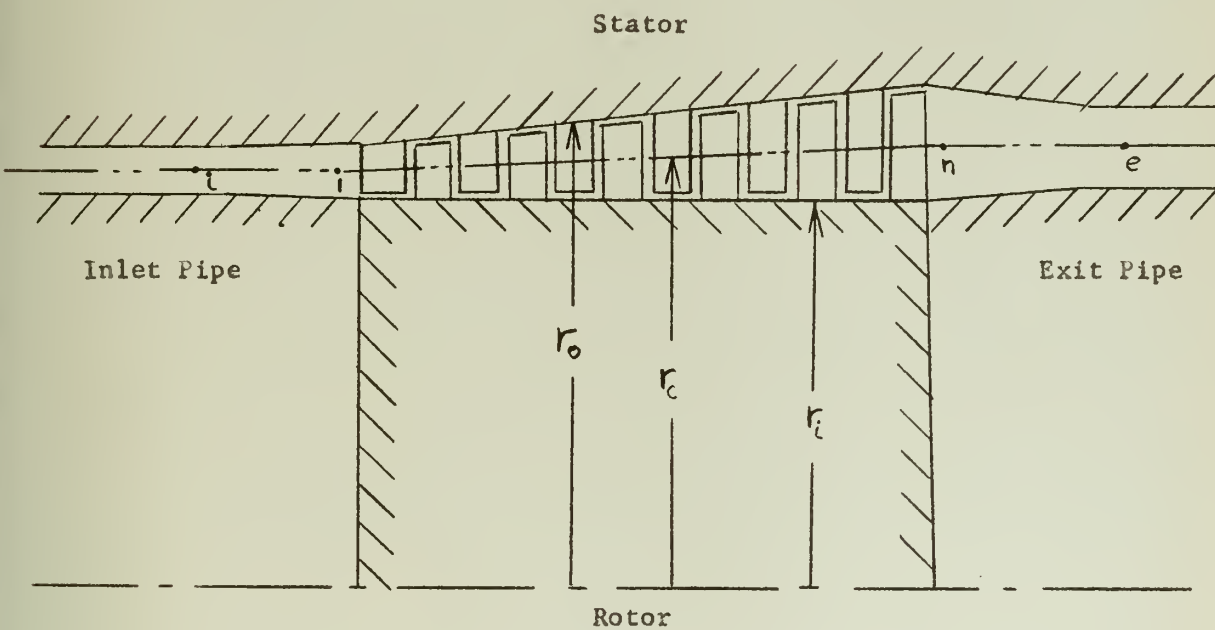
Figure 5-1   Schematic Representation of an Axial Flow Turbine

Figure 5-1 is a sketch of an axial flow turbine showing stream locations i, l, n and e. The inlet and exit sections serve to decelerate and accelerate the flow respectively, since, as we shall see later, the pipe velocities for this cycle are necessarily larger than the through flow velocity. Referring to the enthalpy - entropy diagram in Figure 5-2, the following relations can be written:

$$\left(\Delta H_s\right)_{l,n} = \left(\Delta H_s\right)_{i,e} + \eta_i \left(\frac{V_i^2 - V_l^2}{2gJ}\right) - \frac{1}{\eta_e}\left(\frac{V_e^2 - V_n^2}{2gJ}\right) \quad (5\text{-}1)$$

$$\text{where} \quad \eta_i \equiv \frac{\left(\Delta h_s\right)_{i,l}}{\left(\Delta h\right)_{i,l}} \quad (5\text{-}1a)$$

$$\text{and} \quad \eta_e \equiv \frac{\left(\Delta h\right)_{n,e}}{\left(\Delta h_s\right)_{n,e}} \quad (5\text{-}1b)$$

$$H_i = H_l \quad \text{and} \quad H_e = H_n \quad (5\text{-}2)$$

$$\text{where} \quad H = \frac{V^2}{2gJ} + h \quad (5\text{-}2a)$$

$$\Delta H_B \equiv H_l - H_n \quad (5\text{-}3)$$

$$\eta_T \equiv \frac{\Delta H_B}{\left(\Delta H_s\right)_{i,e}} \quad (5\text{-}4)$$
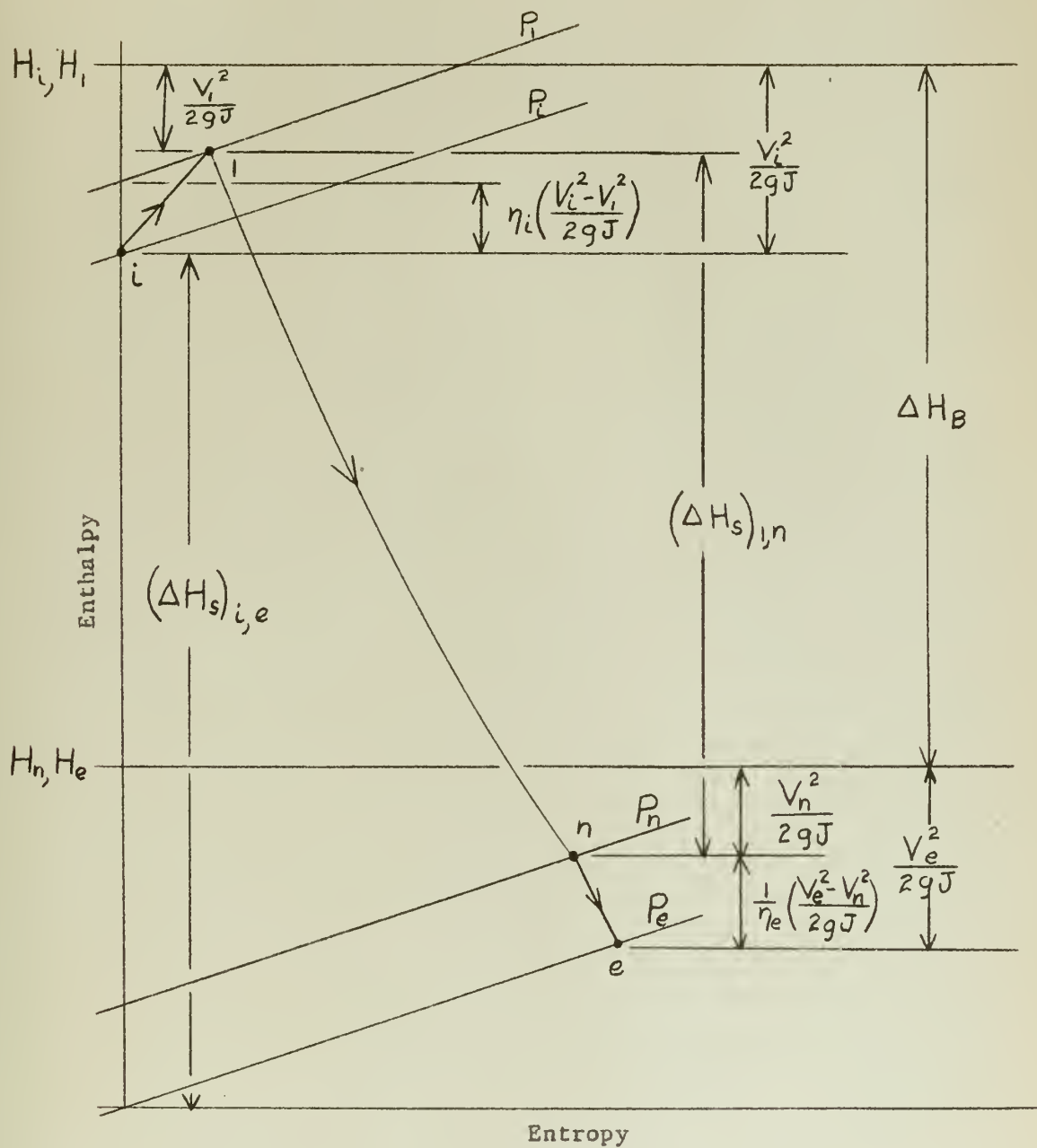
Figure 5-2   Typical Enthalpy-Entropy Diagram for an Axial Flow Turbine
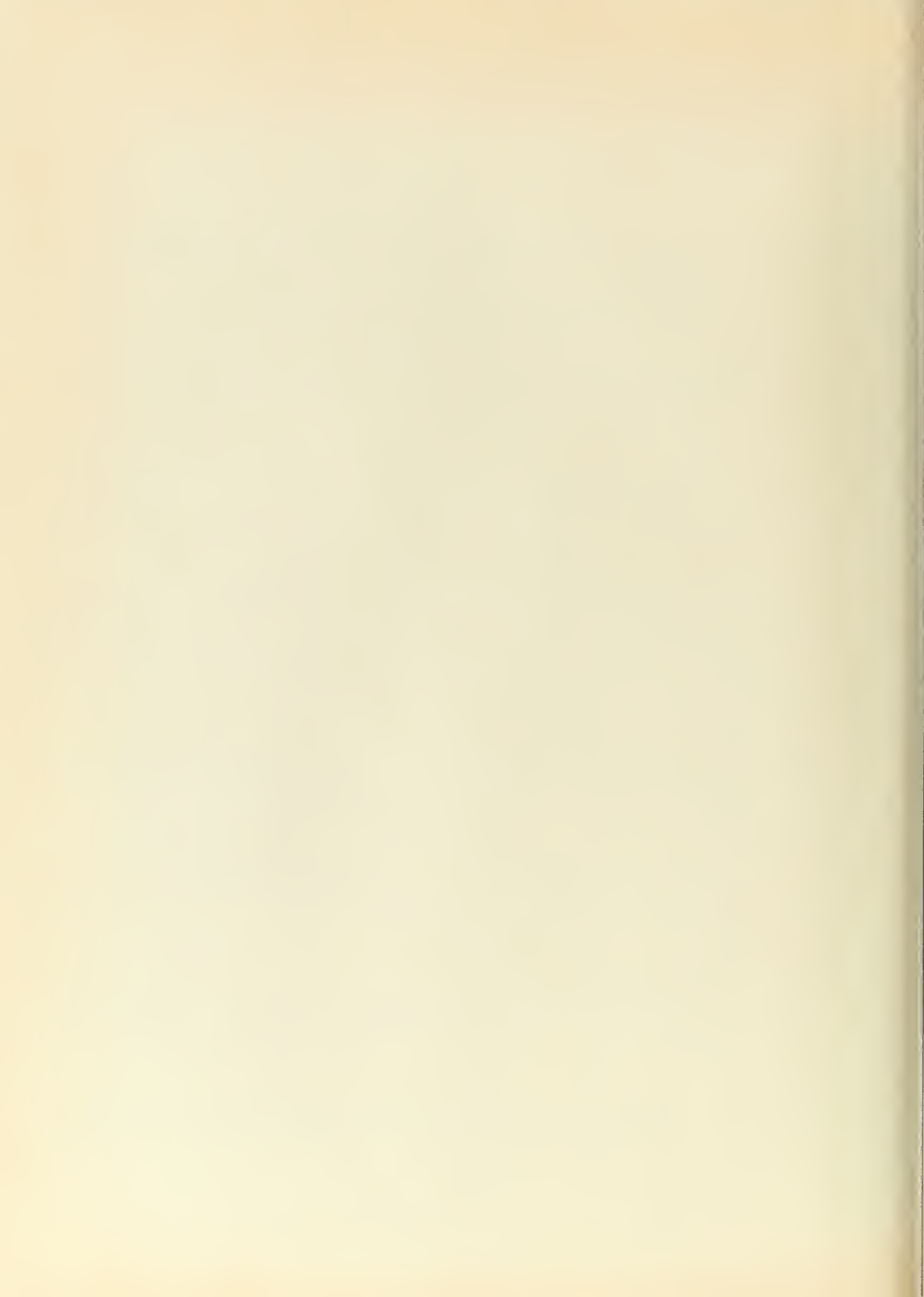
Stage Efficiency

Figures 5-4 and 5-5 are enthalpy - entropy diagrams illustrating absolute flow quantities for the stage and relative flow quantities for the rotor blade respectively.

From Figure 5-4:

$$\left(\Delta h_s\right)' \equiv h_{1'} - h_{3'} \tag{5-5}$$

$$\left(\Delta h_s\right)'' \equiv h_2 - h_{3''} \tag{5-6}$$

$$\left(\Delta h_s\right)''' \equiv h_{2^*} - h_{3'''} \tag{5-7}$$

Assuming zero reheat (f = 0):

$$\left(\Delta h_s\right)'' = \left(\Delta h_s\right)''' \tag{5-6a}$$

$$\phi^2 \equiv \frac{(\Delta h)_{1',2}}{(\Delta h_s)_{1',2}} \tag{5-8}$$

$$\chi' \equiv \frac{\left(\Delta h_s\right)''}{\left(\Delta h_s\right)'} \qquad = \text{isentropic degree} \tag{5-9}$$
$$\text{of reaction}$$

$$\eta_s \equiv \frac{\Delta h_B}{\left(\Delta h_s\right)'} = \frac{\Delta h_B}{\left(\Delta h_s\right)''} \chi' \tag{5-10}$$

87
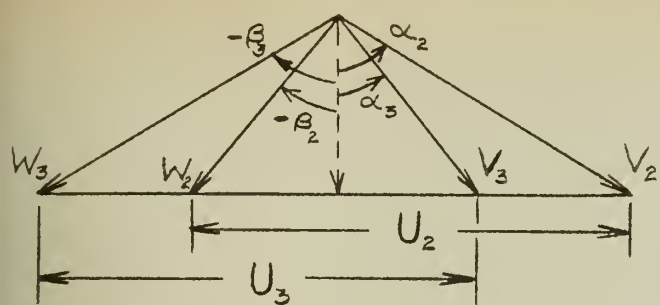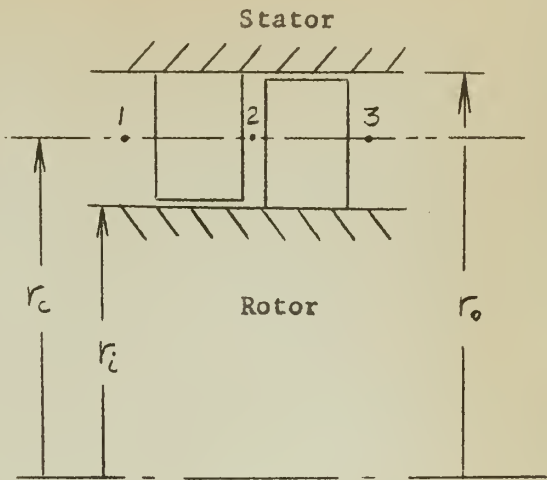
Figure 5-3   Velocity Diagram for an Axial Flow Turbine Stage
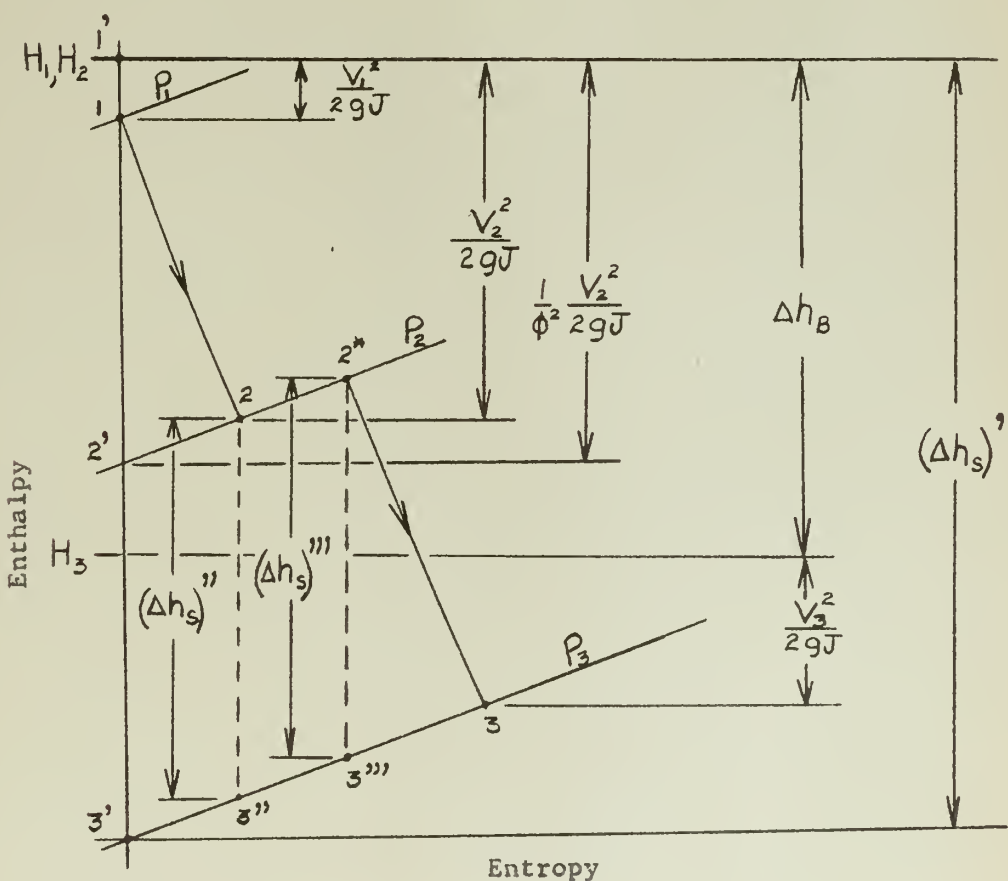
Figure 5-4   Typical Enthalpy-Entropy Diagram for an Axial
Flow Turbine Stage

In equation (5-10) the kinetic energy of the fluid at the exit of the stage is not considered as useful energy. Actually, most of this energy is available for the succeeding stage and another stage efficiency is defined:

$$\eta_s^* \equiv \frac{\Delta h_B}{(\Delta h_s)^*} \tag{5-10a}$$

where $\quad (\Delta h_s)^* = (\Delta h_s)' + K \dfrac{V_3^2}{2gJ} \tag{5-10b}$

and $\quad K \ = \ $ percentage of the kinetic energy leaving a stage that is available for useful work in the succeeding stage
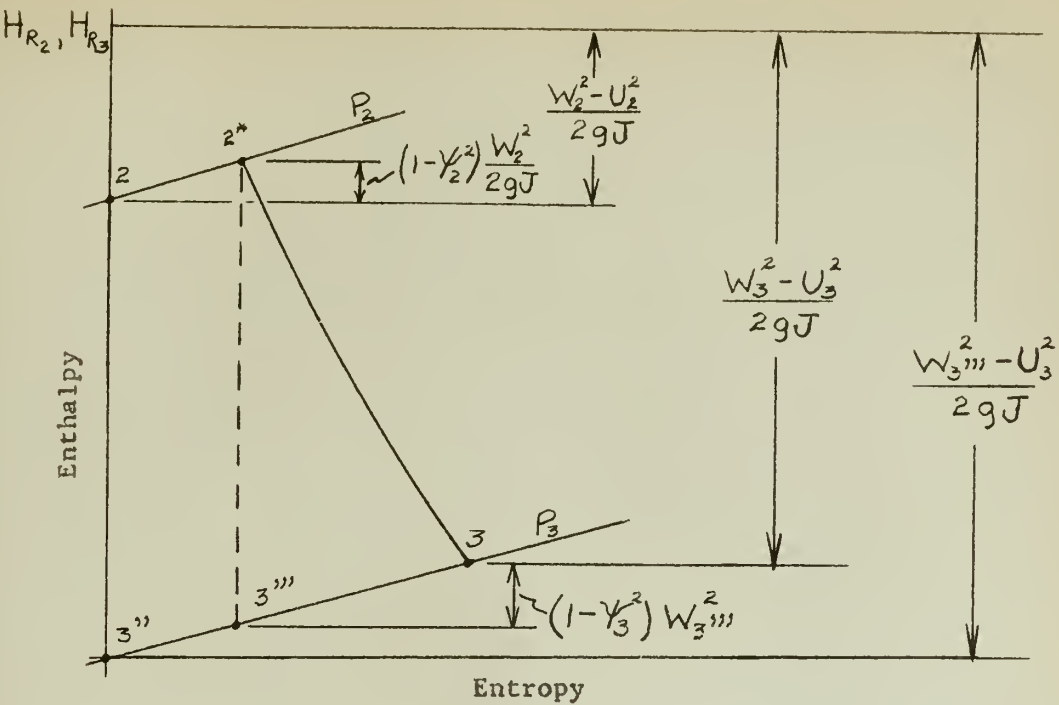
Figure 5-5   Typical Enthalpy - Entropy Diagram for Relative Flow
in a Turbine Rotor Blade

From Figures 5-4 and 5-5:

$$H_{R_2} = H_{R_3} \qquad = \text{constant} \qquad (5\text{-}11)$$

$$\text{where} \quad H_R \equiv h + \frac{W^2}{2gJ} - \frac{U^2}{2gJ} \qquad (5\text{-}11a)$$

$$\psi_2^2 \equiv 1 - \frac{h_{2*} - h_2}{W_3^2 / 2gJ} \qquad (5\text{-}12)$$

90

$$\psi_3 \equiv \frac{W_3}{W_{3'''}} \tag{5-13}$$

$$\frac{W_3^2}{2gJ} = \psi_3^2 \left[(\Delta h_s)''' + \frac{\psi_2^2 W_2^2 + U_3^2 - U_2^2}{2gJ} \right] \tag{5-14}$$

For zero reheat (f = 0):

$$\frac{W_3^2}{U_2^2} = \psi_3^2 \left[\frac{2gJ(\Delta h_s)' x'}{U_2^2} + \frac{\psi_2^2 W_2^2 + U_3^2}{U_2^2} - 1 \right] \tag{5-14a}$$

It is advantageous for subsequent analysis to introduce the following definitions:

$$\nu^2 \equiv \frac{U_2^2}{(\Delta h_s)' (2g\bar{J})} \tag{5-15}$$

$$\lambda \equiv \frac{U_3}{U_2} \tag{5-16}$$

$$\mu \equiv \frac{V_{m_3}}{V_{m_2}} \tag{5-17}$$

From the trigonometry of Figure 5-3, the definitions above and equation (5-14a), several new equations can be derived:

91

$$\left(\frac{W_3}{U_2}\right)^2 = \left(\frac{\psi_3}{\nu}\right)^2 \left[X' + \phi^2 \psi_2^2 (1-X') - \right.$$

$$\left. 2\phi \psi_2^2 \nu \sqrt{1-X'} \sin \alpha_2 + \nu^2 \left(\psi_2^2 + \lambda^2 - 1\right) \right] \quad (5\text{-}14b)$$

$$\frac{V_{u_3}}{U_2} = \lambda - \frac{\psi_3}{\nu} X \quad (5\text{-}18)$$

$$\eta_s = 2\nu \left(\phi \sqrt{1-X'} \sin \alpha_2 + \lambda \psi_3 X - \lambda^2 \nu \right) \quad (5\text{-}19)$$

$$X^2 \equiv X' + \phi^2 \left(\psi_2^2 - \frac{\mu^2}{\psi_3^2} \cos^2 \alpha_2 \right) (1-X') -$$

$$2\phi \psi_2^2 \nu \sqrt{1-X'} \sin \alpha_2 + \nu^2 \left(\psi_2^2 + \lambda^2 - 1 \right) \quad (5\text{-}20)$$

$$\tan \beta_2 = \tan \alpha_2 - \frac{\nu}{\phi \sqrt{1-X'} \cos \alpha_2} \quad (5\text{-}21)$$

The work output per stage can also be expressed in the familiar form:

$$\Delta h_B = \frac{\omega}{gJ} \left(R_2 V_{u_2} - R_3 V_{u_3} \right) \quad (5\text{-}22)$$

If $R_1 = R_2$:

$$\Delta h_B = \frac{U}{gJ} \left(V_{u_2} - V_{u_3} \right) \quad (5\text{-}22a)$$

If $\alpha_2 = 0$:

$$\Delta h_B = \frac{U V_{u_2}}{g J} \qquad (5\text{-}22b)$$

When all stages are similar and produce equal work:

$$\Delta H_B = n \, \Delta h_B \qquad (5\text{-}22c)$$

From the definition of reheat factor and equation (5-10b):

$$(\Delta H_s)_{1,n} \equiv \frac{n(\Delta h_s)'}{1+f} = \left[\frac{n \, \Delta h_B}{\eta_s^*} + \frac{K V_3^2}{2gJ}\right]\frac{1}{1+f} \qquad (5\text{-}23)$$

where $\quad f = f_\infty \frac{n-1}{n} \qquad (4\text{-}28)$

Two additional relations necessary for turbine design are:

$$d_c = \frac{720 \, U}{\pi N} \qquad in. \qquad (5\text{-}24)$$

$$A = \pi d_c h = \frac{m v}{V_m} \times 144 \quad in^2 \qquad (5\text{-}25)$$

Selection of Blading for Turbine No. 1

The type of blading to be selected must permit a good efficiency as well as reasonable dimensions and number of stages for the conditions imposed. The use of low efficiency Curtis impulse stages would not be satisfactory despite the fewer stages required. Generally, it can be expected that reaction stages will have the highest efficiency

93

and require the greatest number of stages. In order to obtain a high efficiency and prevent too many stages a compromise between impulse and reaction stages may be warranted. Two general types of stages were investigated; namely, (1) symmetric or 50 per cent reaction and (2) modified Rateau. The modified Rateau stage differs from the pure impulse stage in that a small amount of reaction is introduced by specifying an axial exit velocity.

Comparisons of the two types have been based on conditions existing at Turbine No. 1, the rotational speed of which is 7000 rpm. The maximum peripheral speed, U, is limited by stress conditions. At temperatures of 1350°F a peripheral speed of about 800 ft/sec seems possible with materials currently available. Losses in the stator and rotor, expressed by the definitions of ϕ, ψ_2, and ψ_3, are estimates based on conventional gas turbine performance tests. For a single stage the differences between U_2 and U_3 can be considered negligible. In addition, the through-flow velocity, V_m, is assumed to be constant.

For each value of V_m there is an efficiency curve which can be plotted as a function of $\dfrac{U}{V_2}$. The choice of V_m depends to a large extent on the ratio of blade height to mean diameter. From Table 2-2:

$$\Delta H_B = 305.9 \quad BTU/lb$$

$$\dot{m}_1 = 182.4 \quad lb/sec$$

$$V_1 = 5.019 \quad ft^3/lb$$

From equations (5-24) and (5-25):

$$d_{c_1} = 27.65 \ \text{in.}$$

$$V_m h_1 = 1517.6 \ \frac{ft-in}{sec}$$

$V_m = 300$ ft/sec results in a first stage $\frac{h}{d_c}$ ratio of 0.18. Velocities less than 300 ft/sec result in higher efficiencies but the blade heights become too large, especially at the last stage.
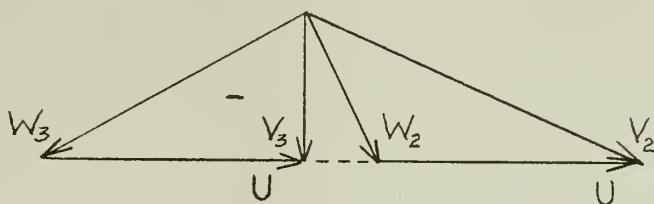
(a) Modified Rateau Stage
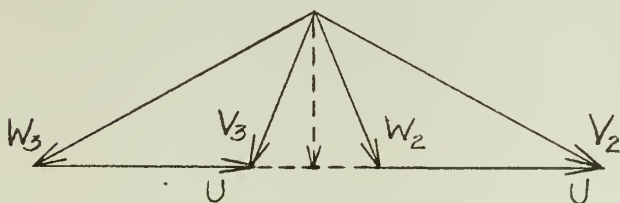
(b) 50% Reaction Stage

Figure 5-6

95

Using the quantities assumed below, the number of stages, n, and stage efficiency, η_s^* , were calculated for the two types of stages indicated in Figure 5-6.

N = 7000 rpm	ϕ = 0.95
U = 800 ft/sec	ψ_2 = 0.95
μ = 1.0	ψ_3 = 0.92
λ = 1.0	K = 0.90

Plots of η_s^* and n vs. $\dfrac{U}{V_2}$ are shown in Figures 5-7 and 5-8. It is apparent that there is little difference in maximum efficiency and that two less stages are required for the modified Rateau stages. For this reason the modified Rateau stage was selected. At the condition of maximum efficiency:

$$\frac{U}{V_2} = 0.7$$

$$\Delta h_B = 35.3 \quad \text{BTU/lb}$$

$$\eta_s^* = 0.854$$

$$x^2 = 0.333$$

$$n = 8.7 \quad \text{theoretical stages}$$

An adjustment must be made in the work per stage to increase the number of stages from 8.7 to 9. For a nine stage turbine having equal work per stage:

$$\left(\Delta h_B\right)_{actual} = \frac{\Delta H_B}{9} = 34.0 \quad BTU/lb$$

Since $\qquad \Delta h_B = \dfrac{U V_{u_2}}{9 J} = \dfrac{U^2}{9 J}\left(\dfrac{V_{u_2}}{U}\right)$ \hfill (5-22b)

Figure 5-7   Effect of $\frac{U}{V_2}$ on Turbine Stage Efficiency

97
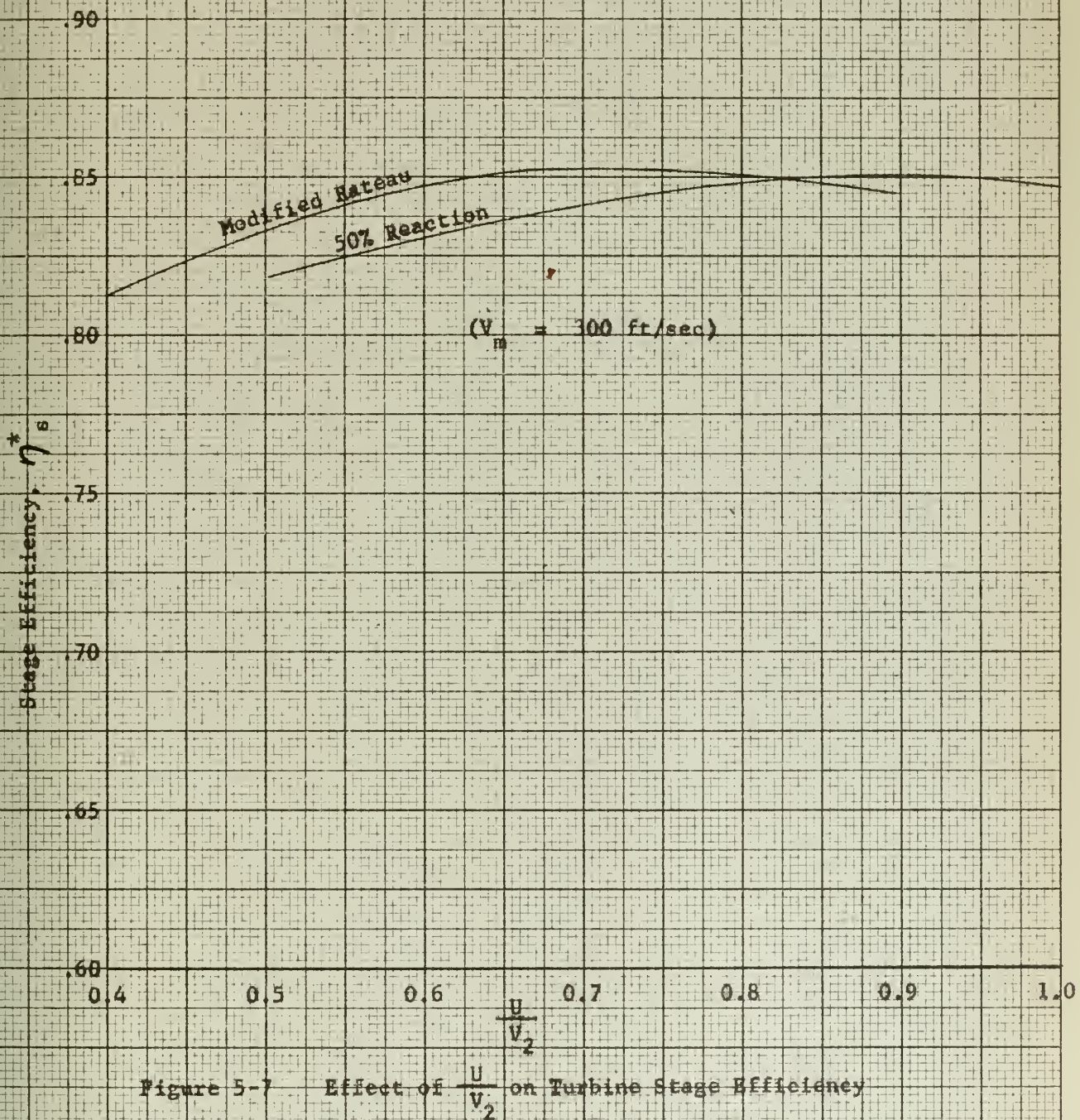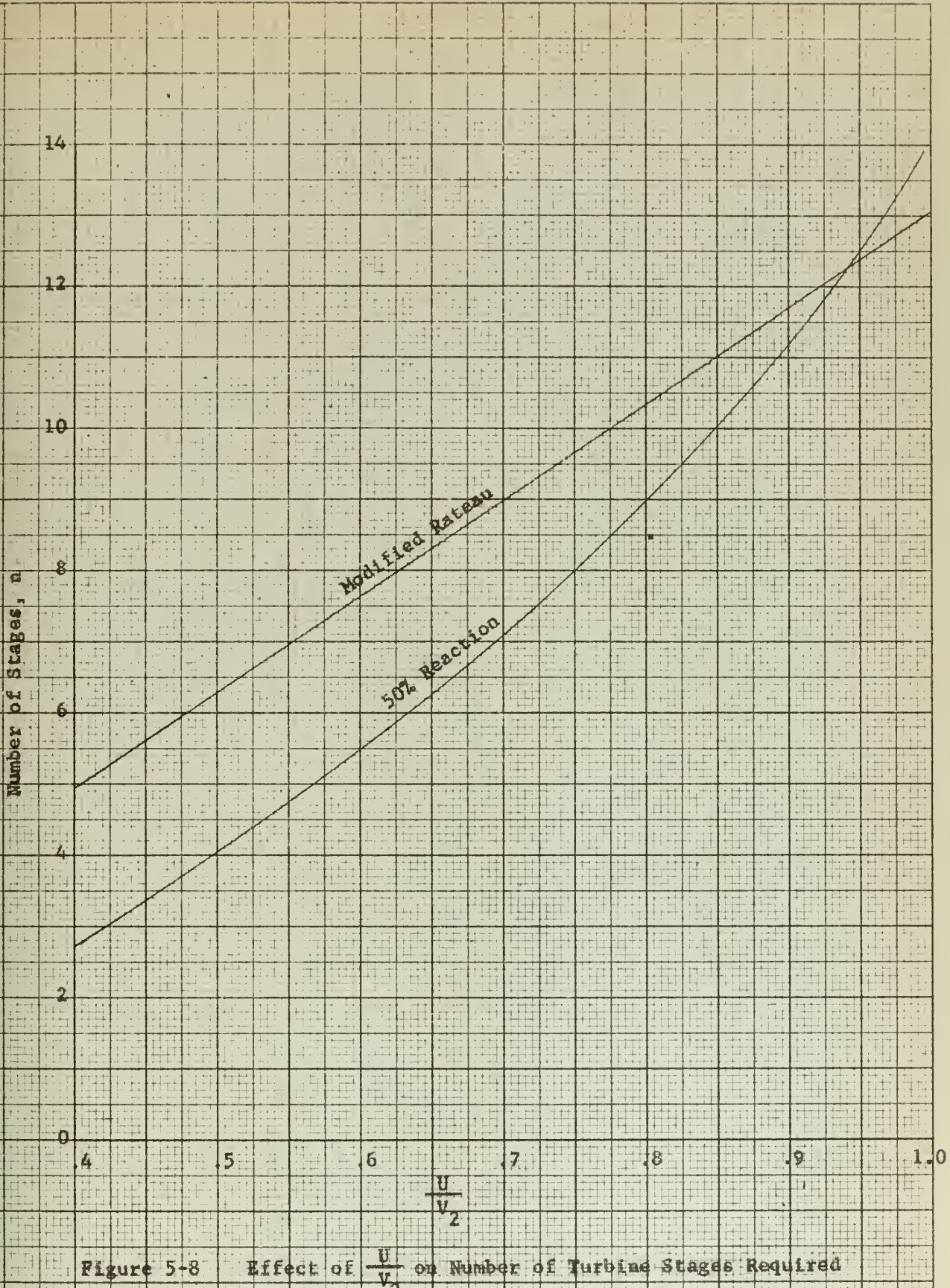
Figure 5-8   Effect of $\frac{U}{V_2}$ on Number of Turbine Stages Required

$$\left(U_2^2\right)_{actual} = \frac{U_2^2 \left(V_{u_2}/U_2\right)}{\left(V_{u_2}/U\right)_{actual}} \times \frac{\left(\Delta h_B\right)_{actual}}{\Delta h_B}$$

To use the same blading, $\dfrac{V_{u_2}}{U_2} = $ constant.

$$\therefore \left(U_2^2\right)_{actual} = U_2^2 \times \frac{\left(\Delta h_B\right)_{actual}}{\Delta h_B}$$

$$\left(U_2\right)_{actual} = \left(\frac{34.0}{35.3}\right)^{\frac{1}{2}} \times 800 = 785 \ ft/sec$$

(5-26)

Recalculation of velocities and dimensions assuming that the blade root diameter, d_i, is constant along the turbine, produces the results contained in Table 5-1.

In calculating the turbine efficiency, η_T, inlet and exit effects and reheat factor must be known. The reheat factor can be calculated by the relation:

$$f = f_\infty \frac{n-1}{n}$$

(4-28)

where f_∞ is obtained from equation (1-9).

To obtain $\left(\Delta H_s\right)_{i,e}$, the values of V_i, V_e, η_i, and η_e must be known. The pipe velocities that are assumed here will be covered in more detail in Chapter VII.

$$V_i = 600 \ ft/sec$$
$$V_e = 500 \ ft/sec$$
$$\eta_i = 0.85$$
$$\eta_e = 0.75$$

Using these data and equations (5-23), (5-1) and (5-4):

$$1+f \quad = \quad 1.0079$$

$$\left(\Delta H_s\right)_{i,n} = \quad 356.9 \quad \text{BTU/lb}$$

$$\left(\Delta H_s\right)_{i,e} = \quad 356.3 \quad \text{BTU/lb}$$

$$\eta_T \quad = \quad 0.858$$

Recalculation of the exit pressure and specific volume is not necessary since the calculated efficiency is only slightly higher than the assumed value. A summary of the first and last stage data for Turbine No. 1 is listed in Table 5-1.

TABLE 5-1

FIRST AND LAST STAGE DATA FOR TURBINE NO. 1

	First Stage	Last Stage	Units
V_2	1121	1162	ft/sec
V_3	294	305	"
α_2	74.78	74.78	degrees
α_3	0	0	"
W_2	418	433	ft/sec
W_3	847	878	"
β_2	45.29	45.29	degrees
β_3	-67.98	-67.98	"
U	785	813	ft/sec
d_i	21.89	21.89	in.
d_c	27.15	28.10	"
d_o	32.41	34.31	"
h	5.26	6.21	"
h/d_c	.194	.221	---

Additional Turbine Data:

$$N = 7000 \text{ rpm}$$

$$\eta_s^* = 0.854$$

$$\eta_T = 0.858$$

$$n = 9 \text{ stages}$$

Turbine No. 2

Unlike Turbine No. 1, this turbine is not restricted to a specific design rpm, thus the speed of this turbine is an additional variable. Since the conditions for this turbine are not very much different from those of Turbine No. 1, a similar type blading is used for simplicity. Thus, U, V_m, μ, λ, ϕ, γ_2, γ_3, and K remain the same. From Table 2-2:

$$\Delta H_B = 193.7 \quad BTU/lb$$

$$\dot{m}_1 = 182.4 \quad lbs/sec$$

$$V_1 = 6.692 \quad ft^3/lb$$

Since
$$d_c = \frac{720\ U}{\pi N} \quad in \qquad (5\text{-}24)$$

and
$$A = \pi d_c h = \frac{\dot{m}V}{V_m} \times 144 \quad in^2 \qquad (5\text{-}25)$$

$$h_1 = \frac{m_1 V_1 N \times 144}{V_{m_1} U_1 \times 720} \qquad = 0.001017\ N \text{ inches}$$

For N = 5500 rpm:

$$h_1 = 5.59 \quad \text{inches}$$

$$d_{c_1} = 33.33 \quad \text{inches}$$

$$h_1/d_{c_1} = 0.168$$

The theoretical number of stages required is 5.5. Using the same

102

method as employed for Turbine No. 1:

$$n = 6 \quad \text{stages}$$

$$V_i = 500 \quad \text{ft/sec}$$

$$V_e = 625 \quad \text{ft/sec}$$

$$\eta_i = 0.85$$

$$\eta_e = 0.75$$

$$1+f = 1.00825$$

$$\left(\Delta H_s\right)_{i,n} = 226.5 \quad \text{BTU/lb}$$

$$\left(\Delta H_s\right)_{i,e} = 231.8 \quad \text{BTU/lb}$$

$$\eta_T = 0.835$$

Since this efficiency is 3.5% larger than assumed in the prelimin-
ary analysis, a recalculation of exit pressure and specific volume is
necessary prior to calculating blade heights and diameters at the last
stage.

$$\left(\frac{P_e}{P_i}\right)^{\frac{Y}{t}} = 1 - \frac{\left(\Delta H_s\right)_{i,e}}{T_i \, c_p} \qquad (1\text{-}7a)$$

$$\therefore \ P_e = 457.6 \quad psia$$
$$V = 8.313 \quad ft^3/lb$$

A summary of first and last stage data for Turbine No. 2 is listed
in Table 5-2.

TABLE 5-2

FIRST AND LAST STAGE DATA FOR TURBINE NO. 2

	First Stage	Last Stage	Units
V_2	1095	1130	ft/sec
V_3	287 '	296	"
α_2	74.78	74.78	degrees
α_3	0	0	"
W_2	408	421	ft/sec
W_3	825	850	"
β_2	45.29	45.29	degrees
β_3	-67.98	-67.98	"
U	765	788	ft/sec
d_i	25.76	25.76	in.
d_c	31.88	32.90	"
d_o	38.00	40.04	"
h	6.12	7.14	"
h/dm	.192	.217	---

Additional Turbine Data:

$$N = 5500 \text{ rpm}$$

$$\eta_s^* = 0.854$$

$$\eta_T = 0.834$$

$$n = 6 \text{ stages}$$

CHAPTER VI

REACTOR

Symbols used in this chapter:

Symbol	Description	Units
A	total heat transfer area	ft^2
a	total coolant flow area	ft^2
c	fission rate per unit of power	fissions/watt - sec
c_p	specific heat at constant pressure	BTU/lb °F
d	diameter of coolant channels	in.
f	thermal utilization factor	---
g	conversion factor, 32.17	$\dfrac{lb_m - ft}{lb_f - sec^2}$
H	height of reactor core	cm or ft
h	convection heat transfer coefficient	BTU/hr - ft^2 - °F
K^2	size-shape factor	cm^{-2}
k	thermal conductivity	BTU/hr - ft^2 - °F/ft
k_∞	multiplication constant for reactor of infinite size	---
k_{eff}	multiplication constant for reactor of finite size	---
L	thermal diffusion length	cm
L_o	thermal diffusion length for pure material	cm
M	mass	grams or lb_m
$\dot{m}$	mass rate of flow	lb/sec
N	number of nuclei/cm^3	---
or	number of coolant channels	---

Symbol	Description	Units
P or	power	— Watts
	pressure	psia
p	resonance escape probability	---
Q	rate of heat transfer	BTU/hr
R	radius of reactor core	cm or ft
t	temperature	°F
V	reactor volume	cm^3 or ft^3
v	specific volume	ft^3/lb
W	coolant velocity	ft/sec
σ	microscopic cross-section	cm^2
μ	absolute viscosity	lb/hr - ft
ϵ	fast fission factor	---
τ	slowing down area for fast neutrons	cm^2
η	neutrons born per absorption	
φ	flux	neutrons/cm^2 - sec
f	friction factor	---
Δ	increment of	

Subscript

a	absorption
av	average
c	graphite
f	fission
He	helium
m	mixture of graphite and uranium

Subscript	Description
u	uranium
w	wall

General

Although the writer has had limited training and no practical
experience in the field of reactor technology, an attempt was made in
this chapter to determine the approximate dimensions of the core of a
helium-cooled enriched reactor, for the primary purpose of establish-
ing the pressure drop of the coolant.

Critical Mass

In determining the core dimensions and the amount of fuel required
to produce a critical mass the following assumptions have been made:

(1) The core consists of a homogeneous mixture of graphite and

U_{235}.

(2) The core shape is a circular cylinder with a height, H,

equal to its diameter, 2R.

(3) The coolant channels occupy 1/3 of the total volume and are

uniformly distributed throughout the core.

(4) The power rating of the reactor is based on a cycle thermal

efficiency of 0.329.

(5) An average flux at full power is of the order 10^{14} neutrons/cm^2

- sec.

(6) The effect of reflector and cooling channel liners is not

included.

(7) No allowance is made for fuel depletion, poison and tempera-

ture effects on reactivity.

For criticality:

$$K_{eff} = 1 = \frac{K_\infty \, e^{-K^2 \tau}}{1 + K^2 L^2} \qquad (6\text{-}1)$$

$$\text{where} \quad K_\infty = \eta \epsilon p f \qquad (6\text{-}2)$$

$$K^2 = \left(\frac{2.4048}{R}\right)^2 + \left(\frac{\pi}{H}\right)^2 \qquad (6\text{-}3)$$

$$L^2 = L_o^2 \left(1 - f\right) \qquad (6\text{-}4)$$

$$f = \frac{1}{1 + \dfrac{N_c \, (\sigma_a)_c}{N_u \, (\sigma_a)_u}} \qquad (6\text{-}5)$$

To calculate these quantities the following nuclear data is known:

$(\sigma a)_c$ = 0.0045 barns   (1 barn = 10^{-24} cm^2)

$(\sigma a)_u$ = 650 barns

L_o^2 = 2500 cm^2

ϵ ≈ 1.0

p ≈ 1.0

η = 2.1

τ = 300 cm^2

Preliminary calculations indicate that for the power and flux requirements:

$$\frac{N_c}{N_u} \approx 14,400$$

Therefore:

$$f = 0.909$$

$$k_\infty = 1.91$$

$$L^2 = 227 \text{ cm}^2$$

By trial and error calculations using equation (6-1):

$$K^2 = 0.0013$$

$$H = 159 \text{ cm} = 5.23 \text{ ft}$$

To allow for the effect of the cooling channels and considering that they are distributed uniformly over the entire core, the following approximations have been made:

(1) L^2 increases to 9/4 of its original value

(2) τ increases to 9/4 of its original value

Referring to equation (6-1) the net effect of K^2 is to decrease it to 4/9 of its original value or:

$$K^2 = 0.000578$$

$$H = 239 \text{ cm} = 7.85 \text{ ft}$$

The ratio of graphite to uranium by mass is:

$$\frac{M_c}{M_u} = \frac{12}{235} \times \frac{N_c}{N_u} = 736$$

Since it can be expected that the density of the graphite will be somewhat less than its pure state (1.65 g/cm^2), it is assumed to be

equal to 1.55 g/cm^3. Then:

$$V_c = 2/3 \ \frac{\pi \ H^3}{4} = 7.175 \times 10^6 \ cm^3 = 253 \ ft^3$$

$$M_c = 7.175 \times 10^6 \times 1.55 = 11.15 \times 10^6 \ grams = 24,600 \ lbs$$

$$M_u = \frac{11.15 \times 10^6}{736} = 15150 \ grams = 33.4 \ lbs$$

$$N_c = \frac{1.55 \times 6.023 \times 10^{23}}{12} = 7.77 \times 10^{22} \ nuclei/cm^3$$

$$N_u = \frac{7.77 \times 10^{22}}{14,400} = 5.4 \times 10^{18} \ nuclei/cm^3$$

The power rating of the reactor, based on a 50,000 HP output at a thermal efficiency of 0.329, is:

$$P = \frac{50,000}{0.329} = 152,000 \ HP$$
$$= 1.135 \times 10^8 \ Watts$$

The average flux is:

$$\phi_{av.} = \frac{c \ P}{N_u \ \sigma_f \ V_m} \qquad \frac{neutrons}{cm^2 - sec} \qquad (6\text{-}6)$$

where $\quad c = 3 \times 10^{10} \qquad$ fissions/watt - sec

$$\sigma_f = 549 \qquad \text{barns}$$

$$V_m \approx V_c = 7.175 \times 10^6 \ cm^3$$

or

$$\phi = 1.6 \times 10^{14} \ \frac{neutrons}{cm^2 - sec}$$

110

The burn-up rate is:

$$U_{235} \text{ used/day} = \frac{\text{No. of fissions}}{\text{day}} \times \frac{\text{No. of absorptions}}{\text{fission}} \times \frac{\text{No. of grams}}{\text{absorption}}$$

$$= (c \times 3600) P \left(\frac{\sigma_a}{\sigma_f}\right)_u \times \frac{235}{6.023 \times 10^{23}} \quad (6\text{-}7)$$

$$= 136 \text{ grams/day at full power}$$

Cooling System

Although the dimensions of the core and the amount of fuel and moderator mixture will increase when allowance is made for the effects of fuel depletion, poison and temperature, it is assumed here that this will have little effect on the characteristics of the cooling system. From the helium properties listed in Table 2-2 for the inlet and exit of the reactor and the dimensions of the core:

$$V_{He} = \frac{1}{3} V = 126.5 \quad ft^3$$

$$a = \frac{V_{He}}{H} = 16.15 \quad ft^2$$

$$W_{av} = \frac{m V_{av.}}{a} = 49 \quad ft/sec$$

For an average wall temperature of 1500°F the heat transferred to the coolant is:

$$Q = h A (t_w - t_{av.}) = c_p \dot{m} (t_{out} - t_{in}) \times 3600 \quad (6\text{-}8)$$
$$BTU/hr$$

111

where $t_w - t_{av}$ = 387.8 °F

$t_{out} - t_{in}$ = 475.5 °F

$\dot{m}$ = 182.4 lb/sec

c_p = 1.24 BTU/lb - °F

or $$h = \frac{1 \times 10^6}{A} \quad BTU/hr - ft^2 - °F$$

$$N = a \times \frac{4}{\pi d^2} \times 144 = \frac{2960}{d^2}$$

$$A = N \frac{\pi d}{12} H = \frac{6090}{d} \quad ft^2$$

$$h = 164 \, d \quad BTU/hr - ft^2 - °F \quad (6\text{-}9)$$

Another expression for h as a function of d is obtained from the turbulent flow heat transfer equation:

$$N_u = 0.023 \, Re^{0.8} \, Pr^{0.4} \quad (3\text{-}16)$$

in which the following gas properties are evaluated for an average coolant temperature of 1119°F:

v = 4.348 ft^3/lb

c_p = 1.24 BTU/lb - °F

μ = 0.10 lb/hr - ft

k = 0.18 BTU/hr - ft^2 - °F/ft

112

.

Equation (3-16) reduces to:

$$h = \frac{179.5}{d^{0.2}} \quad \text{BTU/hr} - \text{ft}^2 - \text{°F} \qquad (6\text{-}10)$$

From equations (6-9) and (6-10):

$$d = 1.08 \text{ inches}$$

$$h = 178 \text{ BTU/hr} - \text{ft}^2 - \text{°F}$$

$$N = 2540 \text{ channels}$$

Pipe Friction

$$\Delta P = \zeta \, \frac{W^2 H}{2 \, g \, v \, d} \qquad (3\text{-}13)$$

$$\zeta = 0.184 \, Re^{-0.2} = 0.0225 \qquad (3\text{-}14)$$

where $R_e = 36{,}500$

$$\therefore \quad \Delta P = 0.117 \text{ psi}$$

113

TABLE 6-1

SUMMARY OF THE REACTOR CORE DATA

H	7.85 ft
M_u	15.15 Kg
M_c	11,150 Kg
V	379 ft^3
W	49.0 ft/sec
d	1.08 inches
N	2,540 channels
P	0.117 psi (Pipe friction only)

CHAPTER VII

INSTALLATION

Symbols used in this chapter:

Symbol	Description	Units
d	diameter	in
g	conversion factor, 32.17	$\dfrac{lb_m - ft}{lb_f - sec^2}$
$\dot{m}$	mass rate of flow	lb/sec
P	pressure	psia
t	thickness	in
V	velocity	ft/sec
v	specific volume	ft^3/lb
Δ	increment	---
η	efficiency	---
σ	stress	psi
ϕ	defined on page 118	---
ψ	defined on page 118	---

Subscripts

i	inside, initial
o	outside
th	thermal
w	wall

General

In the previous chapters each of the major components of the cycle has been analyzed. The following data were obtained:

(1) Basic internal dimensions of the turbo-machines such as diameters and blade heights.

(2) Turbo-machine characteristics such as stage and overall efficiencies, number of stages, and velocity diagrams at the mean radius for the first and last stages.

(3) Heat exchanger dimensions including dimensions and arrangement of tubes, shell inside diameter, and total internal volume.

(4) Heat exchanger pressure losses due to pipe friction.

In order to combine these components in an installation, additional information is necessary. Such items as piping, casings, inlet and exit connections, bearings, couplings, auxiliary equipment, control apparatus, and expansion joints, must be designed. It is beyond the scope of this investigation to cover all of these items, so only those which affect the size of the plant and pressure drops will be considered in this chapter.

Before considering the individual components there follows a review of some of the relations used in this chapter.

Effect of Changes of Specific Volume between Inlet and Exit of Heat Exchangers

In the calculations for pipe friction using equation (3-13) a mean specific volume was used. Given the channel below:

116
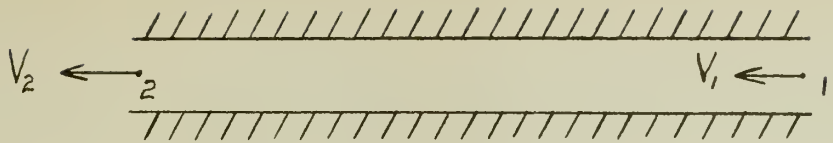
Figure 7-1   Channel of Constant Flow Area

the pressure change between (1) and (2) due to the change in specific volume can be approximated by the equation:

$$P_2 - P_1 \approx \left(\frac{V}{v}\right)^2_{av.} \frac{V_1 - V_2}{g \times 144} \quad psi \qquad (7\text{-}1)$$

Pressure Drop for Flow Acceleration
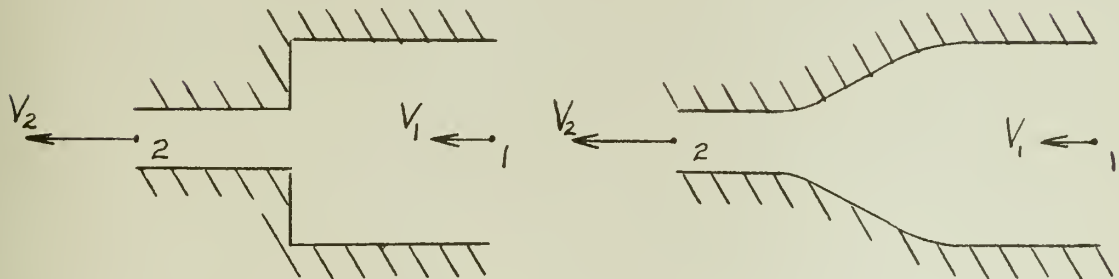
Figure 7-2   Channels of Decreasing Flow Area

$$P_2 - P_1 = \frac{1}{\phi} \left(\frac{V_1^2 - V_2^2}{2\,g\,v \times 144} \right) \quad psi \qquad (7\text{-}2)$$

117

where ϕ is the efficiency of conversion from static pressure to velocity head.

Pressure Increase for Flow Deceleration Due to a Sudden Enlargement
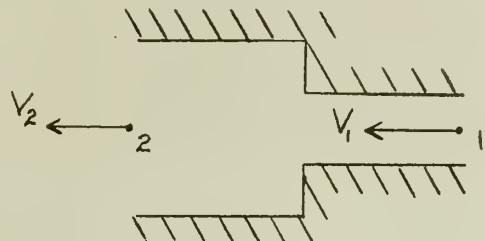
Figure 7-3   Channel with an Abrupt Increase in Flow Area

From the momentum theorem,

$$P_2 - P_1 = \frac{V_2 V_1 - V_2^2}{g v \times 144} \qquad psi \qquad (7-3)$$

Pressure Increase in a Diffuser
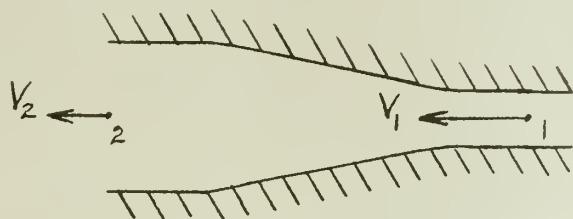
Figure 7-4   Diffuser

$$P_2 - P_1 = \frac{\psi (V_1^2 - V_2^2)}{2 g v \times 144} \qquad psi \qquad (7-4)$$

where ψ is the efficiency of conversion from velocity

118

head to static pressure.

Pipe Dimensions

The internal pipe diameters and flow velocities are related as follows:

$$d_i = \left(\frac{4}{\pi} \frac{\dot{m}v}{V} \right)^{\frac{1}{2}} \times 12 \qquad \text{inches} \qquad (7\text{-}5)$$

The wall thickness, t_w, depends on the allowable circumferential stress, σ :

$$t_w = \frac{(\Delta P) d_i}{2\sigma} \qquad \text{inches} \qquad (7\text{-}6)$$

Piping

In analyzing the turbines and compressors inlet and exit pipe velocities were specified in order that overall efficiencies could be determined. The internal pipe diameters corresponding to these velocities can be calculated from equation (7-5). It is desirable to use standard pipe sizes although these may differ slightly from the calculated diameters. Using the pipe property chart and allowable stress data from Littleton[13], Table 7-1 was compiled with the use of equations (7-5) and (7-6).

The actual outside diameters of some of the installed piping will be greater than those listed by the amount of insulation required. For locations four through eight (Figure 2-1) this will be in the order of six to eight inches. For the other locations none will be required unless some is desired to limit the space temperature.

119

TABLE 7-1

PIPING DATA

Location (Fig. 2-1)	Pipe Schedule	d_o (in.)	t_w (in.)	d_i (in.)	V* (ft/sec)	(psi)	Material (ASTM)
1	30	18.000	0.417	17.125	400	8400	A-155
2	40	16.000	0.500	15.000	400	9000	A-155
3	40	16.000	0.500	15.000	300	9700	A-155
4	80	12.750	0.687	11.376	450	8200	A-155
5	60	16.000	0.656	14.688	600	10100	A-213
6	80	18.000	0.917	16.126	600	8400	Inconel X
7**	40	16.000	0.500	15.000	500	9200	Inconel X
8**	40	16.000	0.500	15.000	625	6600	A-213
9**	Special	20.375	0.425	19.625	200	10000	A-155

* These are velocities assumed for the cycle and differ slightly from those corresponding to the pipe diameters listed.

** Two pipes required.

Regenerator and Precooler

It is convenient to discuss these two units together since they are in series for cooling the hot gas between the power turbine discharge and the inlet to Compressor No. 1. Figure 7-5 illustrates the two units showing approximate dimensions. For an allowable stress of 10,000 psi for the regenerator shell, its thickness is two inches. An allowable stress of 12,000 psi for the precooler shell requires a thickness of one inch. For purposes of calculating pressure changes, schematics of the flow passages are illustrated in Figures 7-6 and 7-7.

Referring to Figure 7-6, the flow has been broken down into the following parts:

(a) Deceleration by means of a diffuser of 2 foot length between (1) and (2), with corresponding pressure recovery.

(b) Deceleration to zero velocity at (3) with no pressure recovery.

(c) Acceleration to V_4.

(d) Pipe friction effects between (4) and (5).

(e) Deceleration from V_5 to zero velocity at (6) with no pressure recovery.

(f) Acceleration to V_7.

(g) - (k) For remainder of the channel between (7) and (12) the effects are similar to those outlined in items (b) - (f) above.

(l) Effects of changes in specific volume between inlet and exit.

A summary of the velocities and pressure changes for the locations specified in Figure 7-6 is listed in Table 7-2. Where applicable, $\gamma = 0.85$ and $\phi = 0.80$.

121
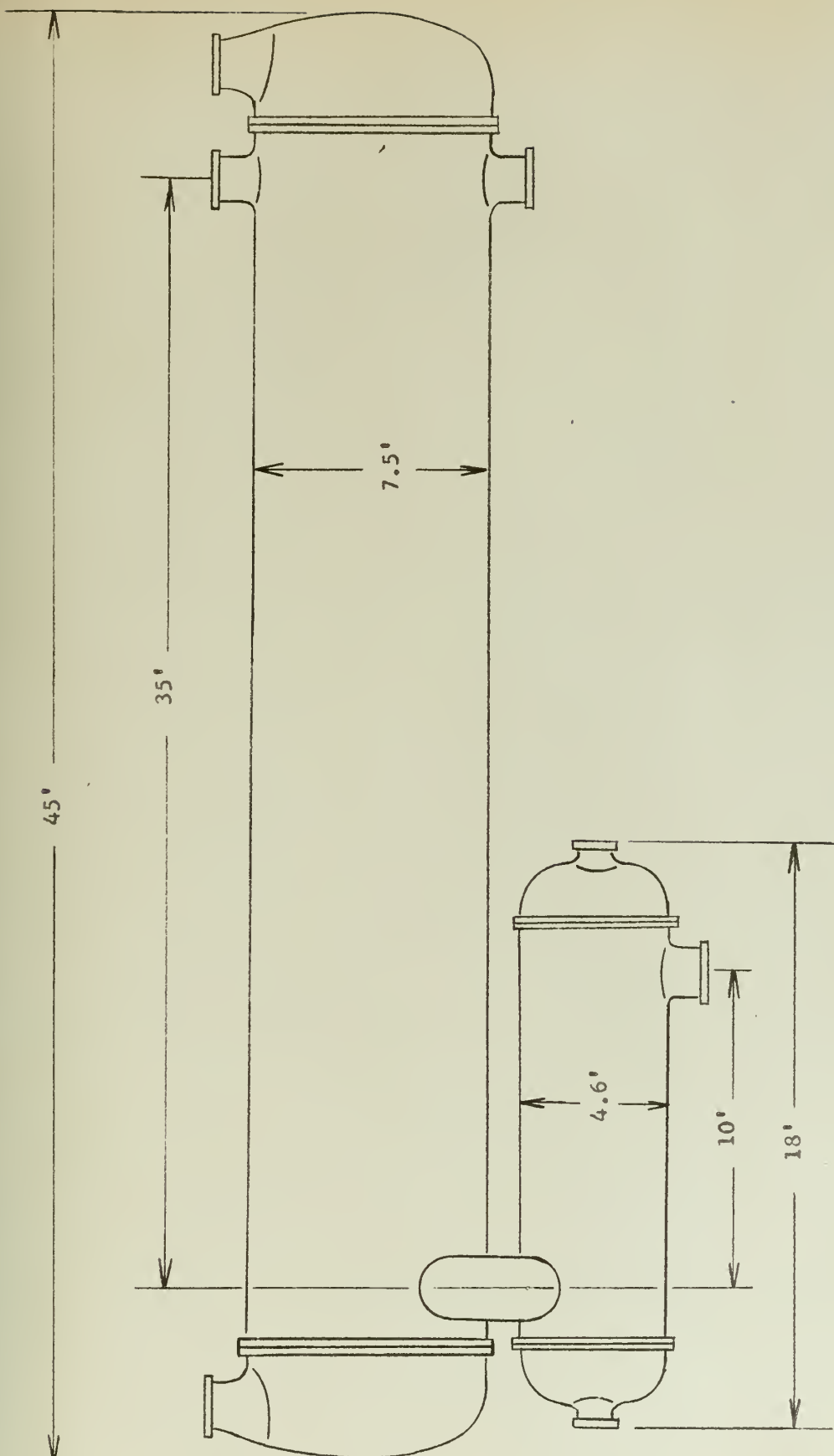
Figure 7-5   Regenerator and Precooler

122
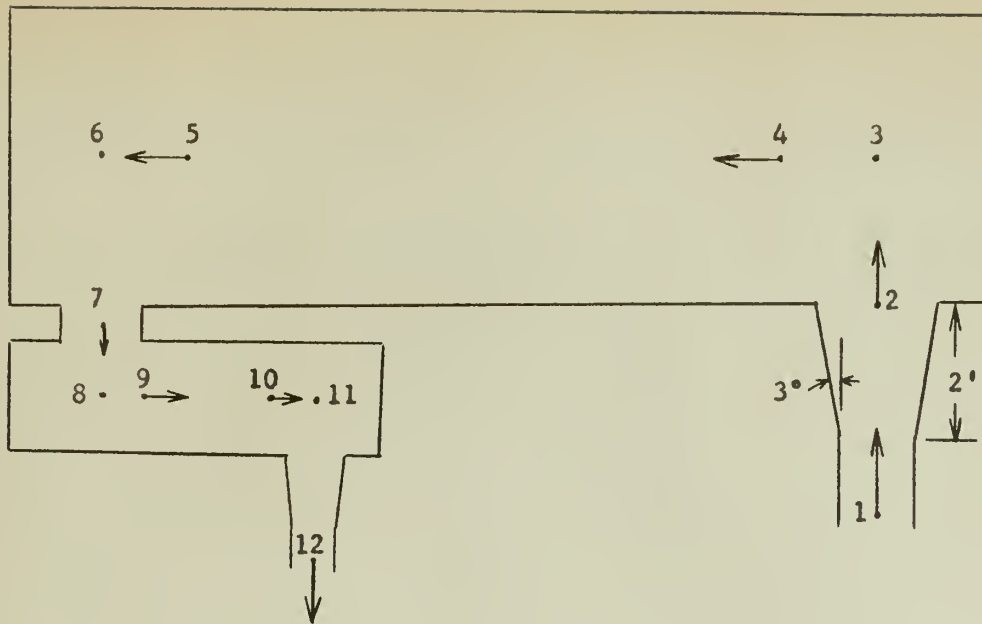
Figure 7-6   Schematic Representation of Flow through the
              Regenerator and Precooler
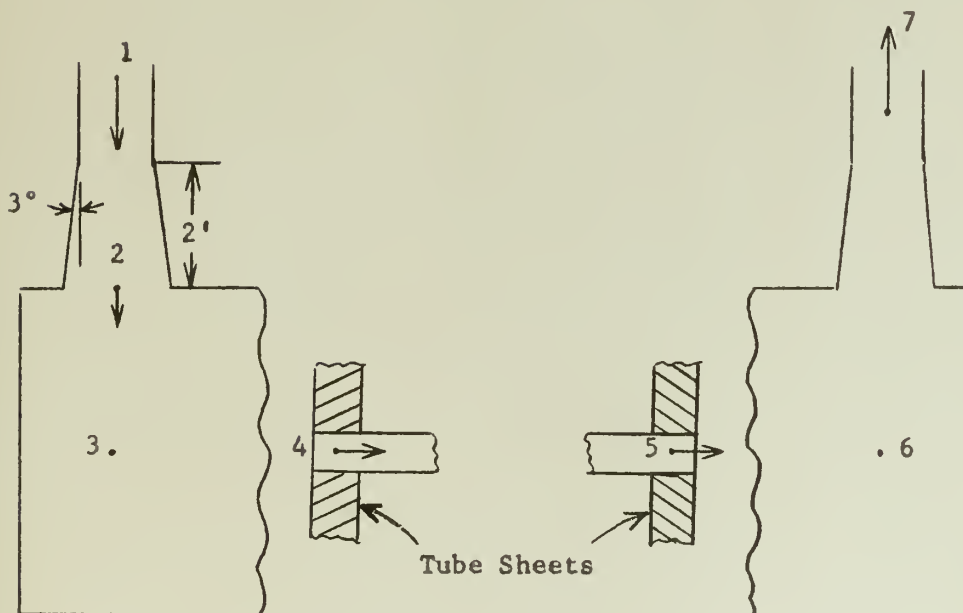
Figure 7-7   Schematic Representation of Flow through the
              Regenerator (H.P. Side)

123

TABLE 7-2

SUMMARY OF PRESSURE LOSSES IN THE REGENERATOR AND PRECOOLER

Location (x) (Figure 7-6)	$v(ft^3/lb)$	$V(ft/sec)$	$P_x - P_{x-1}(psi)$	Equation
1	8.413	625	-----	----
2	"	458	1.97	(7-4)
3	"	0	0	(7-3)
4	"	53.6	-0.05	(7-2)
5	4.607	28.7	-0.76	(3-13)
6	"	0	0	(7-3)
7	"	200	-1.17	(7-2)
8	"	0	0	(7-3)
9	"	86	-0.22	(7-2)
10	3.428	64	-0.72	(3-13)
11	"	0	0	(7-3)
12	"	400	-6.30	(7-2)
Compressibility Effect			0.12	(7-1)

$$\Delta P_{total} = -7.13$$

$$\frac{\Delta P}{P_i} = 0.0158$$

TABLE 7-3

SUMMARY OF PRESSURE LOSSES IN THE REGENERATOR (H. P. SIDE)

Location (x) (Figure 7-7)	$v(ft^3/lb)$	V(ft/sec)	$P_x - P_{x-1}$ (psi)	Equation
1	1.883	450	----	----
2	"	323	7.22	(7-4)
3	"	0	0	(7-3)
4	"	66	-0.31	(7-2)
5	3.677	132	-12.03	(3-13)
6	"	0	0	(7-3)
7	"	600	-13.20	(7-2)
Compressibility Effect			-1.09	(7-1)

$$\Delta P = -19.43$$

$$\frac{\Delta P}{P_i} = 0.0194$$

Considering the conditions inside the tubes of the regenerator, the schematic of Figure 7-7 indicates that items (a) - (f) on page 121 apply. The results are listed in Table 7-3. Where applicable, $\gamma = 0.85$ and $\phi = 0.80$.

125
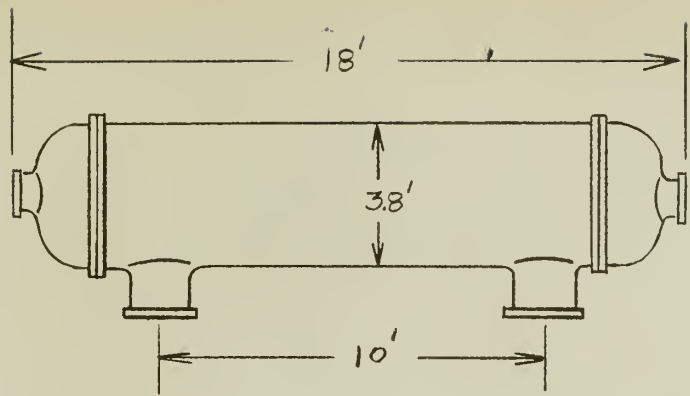
Figure 7-8   Intercooler
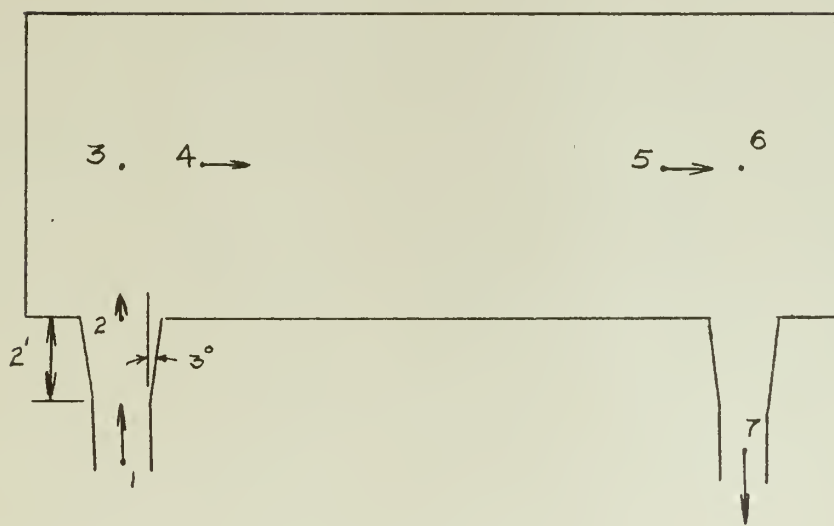
Figure 7-9   Schematic Representation of Flow through the Intercooler

126

Intercooler

The intercooler is similar to the precooler and the flow is broken down in the. same manner. The dimensions indicated in Figure 7-8 are approximate and based on calculations in Chapter III. For an allowable stress of 14,000 psi, the shell thickness is one inch.

TABLE 7-4

SUMMARY OF PRESSURE LOSSES IN THE INTERCOOLER

Location (x) (Figure 7-9)	$v(ft^3/lb)$	$V(ft/sec)$	$P_x - P_{x-1}(psi)$	Equation
1	2.768	400	----	-----
2	"	294	2.43	(7-4)
3	"	0	0	(7-3)
4	"	82	-0.32	(7-2)
5	2.309	68	-1.05	(3-13)
6	"	0	0	(7-3)
7	"	300	-5.26	(7-2)
Compressibility Effect			0.09	(7-1)

$$\Delta P = -4.11$$

$$\frac{\Delta P}{P_i} = 0.0062$$

127

Reactor

As illustrated in Figures 7-10 and 7-11, the flow through the
reactor is similar to that through the heat exchangers. The overall
dimensions are only estimates, since no calculations were made concern-
ing the thickness of shielding and reflector required.

TABLE 7-5

SUMMARY OF PRESSURE DROPS IN THE REACTOR

Location (x)	$v(ft^3/lb)$	$V(ft/sec)$	$P_x - P_{x-1}(psi)$	Equation
1	3.677	600	-----	-----
2	"	434	4.29	(7-4)
3	"	13.8	0.34	(7-3)
4	"	41.5	-0.06	(7-2)
5	5.019	56.5	-0.12	(3-13)
6	"	18.9	0.03	(7-3)
7	"	600	-9.69	(7-2)
Compressibility Effect			-0.04	(7-1)

$$\Delta P \quad = \quad -5.25$$

$$\frac{\Delta P}{P_i} \quad = \quad 0.0054$$

Figure 7-11   Schematic Representation of
Flow through the Reactor
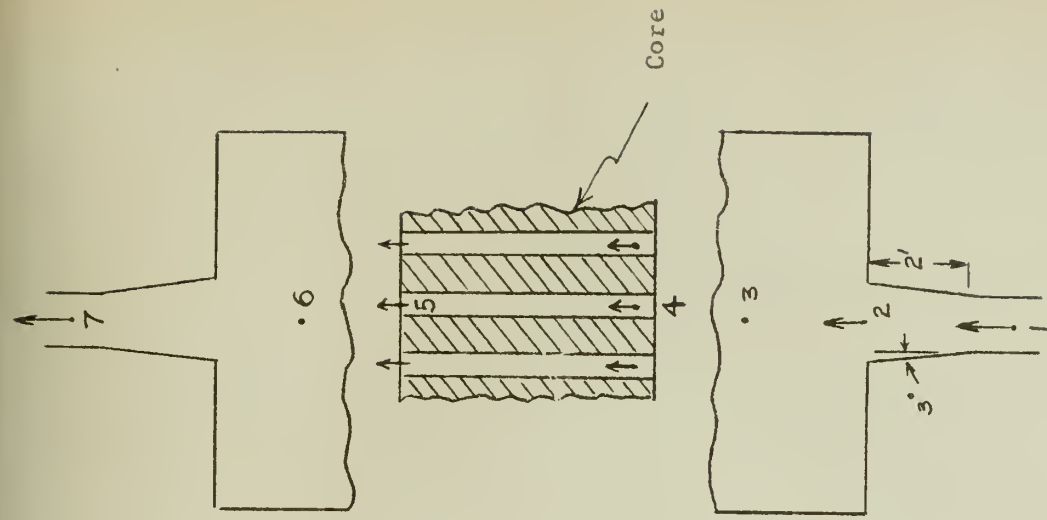
Figure 7-10   Reactor

129
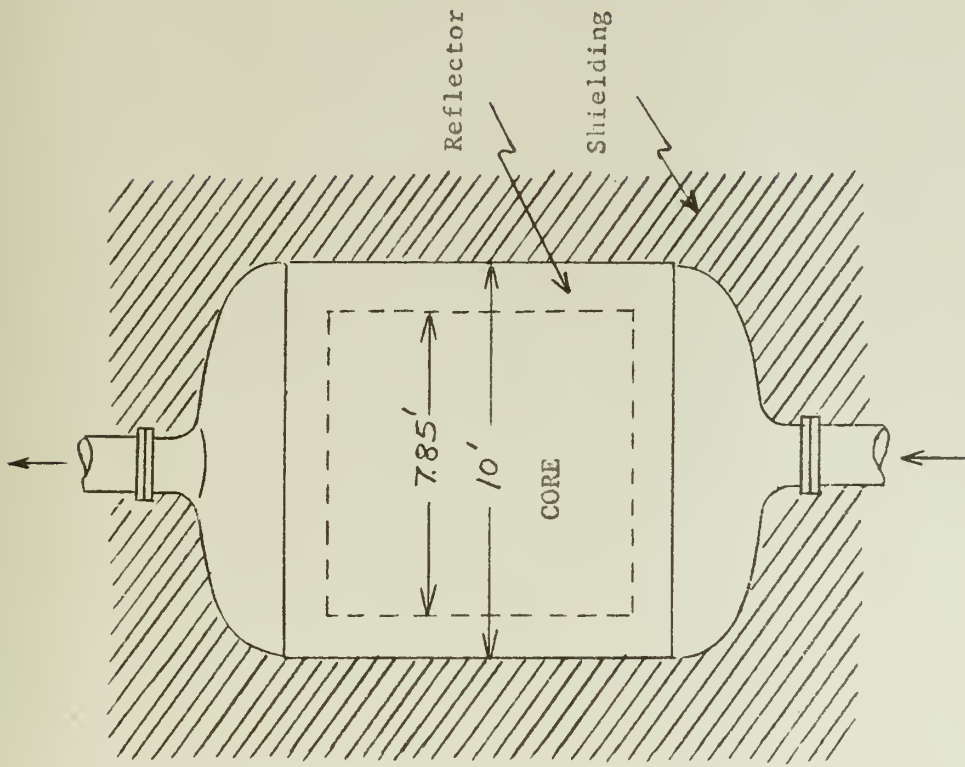
Tables 7-6 and 7-7 compare the calculated machine efficiencies and pressure losses with those assumed in Chapter II. Another cycle analysis using these calculated values results in the following new performance indices:

$$\dot{m} = 162.5 \text{ lb/sec (For 50,000 HP output)}$$

$$\eta \text{ th} = 0.361$$

$$\text{helium rate} = 11.7 \text{ lb/HP - hr}$$

$$\text{work ratio} = 0.424$$

TABLE 7-6

COMPARISON OF ASSUMED AND CALCULATED VALUES OF $\Delta P/P_i$

Unit	$\Delta P/P_i$ (assumed)	$\Delta P/P_i$ (calculated)
Regenerator		
High pressure side	0.015	0.0194
Low pressure side	0.010	0.0158
Precooler	0.0075	
Reactor	0.010	0.0054
Intercooler	0.005	0.0062

TABLE 7-7

COMPARISON OF ASSUMED AND CALCULATED VALUES OF MACHINE EFFICIENCIES

Unit	η (assumed)	η (calculated)
Compressor No. 1	0.84	0.867
Compressor No. 2	0.80	0.840
Turbine No. 1	0.85	0.858
Turbine No. 2	0.80	0.835
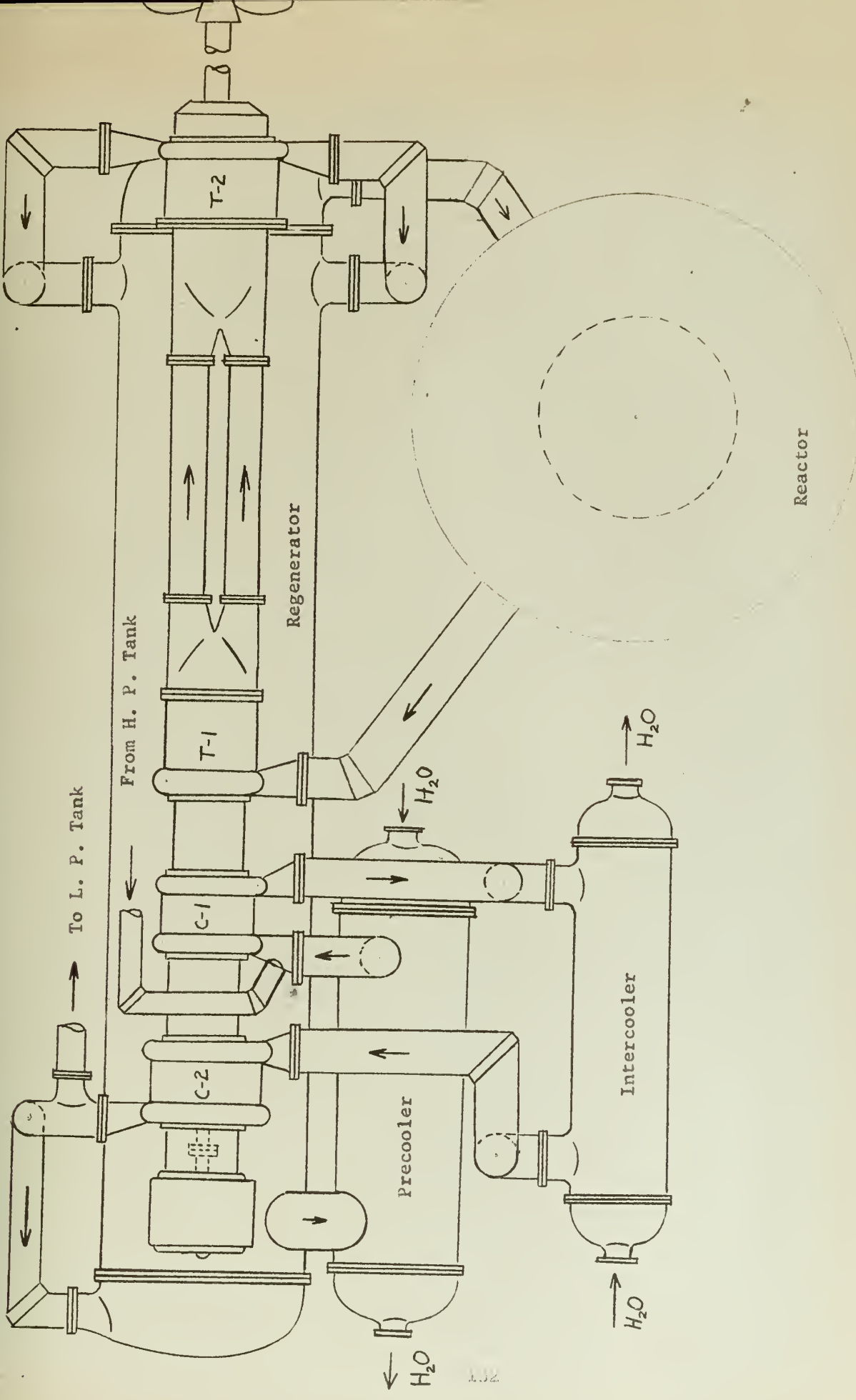
Figure 7-12   Power Plant Arrangement

CHAPTER VIII

STRESSES

Symbols used in this chapter:

Symbol	Description	Units
A	area	in^2
b	width of turbine disk	in
c	chord	in
c_P	specific heat at constant pressure	BTU/lb - °F
F	force	lb_f
g	conversion factor, 32.17	$\dfrac{lb_m}{lb_f} \dfrac{ft}{sec^2}$
h	blade height	in
or	enthalpy	BTU/lb
I	moment of inertia	in^4
J	conversion factor, 778	ft - lb/BTU
K	coefficient defined in equation (5-10b)	---
M	bending moment	in - lb
m	mass	lb_m
$\dot{m}$	mass rate of flow	lb/sec
N	rotational speed	rpm
P	pressure	psia
q	centrifugal loading	lb/in
r	radius	in
s	spacing	in
T	absolute temperature	°R

Symbol	Description	Units
t	temperature	°F
U	peripheral speed	ft/sec
V	absolute velocity	ft/sec
v	specific volume	ft^3/lb
W	relative velocity	ft/sec
Z	no. of blades	---
α	absolute flow angle	degrees
β	relative flow angle	degrees
γ, γ'	angles defined by Figure 8-3	degrees
δ, δ'	angles defined by Figure 8-2	degrees
ϕ	acute angle between y-axis and $\overline{F}_g$	degrees
θ	acute angle between $\overline{F}_g$ and $\overline{m}$	degrees
σ	stress	psi
ω	rotational speed	rad/sec
Δ	increment	---
ρ	density	lb/ft^3
χ	degree of reaction	---
η	efficiency	---

Subscript	Definition
c	centrifugal or center
CG	center of mass
g	gas force
i	inner
m	axial
min	minimum

Subscripts	Definition
max	maximum
o	outer
R	rotor
s	stator, isentropic, stage
x, y	coordinates
overscore	vector

General

Of the quantities that were assumed in the analysis of the turbo-machines the most critical were the allowable peripheral speeds. These had an effect on the machine efficiencies, radial dimensions and the number of stages required. The choice of the allowable speeds was made for both the compressors and turbines on the premise that the blade and rotor stresses would not exceed safe limits. It is the objective in this chapter to investigate the parts of the machines where the stresses will be the greatest; namely, the first and last stages of Compressor No. 1 and the first stage of Turbine No. 1.

Compressor Blades
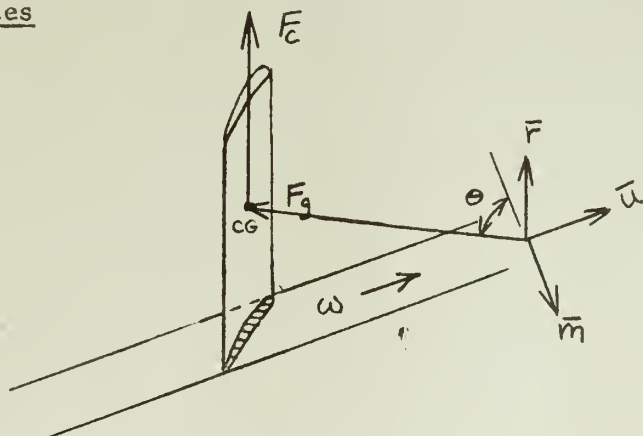
Figure 8-1   Forces Acting on a Compressor Rotor Blade

For free-vortex flow and equal work input at all radii:

$$rV_u = \text{constant}$$

$$V_m = \text{constant}$$

From the first and last stage data given in Tables 4-2 and 4-5, the equations above, and Figure 4-3, the velocity diagrams for the inner, center and outer radii have been determined as indicated in Tables 8-1 and 8-2.

TABLE 8-1

VELOCITY DIAGRAM DATA FOR THE FIRST STAGE OF COMPRESSOR NO. 1

	Inner	Center	Outer	Units
r	19.435	20.25	21.065	in.
$V_1 = V_3 = V_m$	436	436	436	ft/sec
V_2	616	604	593	"
V_{u_1}	0	0	0	"
V_{u_2}	435	418	402	"
W_1	1263	1310	1358	"
W_2	868	928	987	"
W_{u_1}	1135	1235	1285	"
W_{u_2}	750	819.	883	"
U	1185	1235	1285	"
β_1	69.8	70.6	71.2	degrees
β_2	59.8	62.0	63.7	"
α_1	0	0	0	"
α_2	45.0	43.8	42.7	"
c	0.82	0.82	0.82	in.
s_R	0.79	0.82	0.85	"
s_s	0.37	0.39	0.41	"

TABLE 8-2

VELOCITY DIAGRAM DATA FOR THE LAST STAGE OF COMPRESSOR NO. 1

	Inner	Center	Outer	Units
r	19.435	20.10	20.765	in.
$V_1 = V_3 = V_m$	432	432	432	ft/sec
V_2	609	599	591	"
V_{u_1}	0	0	0	"
V_{u_2}	429	415	402	"
W_1	1262	1300	1333	"
W_2	869	920	964	"
W_{u_1}	1185	1225	1267	"
W_{u_2}	756	810	865	"
U	1185	1225	1267	."
β_1	70	70.6	71.1	degrees
β_2	60.2	62.0	63.4	"
α_1	0	0	0	"
α_2	44.8	43.8	43.0	"
c	0.82	0.82	0.82	in.
s_R	0.79	0.82	0.85	"
s_s	0.38	0.39	0.40	"

Blade Profiles

The profiles selected for the rotor and stator blades are NACA
Airfoil 6309 and modified Joukowsky Airfoil 603, respectively. These

are illustrated in Figures 8-2 and 8-3 showing important dimensions.
Table 8-3 lists important section properties. Angles γ and δ
depend on space/chord ratio, the velocity diagrams, and the type of
profile. Actual values of δ were obtained from de Haller[14] whereas
values for γ were obtained from Vavra[15]. These are tabulated in
Table 8-4.

TABLE 8-3

AIRFOIL SECTION PROPERTIES FOR A CHORD OF 0.82 INCHES

	NACA 6309	Joukousky 603	
Area	0.042	0.0532	in^2
$I_{min} = I_x$	1.46×10^{-5}	5.4×10^{-5}	in^4
$I_{max} = I_y$	1.565×10^{-3}	1.89×10^{-3}	in^4

TABLE 8-4

VALUES OF γ AND δ (FIGURES 8-2 AND 8-3)

	First Stage			Last Stage		
	Inner	Center	Outer	Inner	Center	Outer
δ	27.2	25.2	23.5	27.3	25.3	23.8
δ'	27.5	25.5	23.8	27.6	25.6	24.1
γ	26.0	25.0	24.8	----	----	----
γ'	29.1	28.1	27.9	----	----	----
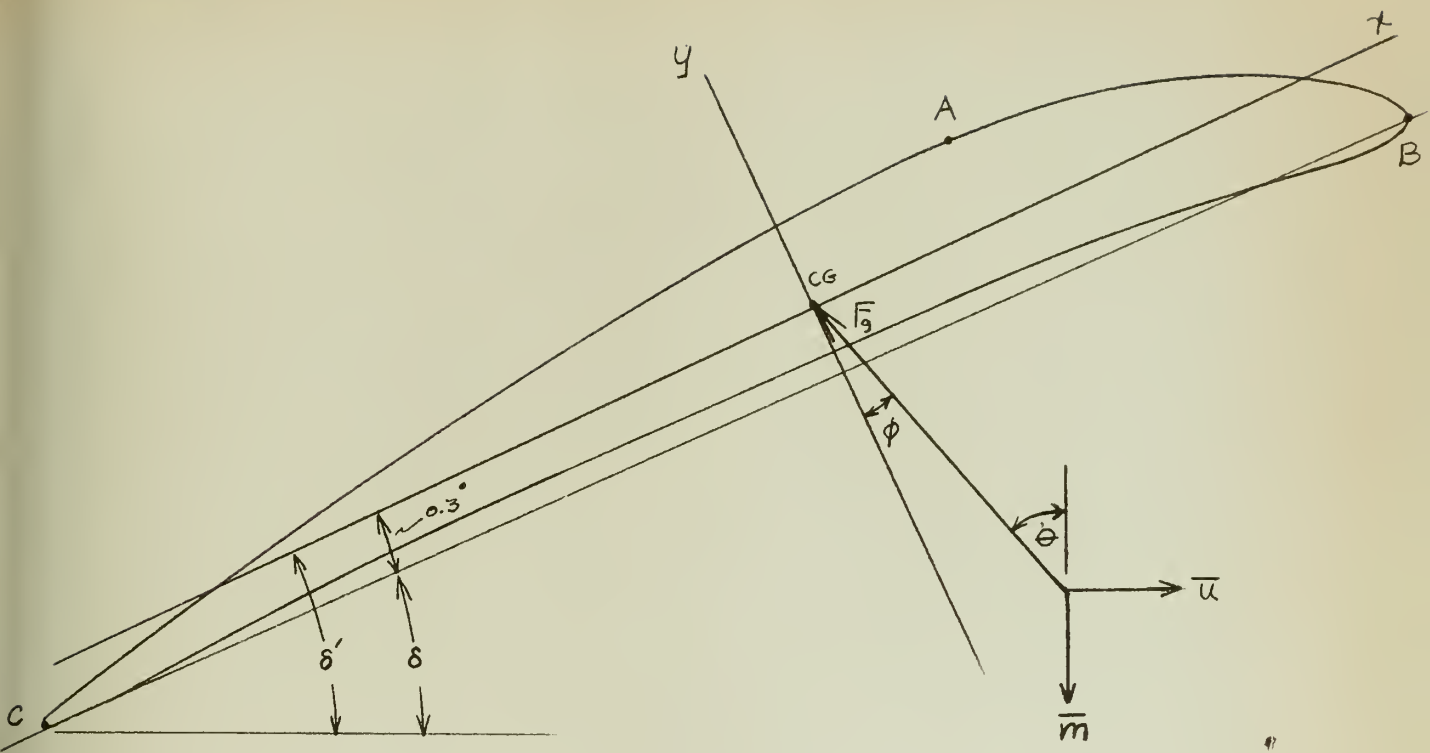
Location	x (in)	y (in)
A	0.0928	0.0492
B	0.347	-0.041
C	0.473	-0.034

Figure 8-2   First Stage Rotor Blade for Compressor No. 1
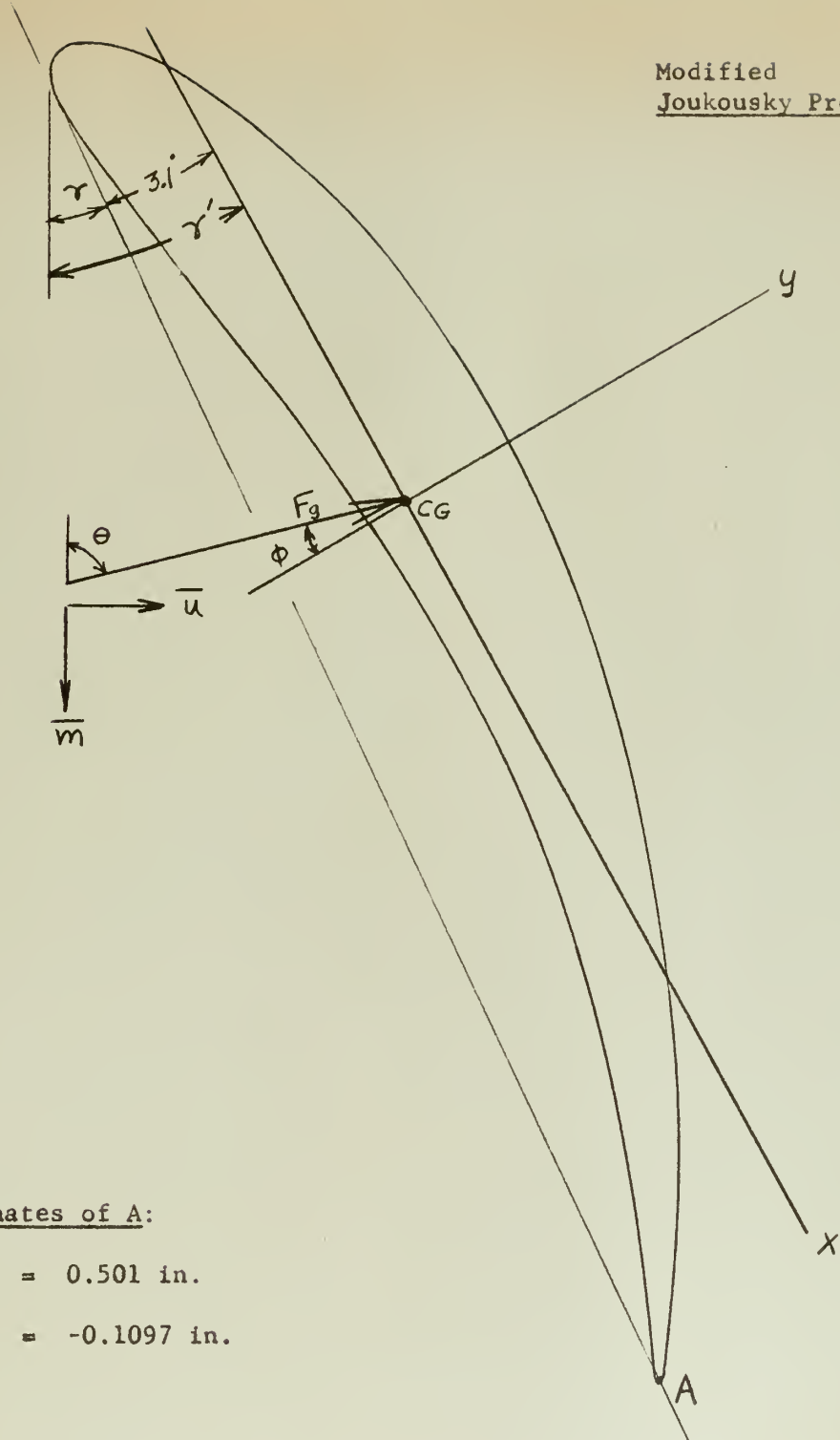
Coordinates of A:

x = 0.501 in.

y = -0.1097 in.

Figure 8-3   First Stage Stator Blade for Compressor No. 1

141

Centrifugal Blade Forces

The maximum blade stress will occur at the blade root. A portion of this stress for the rotor blade will be due to the centrifugal force effects and can be calculated from the following equations:

$$F_c = \frac{m}{g} \frac{r_{CG}}{12} \omega^2 \quad lb_f \qquad (8\text{-}1)$$

$$\sigma_c = \frac{F_c}{A} \qquad (8\text{-}2)$$

For constant chord blades of low alloy steel ($\rho = 0.282$ lb/in^3) the centrifugal forces and stresses are as listed in Table 8-5.

TABLE 8-5

CENTRIFUGAL FORCES AND CORRESPONDING STRESSES FOR

THE ROTOR BLADES OF COMPRESSOR NO. 1

	First Stage	Last Stage	Units
	733	733	rad/sec
r_{CG}	20.25	20.10	in.
m	0.0193	0.0158	lb_m
F_c	544	442	lb_f
σ_c	12,950	10,500	psi

Gas Bending Force

The force acting on the blades due to the pressure differential and the change in momentum of the flow can be calculated by means of

the momentum theorem.

(a) Rotor   (b) Stator
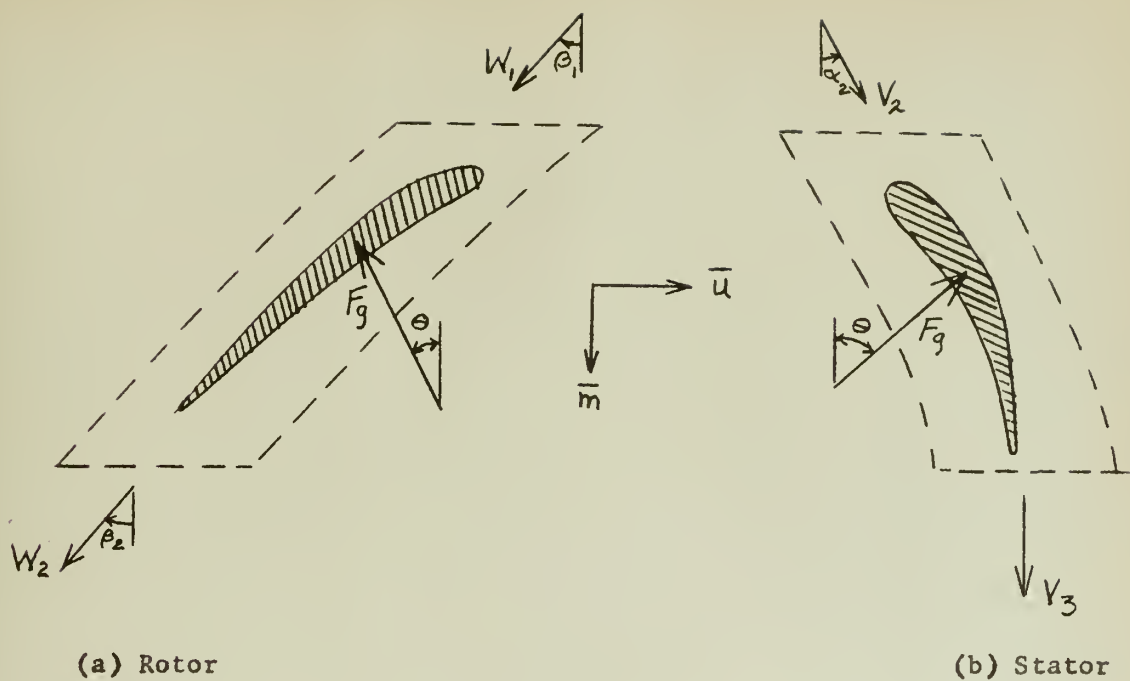
Figure 8-4   Momentum Theorem Control Surfaces for the Blades
of Compressor No. 1

Referring to Figure 8-4 and using the dashed line as a control
surface, the momentum equations become:

For Rotor:

$$- \frac{\dot{m}_z}{g} \overline{W}_1 + \frac{\dot{m}_z}{g} \overline{W}_2 = \left(P_1 A_1 - P_2 A_2 \right) \overline{m} - \overline{F}_g \qquad (8\text{-}3)$$

$$\text{where} \quad A_1 = A_2 = sh$$

For Stator:

$$- \frac{\dot{m}_z}{g} \overline{V}_2 + \frac{\dot{m}_z}{g} \overline{V}_3 = \left(P_2 A_2 - P_3 A_3 \right) \overline{m} - \overline{F}_g \qquad (8\text{-}3a)$$

$$\text{where} \quad A_2 = A_3 = sh$$

143

Solving these equations for $\bar{F}_g$ requires knowledge of the number of blades, Z, and the pressure rise across the blades in addition to quantities previously determined.

$$Z = \frac{2\pi r}{s} \quad blades \tag{8-4}$$

The pressure rise for the first stage is easily calculated from equation (1-6a) since T_1 and P_1 are known from Table 2-2 and Δh_s from Table 4-4. Although the degree of reaction, χ, is defined in terms of enthalpies, it can be expressed in terms of pressure rise with little error.

$$\chi = \frac{h_2 - h_1}{h_3 - h_1} \approx \frac{P_2 - P_1}{P_3 - P_1} \tag{4-15}$$

For the last stage, the quantities Δh_s and T_1 must be calculated. This can be done by equations (4-24) and (1-5a) since h_3, U, τ and ηs are known. The pressure rise can then be calculated from equations (1-6a) and (4-15).

Table 8-6 indicates values of Z, ΔP and $\bar{F}_g$.

TABLE 8-6

GAS FORCES ACTING ON THE BLADES OF COMPRESSOR NO. 1

	First Stage		Last Stage		Units
	Rotor	Stator	Rotor	Stator	
Z	155	326	144	324	Blades
ΔP	24.2	4.9	29.8	6.1	psi
F_g	36.0	7.92	35.9	---	lbs
Θ	26.2	66.7	25.2	---	degrees

The gas bending stresses have been calculated for three locations on the rotor blades and one on the first stage stator blade.

Referring to Figures 8-2 and 8-3, the stresses can be expressed as:

$$\sigma_g = \frac{M_x y}{I_x} - \frac{M_y x}{I_y} \qquad\qquad (8-5)$$

where
$$M_y = -\frac{h}{2} F_g \sin \phi$$
$$M_x = -\frac{h}{2} F_g \cos \phi$$
$$\phi = \Theta - \delta' \quad \text{for rotor}$$
$$\phi = (\Theta - 90) + \gamma' \quad \text{for stator}$$

TABLE 8-7

BLADE ROOT STRESSES DUE TO GAS FORCES

| | Rotor | | Stator | |
	First Stage	Last Stage	First Stage	Units
ϕ	-1.3	-2.4	+4.6	degrees
M_x	-29.3	-23.8	-6.42	in - lb
M_y	0.62	1.0	+0.52	in - lb
$(\sigma_g)_A$	-99,000	-80,300	+12,850	psi
$(\sigma_g)_B$	+82,350	+66,600	----	psi
$(\sigma_g)_C$	+68,500	+55,800	----	psi

Applying the centrifugal force stresses to the gas force stresses, a maximum stress of 95,300 psi occurs at point B of the first stage rotor blade. This stress is higher than normal long-life design criteria and would preferably be reduced to 50,000 psi or less. Lower stresses can be obtained by modifying the blades. Instead of using a 9% thick blade at all sections, a tapered blade 12% thick at the root would reduce the stress to 53,700 psi. If, in addition, the chord is increased by 10%, the stress is further reduced to about 40,400 psi.

There are many low-alloy, high-strength steels that would be suitable for the compressor blades such as AISI Nos. 4140, 4340, 6150, 8640 and 8740.

As one might expect, the stresses in the stator are small compared to the rotor stresses since most of the pressure rise is in the rotor blades. Providing there is no serious vibration problem, no major design changes would have to be made to permit a mean peripheral speed

of 1235 ft/sec.

Turbine Blades
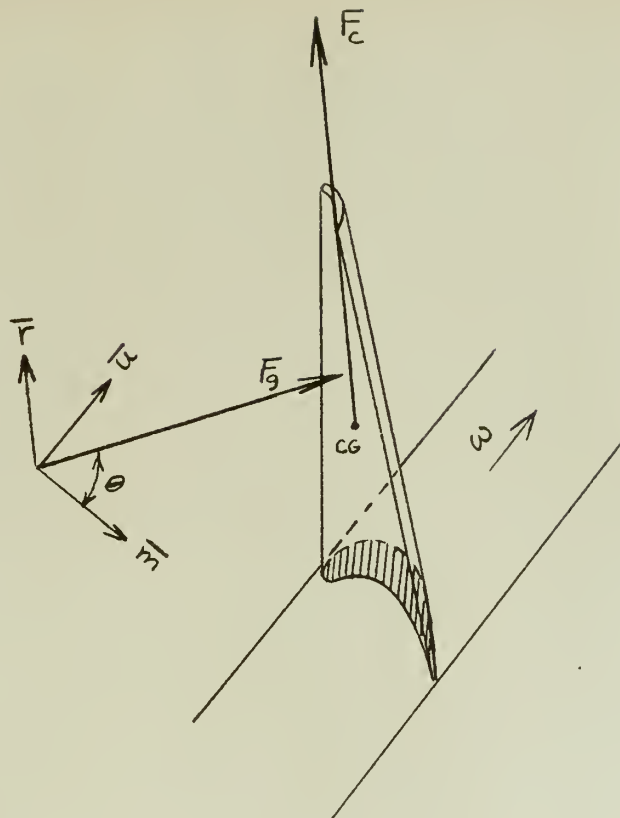
Figure 8-5   Forces Acting on a Turbine Rotor Blade

For free-vortex flow and equal work output at all radii:

$$rV_u = \text{constant}$$

$$V_m = \text{constant}$$

From the first stage data given in Table 5-1, the equations above, and Figure 5-3, the velocity diagrams for the inner, center and outer radii have been determined as indicated in Table 8-8.

147

TABLE 8-8

VELOCITY DIAGRAM DATA FOR FIRST STAGE OF TURBINE NO. 1

|	Inner	Center	Outer	Units
r	10.945	13.575	16.205	in.
V_2	1370	1121	9.52	ft/sec
$V_1 = V_3 = V_m$	294	294	294	"
V_{u_2}	1339	1080	904	"
V_{u_3}	0	0	0	"
W_2	763	418	296	"
W_3	696	847	982	"
W_{u_2}	706	295	-33	"
W_{u_3}	-633	-785	-937	"
U	633	785	937	"
β_2	67.4	45.29	-6.4	degrees
β_3	-65.0	-67.98	-72.6	"
α_2	77.6	74.78	72.0	"
α_3	0	0	0	"
s_R	0.81	1.0	1.19	in.
s_s	0.97	1.2	1.43	"

Also: N = 7000 rpm

h = 5.26 in.

Z_R = 85

Z_s = 71

148

Rotor Blades

The root, center and tip profiles of the first-stage rotor blade are illustrated in Figure 8-6. This is a tapered blade in which the centroids of each section lie on a radial line. The maximum blade stresses occur at the blade root, hence only these section properties have been determined. As in the compressor, the stress is due to a combination of gas bending force and centrifugal force effects.

Centrifugal Force

The volume and center of mass of the tapered blade having root, center and tip sections as shown in Figure 8-6 can be determined from the following plot:

Distance from Blade Root (in.)
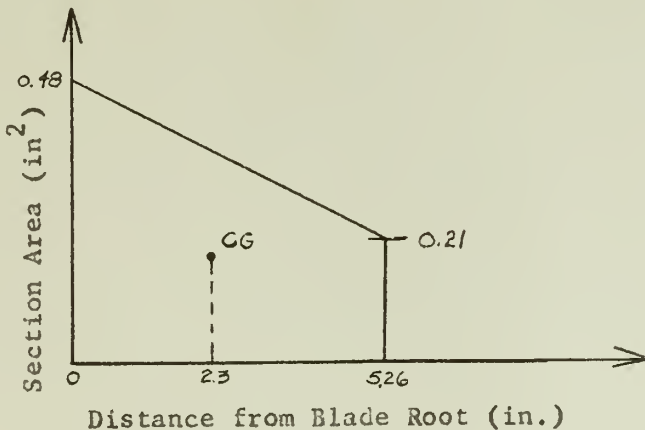
Blade Volume $= \dfrac{0.21 + 0.48}{2} \times 5.26 = 1.82 \text{ in}^3$

$r_{CG} = 10.94 + 2.30 = 13.24 \text{ in}$

For alloy S-816: ($\rho = 0.310 \text{ lb/in}^3$)

$m = 0.564 \text{ lb per blade}$

$F_c = 10,500 \text{ lb per blade}$

$\sigma_c = 21,900 \text{ psi}$

149

Tip

Area = 0.21 in^2

Spacing = 1.19 in.

Center

Area = 0.345 in^2

Spacing = 1.0 in.

Root

Area = 0.48 in^2

Spacing = 0.81 in.

$I_x = I_{min} = 0.014$ in^4

$I_y = I_{max} = 0.068$ in^4
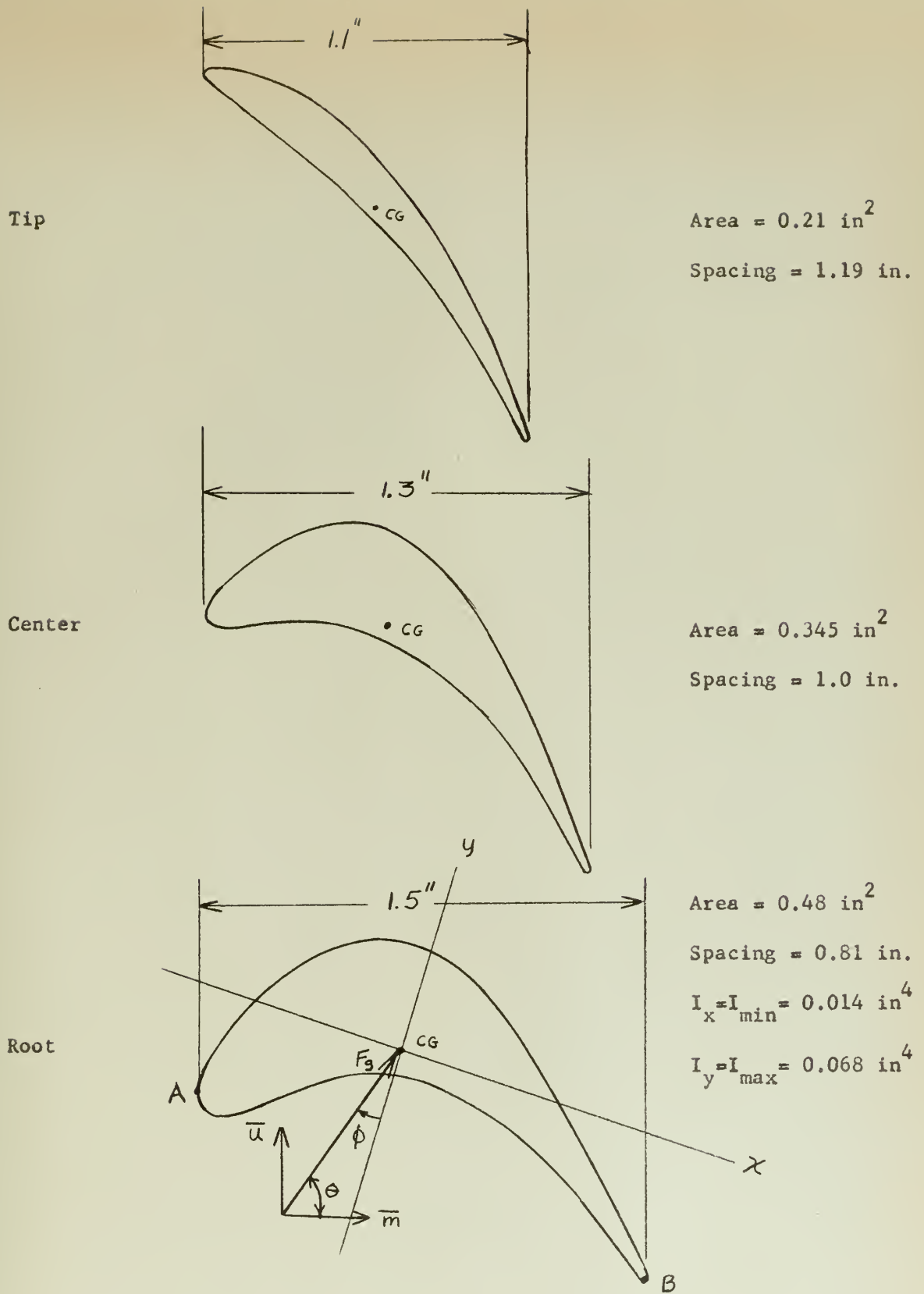
Figure 8-6   First Stage Rotor Blade Profiles for Turbine No. 1

Gas Force

Before the gas force can be calculated by means of the momentum theorem, the pressure differential between the inlet and exit to the rotor blade must be calculated.

Referring to Figures 5-4 and 5-5, the following relations are apparent:

$$\left(\Delta h_s\right)_{1,2} = \frac{1}{\phi^2} \frac{V_2^2}{2gJ} - \frac{V_1^2}{2gJ} \tag{8-6}$$

$$h_{2*} = h_2 + \left(1 - \gamma_2^2\right) \frac{W_2^2}{2gJ} \tag{5-12}$$

$$h_2 = h_1 - \frac{\left(V_2^2 - V_1^2\right)}{2gJ} \tag{8-7}$$

$$\left(\Delta h_s\right)'' = \left(\Delta h_s\right)' - \frac{1}{\phi^2} \frac{V_2^2}{2gJ} \tag{8-8}$$

Also:

$$\left(\Delta h_s\right)_{1,2} = T_1 \, c_p \left[1 - \left(\frac{P_2}{P_1}\right)^{\gamma_t}\right] \tag{1-7a}$$

$$t_{2*} = \frac{h_{2*} - h_{600°F}}{1.24} + 600 \tag{1-5}$$

151

$$\left(\Delta h_s\right)^* = \frac{\Delta h_\beta}{\eta_s^*} \tag{5-10a}$$

$$\left(\Delta h_s\right)^* = \left(\Delta h_s\right)' + K\frac{V_3^2}{2gJ} \tag{5-10b}$$

Combining equations (8-8), (5-10a) and (5-10b):

$$\left(\Delta h_s\right)'' = \frac{\Delta h_\beta}{\eta_s} - K\frac{V_3^2}{2gJ} - \frac{1}{\phi^2}\frac{V_2^2}{2gJ} \tag{8-9}$$

Also:

$$\left(\Delta h_s\right)'' = T_2\, c_p\left[1 - \left(\frac{P_3}{P_2}\right)^{\frac{\gamma_t}{}}\right] \tag{1-7a}$$

From these equations, Tables 2-2, 8-8 and Chapter V, the pressure rises are:

$$P_1 - P_2 = 27.7 \text{ psi}$$

$$P_2 - P_3 = 11.5 \text{ psi}$$

Using the dashed line of Figure 8-7 as a control surface, the momentum theorem becomes:

$$-\frac{\dot{m}_z}{g}\overline{W}_2 + \frac{\dot{m}_z}{g}\overline{W}_3 = \left(P_2 A_2 - P_3 A_3\right)\overline{m} - \overline{F_g}$$

where $A_2 = A_3 = sh$
$$\overline{F_g} = 60.5\,\overline{m} + 72.0\,\overline{u}$$
or $\quad \overline{F_g} = 94.3 \text{ lb}; \quad \Theta = 49.9°$

152
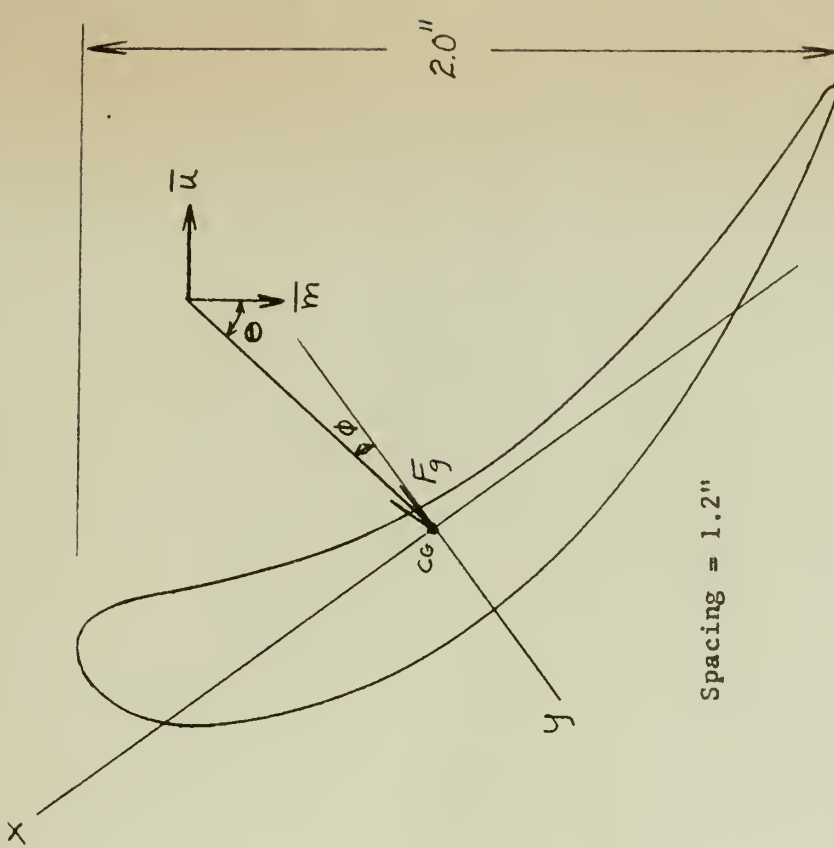
Figure 8-8   Turbine Nozzle Profile
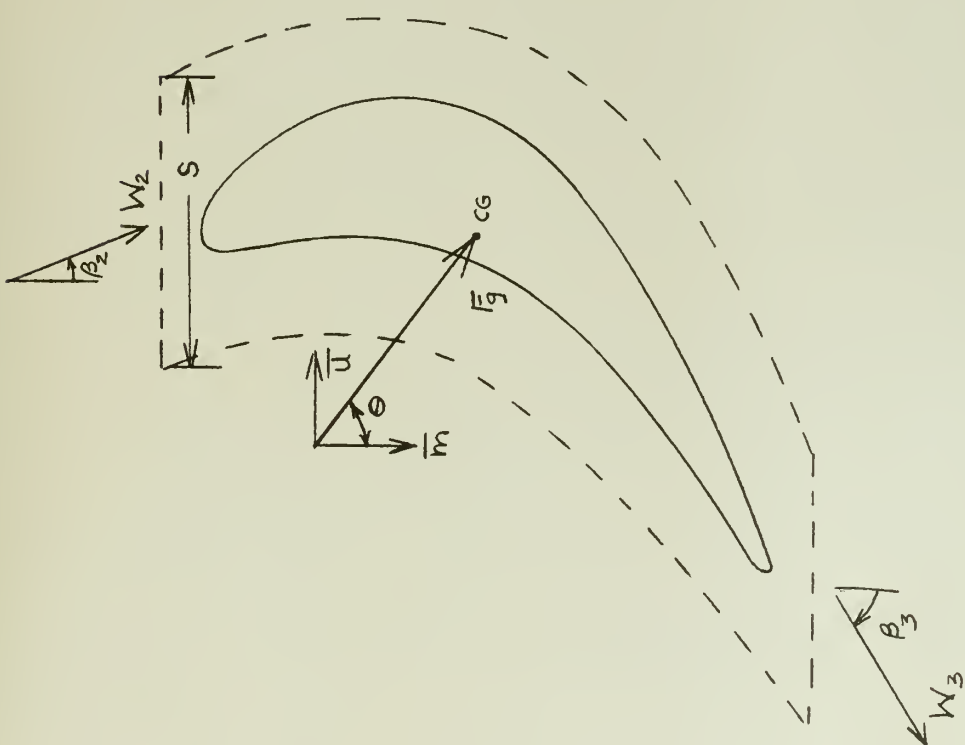

Figure 8-7   Momentum Theorem Control
Surface for a Turbine
Rotor Blade

153

The fibers most heavily stressed in the root cross section are indicated by A and B in Figure 8-6. Axes x and y are principal axes.

$$\sigma = \frac{M_x y}{I_x} - \frac{M_y x}{I_y} \qquad (8\text{-}5)$$

$$\text{where } M_x = -\frac{h}{2} F_g \cos \phi$$

$$M_y = \frac{h}{2} F_g \sin \phi$$

$$\phi = 72.5° - \Theta = 22.6°$$

$$\therefore (\sigma_g)_A = 7080 \text{ psi}$$
$$(\sigma_g)_B = 6610 \text{ psi}$$

A total stress of 29,000 psi exists at A. Jennings[16] states that the blade root temperature will normally be 175-300°F lower than the gas stagnation temperature or a temperature of about 1100°F here. The stress-to-rupture in 100,000 hours for S-816 alloy is 47,000 psi at 1100°F. Therefore, the rotor blade stresses are not excessive for the blading of Figure 8-6 providing no serious vibration problem exists.

Stator Blades

There is no attempt here to do a detailed stress analysis on the nozzles. Figure 8-8 illustrates a typical profile for the root section. The gas force has been calculated to be 200 lbs at $\Theta = 25.6°$. The minimum section modulus, $\frac{I_{min}}{y_{max}}$, of the profile is approximately 17.6 x 10^{-3} in^3 and can be increased by increasing the % thickness and/or chord length.

154

$$\sigma_{max} \approx \frac{M_x \, y_{max}}{I_x} \qquad = \quad 30,000 \text{ psi}$$

Since the stator blade temperatures will be higher than the rotor blades, a maximum stress of less than 25,000 psi is desirable and this can easily be achieved by slight modification of the blade.

Turbine Disks
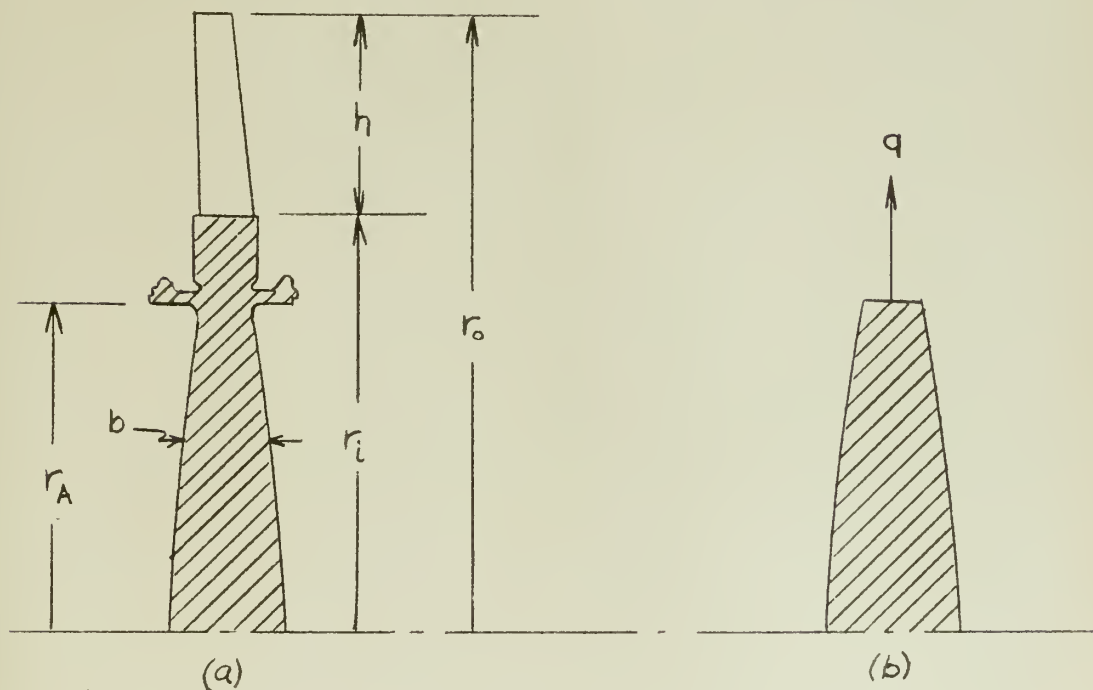
Figure 8-9   Turbine Disk

155

The type of disk being considered is illustrated in Figure 8-9.
All dimensions except the disk width, b, are known from blade data and
practical considerations. The value of b depends on stress conditions
due to the centrifugal forces. The stresses in the rim ($r_A < r < r_i$) are
substantially smaller than the blade root stresses so they need not be
calculated here. Since we are interested in the stresses and dimensions
of the remainder of the disk, the blade and disk assembly can be replac-
ed by the hub portion only ($0 < r < r_A$) with an external load due to
centrifugal forces of the mass of the blades and the rim (Figure 8-9(b)).

Because of the irregular shape of the rim it is divided into sec-
tions (Figure 8-10) for the purpose of determining centrifugal forces.
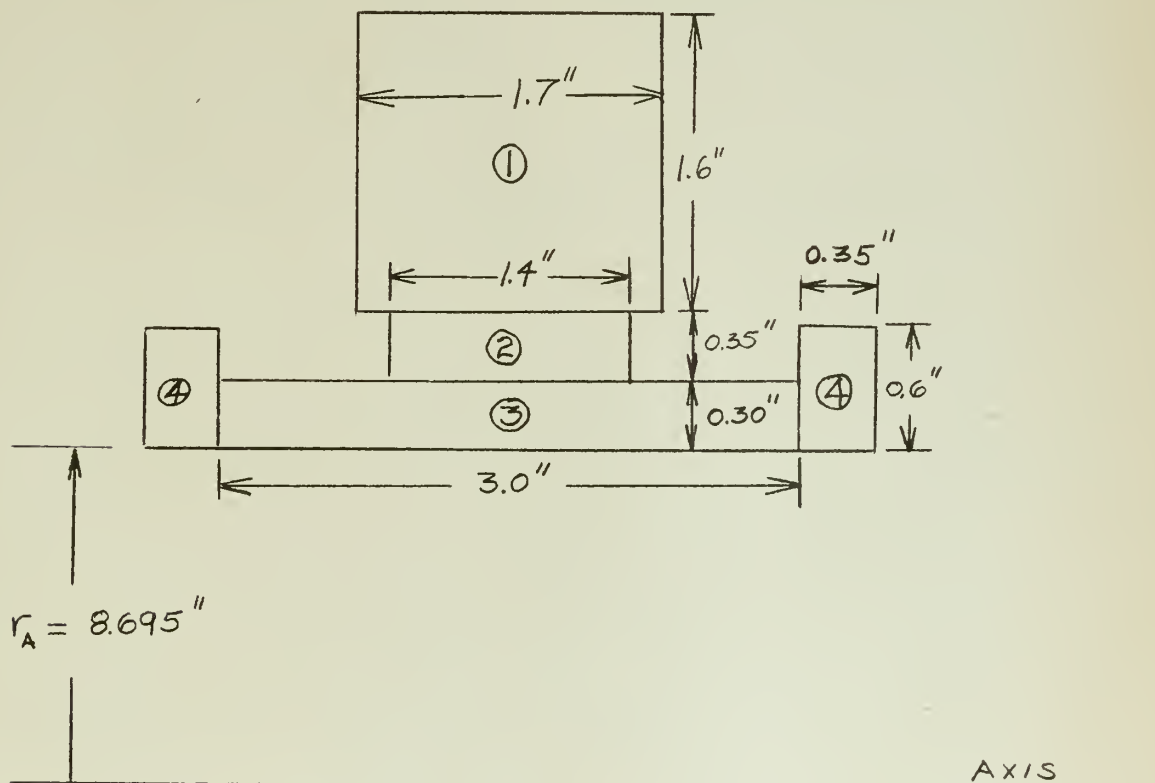
Figure 8-10   Approximate Cross Section of Turbine Disk Rim

TABLE 8-9

### CENTRIFUGAL LOADING ON THE TURBINE DISKS

Item	Material	ρ (lb/in^3)	r_{CG} (in)	m(lb/in at A)	q(lb/in at A)
1	Fir Tree: S-816 Rim: 16-25-6	0.300	10.145	0.957	13,600
2	16-25-6	0.291	9.170	0.150	1,920
3	16-25-6	0.291	8.845	0.266	3,270
4	16-25-6	0.291	8.995	0.126	1,580
				$q_{rim} =$	20,370

Loading at A due to blades:

$$q(blades) = \frac{F_c \, Z}{2\pi \, r_A} = 16{,}350 \quad lb/in \ at \ A$$

Total loading:

$$q(total) = 16{,}350 + 20{,}370 = 36{,}720 \ lb/in \ at \ A$$

For a constant stress disk:

$$b = b_A \, e^{\frac{\rho \omega^2}{2g\sigma}\left(r_A^2 - r^2\right)} \tag{8-10}$$

Since the disk temperature will be approximately 1000°F at A and 500°F at the center, an allowable stress of 25,000 psi is assumed, based on 100,000 hour stress-to-rupture data of 16-25-6 alloy.

$$b_A = \frac{q}{\sigma} = \frac{36720}{25000} = 1.47 \ in.$$

Values of b for various radii are tabulated in Table 8-10.

TABLE 8-10

WIDTHS OF CONSTANT STRESS DISK

r (in.)	b (in.)
0	3.15
1.0	3.12
2.0	3.02
3.0	2.87
4.0	2.68
5.0	2.45
6.0	2.19
7.0	1.96
8.0	1.65
8.695	1.47

Figure 8-11 illustrates the first and second stage rotor and nozzle assemblies.

It appears from the foregoing stress calculations that the peripheral speed that was assumed is not excessive. There is, of course, the possibility of much higher blade stresses if the unsteady gas force frequency is close to the blade natural frequencies. This problem will not be investigated here since normally these effects can be minimized by modification of the blading rather than major redesign of the turbine.

158
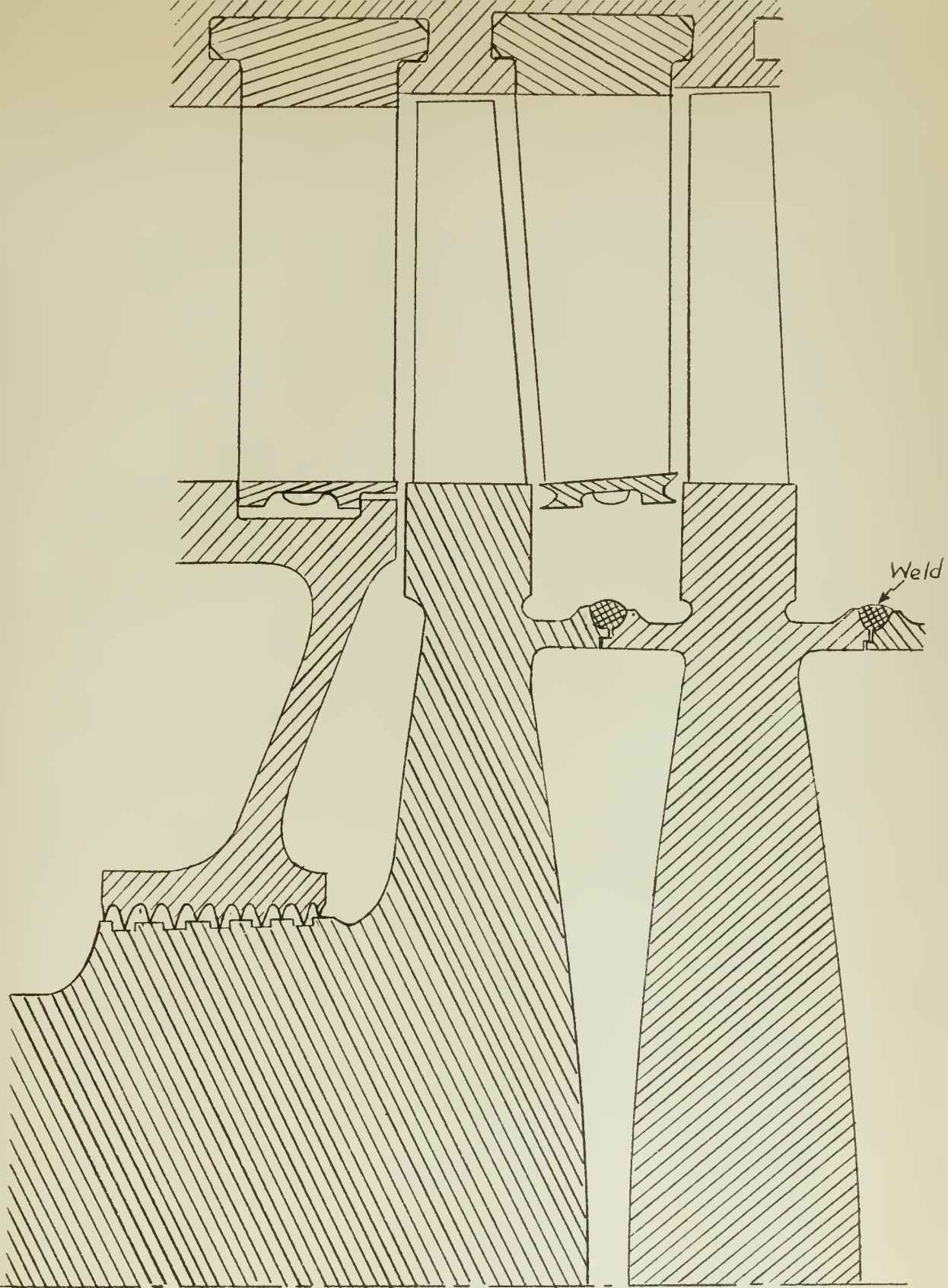
Figure 8-11   First and Second Stages of Turbine No. 1

CHAPTER IX

SUMMARY AND CONCLUSIONS

In this report, a limited design study was performed for each of the major components of a 50,000 HP closed-cycle gas turbine power plant employing helium as the working fluid and a nuclear reactor as the heat source. The descriptive data tabulated in Table 9-1 should be considered representative rather than optimum for a cycle having a maximum pressure of 1000 psia and a maximum temperature of 1350°F. It is believed that comparable sizes and performance would be obtained if different choices are made for such variables as compressor and turbine rpm, type of blading, ratio of blade spacing to chord, type of heat exchanger surfaces, and reactor cooling channel arrangement.

The thermal efficiency of the cycle is in the order of 33-36% depending on the accuracy of the machine efficiencies and pressure drops. For temperatures of 1450 - 1500°F it is estimated that the cycle efficiency would increase to about 40%. The size of the components would be reduced substantially from those herein if higher pressures were employed.

Although this design study was based on a ship propulsion plant, no mention has been made as to its operational requirements. One of these requirements is astern power. It may be possible to use an astern gas turbine in an arrangement similar to that of a conventional steam propulsion plant.

Another operational problem of critical importance concerns the control of the cycle. The primary control consists of raising and

TABLE 9-1

SUMMARY OF DESCRIPTIVE DATA FOR THE MAJOR COMPONENTS

Unit	Stages	RPM	Max. Blade Tip Diameter (in.)	Max. Blade Height (in.)	Efficiency
Compressor #1	7	7000	42.1	1.6	0.867
Compressor #2	10	7000	40.9	1.5	0.840
Turbine #1	9	7000	34.3	6.2	0.858
Turbine #2	6	5500	40.0	7.1	0.834

	Overall Length (ft)	Outer Diameter (ft)	Tube Length (ft)	Tube I. D. (in.)	No. of Tubes	$\frac{\Delta P}{P_i}$
Regenerator	45	7.5	35.7	0.30	10,330	0.0194
Precooler	18	4.6	10.2	0.40	2,690	0.0158*
Intercooler	18	3.8	9.9	0.40	1,700	0.0062
Reactor Core	7.85	7.85	7.85	1.08	2,540	0.0054

* Includes the low pressure side of the regenerator.

lowering the upper pressure level by means of an auxiliary system containing high pressure and low pressure helium accumulators. The speed with which this control functions will have an effect on ship maneuverability. Due to the large inventory of helium in the cycle this method of control may be sluggish compared to that of conventional steam plants. One important characteristic of this type of cycle is its good efficiency over a wide range of power.

Since helium is unavailable at sea except for a limited reserve supply, there must be practically zero leakage. This is very difficult to achieve when rotating machinery is involved. The main leakage problem occurs at Turbine No. 2 where the shaft leaves the casing. The remainder of the cycle can be enclosed in a leakproof casing. Bearing lubrication then becomes a problem. If oil is used as the lubricant, a rather complex system of separating helium from the oil is required in order that the helium can be returned for further use. It is possible to design the bearings so that high pressure helium is the lubricant while the machines are operating. With this arrangement, an auxiliary oil system would be required for starting.

Long half-life fission products must be prevented from being carried to all parts of the cycle by proper design of the cooling channels and filtering system. Then, only the reactor would have to be shielded.

These are only some of the problems that would have to be thoroughly investigated before a meaningful appraisal of the closed-cycle helium gas turbine plant can be made. However, on the basis of the limited investigation of this report, such a cycle has definite advantages and is worthy of further study.
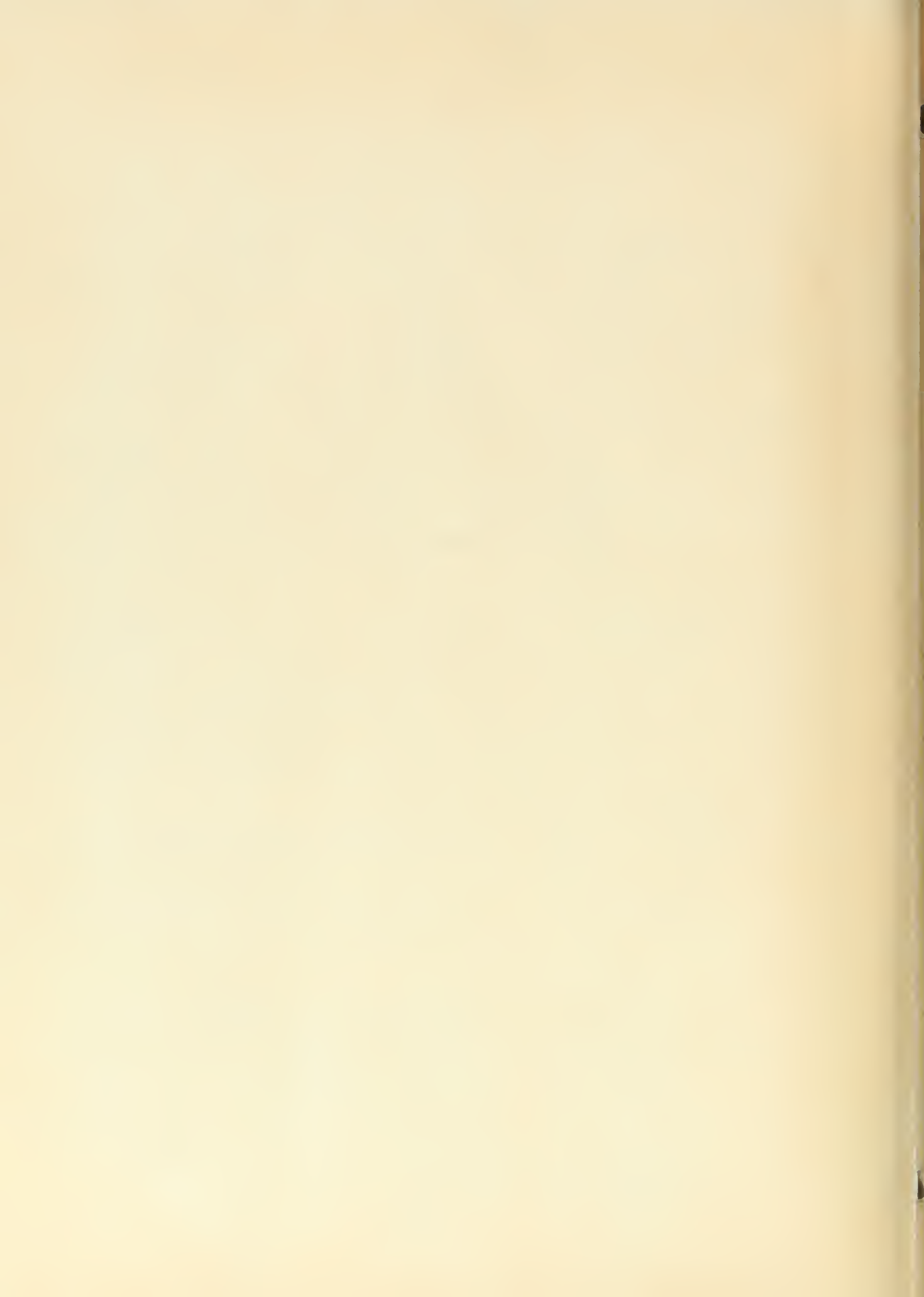
BIBLIOGRAPHY

1. Akin, S. W.   "The Thermodynamic Properties of Helium", ASME Transactions, Vol. 72, 1950

2. Keesom, W. H.   "Helium", Elsevier, Amsterdam, Holland, 1942

3. Keller, C.   "The Escher-Wyss A-K Closed-Cycle Turbine", ASME Transactions, Vol. 68, 1946

4. Kays, W. M.,
    London, A. L. and
    Johnson, D. W.   "Gas Turbine Plant Heat Exchangers", ASME Copyright 1951

5. Traupel, W.   "The Dimensionless Theory of Heat Exchange Apparatus", Sulzer Technical Review No. 1, 1944

6. Bowman, R. A.,
    Mueller, A. C. and
    Nagle, W. M.   "Mean Temperature Difference in Design", ASME Transactions, Vol. 62, 1940

7. Gardner, K. A.   "Efficiency of Extended Surface", ASME Transactions, Vol. 67, 1945

8. McAdams, W. H.   "Heat Transmission", 2nd Edition, McGraw-Hill Book Company, New York, N. Y., 1942

9. Gloyer, W.   Discussion of Gardner's "Efficiency of Extended Surface", ASME Transactions, Vol. 67, 1945

10. Von Karman, T.   "Uber Laminare und Turbulente Reibung", Zeit. fur Angew. Mathematik und Mechanik, Vol. 1, 1921

11. Howell, A. R.   "Fluid Dynamics of Axial Compressors", Development of the British Gas Turbine Jet Unit, Institution of Mechanical Engineers, London, January 1947

12. Murray, R. L.   "Introduction to Nuclear Engineering", Prentice-Hall, Inc., New York, N. Y., 1954, Chapter 11

13. Littleton, C. T.   "Industrial Piping", McGraw-Hill Book Co.,
                              1951

14. de Haller, P.   "Das Verhalten von Tragfluegelgittern in
                              Axialverdichtern und im Windkanal", Brenn-
                              stoff-Warme-Kraft, Vol. 5, No. 10, October
                              1953

15. Vavra, M. H.   Personal papers

16. Jennings, B. H. and
    Rogers, W. L.   "Gas Turbine Analysis and Practice",
                              McGraw-Hill Book Co., 1953
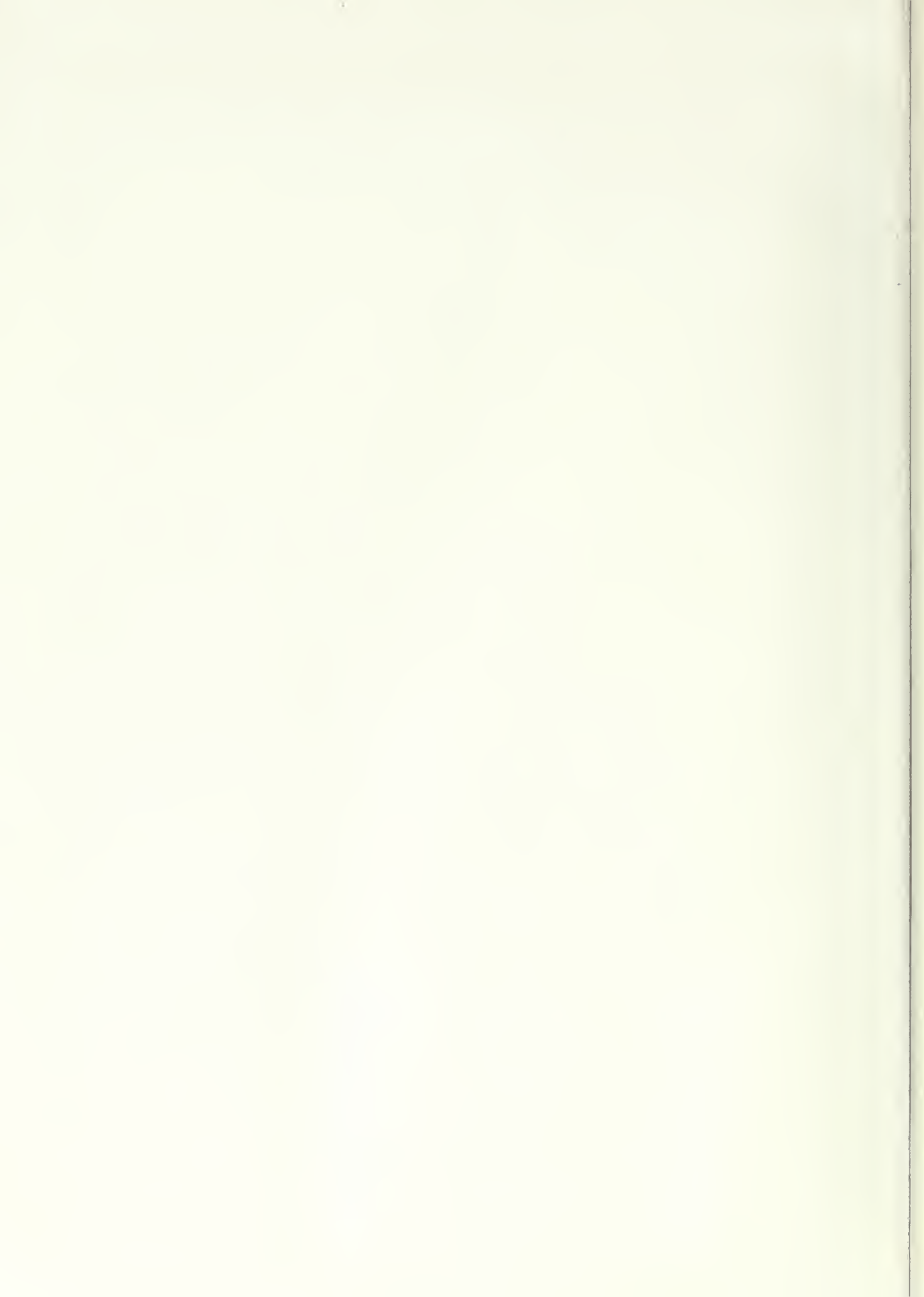
MR 6 57   4 6 8 9
OC 10 58   4 9 5 1
12 MAY 72   7 0 3
OC 25 60
12 MAY 72   7 0 3
17 SEP 76

P484   Phillips   28915
        Helium gas turbines for
    nuclear power.

    MR 6 57   4 6 8 9
    SE 25 58   4 9 5 1
   OC 10 58   4 9 5 1
    OC 25 60   9 4 4 3
    12 MAY 72   7 0 3
    17 SEP 76   2 3 8 6 3

P484   Phillips   28915
        Helium gas turbines for nuclear
    power.